# HIGH PRECISION GPS DATA PROCESSING FOR THE SURVEY OF SOUTH AFRICAN TIDE GAUGES

By

Robert Zimba

Thesis is presented in fulfilment of the requirement for the award of the degree

MSc (Eng.),

in the

Department of Geomatics, University of Cape Town

February 2000.

# Acknowledgements

I wish to express my sincere gratitude to the following individuals and organisations for their assistance and support during the course of this project,

My supervisor, Associate Professor Charles Merry of the University of Cape Town, for his guidance and inspiration throughout this project's course.

Ms. Jennifer Whittal for her encouragement and supervision in the initial stages of this work.

The Bureau for International Activities at the Eindhoven University of Technology for this scholarship. Special thanks to Mrs. Lutgart van Kollenburg for successfully coordinating my fees and finances.

The various teams that carried out the field observations and the organisations that provided the funds for this project, for doing a commendable job.

The South African agents of Geodetic Systems for loaning the Geogenius software to this project.

Mr. Trevor Venter of Optron (Pty) Ltd., for providing the GPSurvey (version 2.30) software for use in this project. His assistance is greatly appreciated.

The entire Staff and Students in the department of Geomatics at UCT for their support and the friendly work environment.

Lastly, my family and friends for their unfading support throughout my stay at University.

# Abstract

This thesis describes the work leading up to the computation of the ITRF97, epoch 1998.0 coordinates of South Africa's nine major tide gauge sites. The primary objective was to determine the ellipsoidal heights of these tide gauges to an accuracy of 1-2 cm. GPS measurements were carried out at the tide gauges as well as at IGS fiducial stations at Hartebeesthoek and Sutherland. The baselines ranged from just under a kilometre to about 1132 km.

The observations were processed in the baseline mode using Trimble's GPSurvey software (version 2.30). An extensive evaluation of the effects of the ionosphere, troposphere, antenna phase centre variations and orbits biases was carried out. This was achieved by analysing and comparing results from processing with and without the particular nuisance parameter of interest. For instance, the amount of error due to the troposphere was investigated by comparing results from processing with and without tropospheric refraction correction. In the end, an optimal processing algorithm (Precise $L1c_{(NOAA)}$) was devised in an effort to meet this project's objective. Precise $L1c_{(NOAA)}$ used IGS precise orbits and eliminated the scale error introduced by the ionosphere, using the ionosphere free observable (L1c). Tropospheric refraction and tropospheric zenith delay corrections were effected using standard meteorological data on the Hopfield model. Antenna phase centre variations were corrected for using the NOAA antenna calibration table of 1996 for the antenna used by this project.

The solution for coordinates was based on the constrained network adjustment, with the coordinates of two IGS-GPS stations at Hartebeesthoek and Sutherland fixed. A series of statistical tests within the processing software (and independent of it) were used to determine the relative quality of the processed data. No major problems were noted in the data. Position accuracy was determined to an accuracy range of a few millimetres. The largest position standard error was a meagre 6 mm at Port Nolloth (PNTG). In contrast, the resulting standard errors for the heights at the tide gauges ranged from 2-3 cm. This was a very good result considering that the software used

was not exactly suitable for this application. The more suitable specialist software packages were unavailable to this project. Under the circumstances, GPSurvey performed exceptionally well, providing accuracy better than 0.1 ppm.

# Contents

# List of Figures

# List of Tables

# ABBREVIATIONS

| | |
|---|---|
| ARP | Antenna Reference Point |
| ASCII | American Standard Code of Information Interchange |
| C/A-code | Coarse Acquisition code |
| CDDIS | Crustal Dynamics Data Information System |
| COGR | Continuously Operating GPS Receiver |
| CTS | Conventional Terrestrial System |
| DMA | Defense Mapping Agency (USA) |
| DNTG | Durban Tide Gauge |
| DoD | Department of Defense (USA) |
| ELTG | East London Tide Gauge |
| GLOSS | Global Sea Level Observing System |
| GPS | Global Positioning System |
| HARK | Hartebeesthoek Satellite Remote Sensing Centre (replaced HART) |
| HART | Hartebeesthoek Satellite Remote Sensing Centre (destroyed) |
| HRAO | Hartebeesthoek Radio Astronomical Observatory |
| IERS | International Earth Rotation Service |
| IESSG | Institute of Engineering Surveying and Space Geodesy |
| IGS | International GPS Service |
| ITRF | International Terrestrial Reference Frame |
| LSML | Least Squares modification of Stoke's formula |
| MBTG | Mossel Bay Tide Gauge |
| MSL | Mean Sea Level |
| NASA | National Aeronautics and Space administration (USA) |
| NGS | National Geodetic Surveys (USA) |
| NGWLMS | Next Generation Water Level Measuring Systems |
| NKG-89 | Nordic Geodetic Commission 1989 |
| NOAA | National Oceanic and Atmospheric Administration |
| NSWC | Naval surface Warfare Centre (USA) |
| P-code | Precise or Protected code |
| PETG | Port Elizabeth Tide Gauge |
| PNTG | Port Nolloth Tide Gauge |
| PPM | Parts Per Million |
| PRN | Pseudo-Random Noise |
| PSMSL | Permanent Service for Mean Sea Level |
| RBTG | Richard's Bay Tide Gauge |
| RINEX | Receiver INdependent EXchange |
| RMS | Root Mean Square |
| SA | Selective Availability |
| SATG | Saldanha Bay Tide Gauge |
| SBTG | Simon's Bay Tide Gauge |
| SE | Standard Error of unit weight |
| SLR | Satellite Laser Ranging |
| SSLR | Sutherland Satellite Laser Ranger |
| SUTH | Sutherland IGS-GPS Station |
| TBTG | Table Bay Tide Gauge |
| TEC | Total Electron Content |
| TGBM | Tide Gauge Bench Mark |
| TGGS | Tide Gauge GPS Station |
| UCTN | University of Cape Town North |
| UK | United Kingdom |
| USA | United States of America |
| VLBI | Very Long Baseline Interferometry |
| WAVE | Weighted Ambiguity Vector Estimator |
| WGS-84 | World Geodetic System 1984 |

# Chapter 1

## INTRODUCTION

Tide gauges are devices that measure sea level relative to a local set of monuments to which they have been related by geodetic levelling. The need to monitor their stability is of great concern as tidal records contribute to the solutions of specific scientific and oceanographic problems. Changes in sea level may be due to changes in the volume of the seas or vertical movement of the land at tide gauge sites (Carter et al., 1998). Therefore, there exists a great need to distinguish one signal from the other. GPS measurements at tide gauges have been recommended by a number of renowned researchers as a means of attaining this objective (Carter et al., 1986; Pugh, 1987). The measurements are designed to determine the absolute heights of a global set of tide gauge reference marks (TGBM's) in a single and unified three-dimensional absolute system.

Some of the most widely encountered applications of GPS measurements at tide gauge sites include the following:

- Referencing of global sea level measurements to a single and unambiguous reference surface
- The detection and modelling of vertical crustal motion at the tide gauge sites, in order to separate this signal from that of sea level variations
- Calibration and validation of precise satellite altimeter measurements

There are many reasons for measuring sea level. These range from immediate maritime operational requirements to long term predictions of global sea level change due to climate variations (Pugh, 1987). Other long term applications of tidal records include coastal development, harbour design and datum definitions for both hydrographic charts and land surveys. Coastal defences against flooding are also designed on the basis of long term tidal statistics. Protracted height measurements at the tide gauges also lead to an important empirical definition-the Mean Sea Level (MSL). MSL subsequently leads to the definition of the geoid. These geodetic features are the initial steps leading to the refinement, unification

and re-establishment of the vertical as well as horizontal datum, in the frame of a geocentric coordinate system.

Global sea level rises by about 1-2 mm per year (Carter et al., 1988). To separate this signal from vertical crustal motion, GPS must detect changes in the vertical positions of the tide gauge reference marks to better than 1 mm per year (Bevis, 1998). Calibration of satellite altimeters on the other hand requires absolute height accuracy of 1-2 cm, while other applications would require accuracy of 2-5 cm.

As suggested by its name, GPS serves to provide a global absolute positioning capability with respect to a consistent terrestrial reference frame. The World Geodetic System 1984 (WGS-84) defines the ellipsoid and realisation of the Conventional Terrestrial System (CTS) that the GPS system uses presently. However, the International Terrestrial Reference Frame-ITRF, as defined by the International Earth Rotation Service-IERS, is a more practical depiction of the CTS. ITRF has its origin at the centre of mass of the earth, rotates with the earth and is earth fixed. It is thus the recommended frame for determining positions of points on the earth (Merry, 1995; Woodworth, 1997). The latest realisation of this frame is the ITRF97 (ITRF web page - http://lareg.ensg.ign.fr/ITRF/). This thesis discusses the steps leading up to the computation of the precise ITRF coordinates of the nine major tide gauge sites around South Africa's coastline.

## 1.1 AIM OF PROJECT

The objective of this thesis was to determine the coordinates of South Africa's nine major tide gauges, to an accuracy of 1-2 cm, in the ITRF97 and at epoch 1998.0. Differential carrier phase techniques are of course capable of achieving millimetre accuracy (Hofmann-Wellenhof et al., 1997). However, the rule of thumb is that the heights are less accurate than the positions by factors of about 1.5-2. In the light of that, the 1-2 cm accuracy range is with regard to the heights.

## 1.2 GPS-TIDE GAUGE NETWORK

The design of the tide gauges has been improved upon. They are now state of the art sonar devices that record data digitally. The hydrographic office of the South African Navy

subsequently processes these data. The reference marks at the tide gauge stations are brass studs with female $\frac{5}{8}$" Whitworth threads, set in concrete jetties for maximum stability. These GPS stations or reference marks are within 50 m of the tide gauge and within 20 m of the tide gauge benchmark. Further, they have good overhead visibility and are clear of buildings, thus providing minimal multipath. Multipath is the undesirable effect of the GPS signals bouncing off surfaces near the antenna interfering with the direct signal.

Three dual frequency Z-12 Ashtech receivers belonging to the University of Cape Town were used for the field campaigns. Ideally, GPS receivers should be permanently and continuously operated at the tide gauges (Bevis, 1998). Unfortunately, this is not a feasible undertaking in the South African context due to the expensive nature of geodetic quality receivers. To make efficient use of the available equipment, the three receivers were operated simultaneously at three sites. The observations at each site lasted 24 hours, except for some inevitable breaks in the observations at certain sites. Thereafter one or two of the receivers would be moved to the next site to observe the next 24-hour session. In the end a network of independent vectors was created. Figure 1 shows the final network generated by this project.

### 1.3 ITRF FIDUCIAL STATIONS

The mainland stations designated HRAO, HARK and SUTH have permanently operating GPS receivers. These Turbo Rogue receivers continuously receive and record the L-band dual frequency signals transmitted by the satellites. The three stations are South Africa's contribution to the dense polyhedron of points around the world that constitute the International GPS Service (IGS) network of tracking stations (Beutler et al., 1998). GPS observation data from these tracking stations are collected, archived and distributed by the IGS in support of the various application and research activities. The IGS also uses the GPS data in conjunction with the Satellite Laser Ranging (SLR) and Very Long Baseline Interferometry (VLBI) measurements to generate the ITRF. As a by-product, the coordinates of the tracking stations are determined to an accuracy of a few centimetres. At this level of accuracy, the effects of crustal motion are taken into consideration and as such the solution for coordinates includes their velocity vectors (Merry, 1995). The three points are ideal fiducial points since they are closely monitored by the IGS and their coordinates are precisely known in the ITRF97. They were used as such by this project. Prior to 1997, HART at the Satellite Remote Sensing Centre in Hartebeesthoek was the sole IGS station in South Africa.

This receiver was moved by a few metres in 1997 and renamed HARK. In the same year, another IGS station was established at the Hartebeesthoek Radio Astronomical Observatory, about 2 km from HARK. This station was labelled HRAO. This project intended to use data

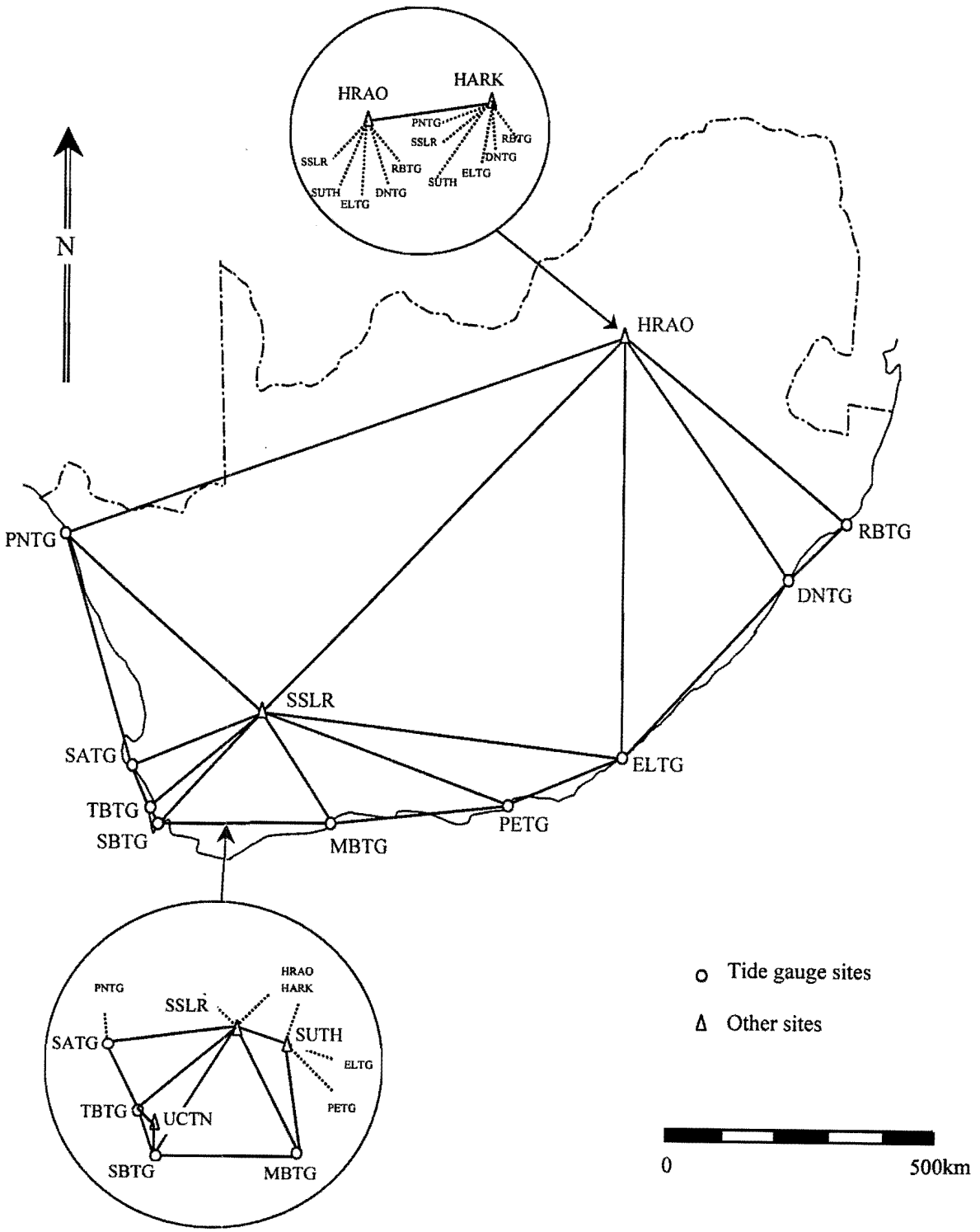


**Figure 1:** GPS Tide Gauge Network

from HRAO throughout the GPS survey. However, HRAO was unavailable in the initial stages of the field survey, as it had been struck down by lightning. Consequently, data from HARK was used to provide an additional check vector to Port Nolloth. In the latter campaigns HRAO became available while HARK failed. Both sites were subsequently used to generate the network shown in figure 1.

When this project commenced, the only point of interest at Sutherland was the Satellite Laser Ranging site as it had been included in the ITRF96. This point was designated SUTH and occupied by one of the Ashtech receivers during the field campaigns. However, early in 1998 a new IGS-GPS station was established several hundred metres from the SLR site and labelled SUTH (Merry, 1999). To avoid the eminent confusion, the point at the Satellite Laser Ranging site was re-labelled SSLR by this project. Both these points were included in the ITRF97 and have subsequently been used in this project. SSLR consist of a labelled brass stud set in a stainless steel disk engraved with three grooves at 120° to each other. The GPS antenna was mounted on a tribrach on a beacon plate that was centred by putting its feet in the grooves of the centring disk.

UCTN is the point at the University of Cape Town on the roof of the Menzies building. It forms part of the network of precise three-dimensional GPS control points in South Africa (Krynski and Swiatek, 1998). This project sought to compute its coordinates along with those for the tide gauges. UCTN consists of a brass disk with three grooves at 120° to each other on a 0.5 m concrete pillar. The GPS antenna was placed over this point as at SSLR.

## 1.4 FIELDWORK

The fieldwork had to be split into three separate campaigns. Financial constraints, the limited availability of geodetic quality equipment and a lack of field observers prompted this. The first campaign extended over the period 10-16$^{th}$ December 1997. It covered the tide gauges on the western sea board. These were Port Nolloth, Saldanha Bay, Table Bay, Simon's Bay and Mossel Bay (respectively, PNTG, SATG, TBTG, SBTG, and MBTG). It also covered the points, SSLR at Sutherland and UCTN at the University of Cape Town.

The second campaign was undertaken from 17-24$^{th}$ March 1998. Mossel Bay was reoccupied in this extension of the tide gauge network to the eastern sea board. The stations surveyed

were Port Elizabeth, East London, Durban and Richard's Bay (PETG, ELTG, DNTG, RBTG). SSLR was to be reoccupied so as to provide additional check vectors to the points PETG and ELTG. However, the receiver earmarked for that station failed prior to this field campaign. The work went ahead on the strength that data from the new IGS station at Sutherland (SUTH) would be available. Unfortunately, this station also failed over the observation period thus prompting a third campaign.

The third and final campaign served to provide the missing check vectors to MBTG, PETG and ELTG. It ran from 11-15$^{th}$ May 1998 using the two functional Ashtech receivers. One was stationed at SSLR while the other roved from MBTG to PETG and finally to ELTG. However, data from SUTH were also collected over this period, as it had become functional again. Preliminary processing results from Zimba and Merry (1999) showed SUTH as providing more stable checks to PETG and ELTG, than SSLR. Consequently, SUTH was the preferred fiducial station at Sutherland. The final network does however incorporate both points.

# Chapter 2

## STATIC GPS SURVEYING

The recommended baseline observation technique for long baselines and high order control work is the static relative positioning by carrier phases (Merry, 1995; Hofmann-Wellenhof et al., 1997). Static GPS surveying requires the use of two or more receivers held at selected points for a common period of time to collect GPS measurements. The differential technique is necessary to overcome the accuracy limitations imposed by the policy of Selective Availability (SA), orbit and propagation media errors. Processing of the GPS measurements result in precise three-dimensional vectors between the receivers, in the WGS84 Datum, consisting of three components, $\Delta x$, $\Delta y$, $\Delta z$ (Merry, 1995).

An observation session using three receivers produces three vectors; each is one side of the triangle of receivers. However, only two of these vectors are actually measured while the third is merely computed (Craig, 1996; Reilly, 1998). The two measured vectors are independent baselines whereas the computed vector (the third vector) is a dependent baseline. The choice of which vectors are to be independent or dependent must be made at the network design stage. The third vector should be determined in an independent session (Craig, 1996; Hofmann-Wellenhof et al., 1997). The network of independent vectors shown in figure 1 was designed on the basis of this principle. The inclusion of trivial or dependent vectors in a network will lead to over optimistic error estimates in the network adjustment. This is because more weight is given to the vectors of that session. Loop closures will also be smaller when trivial baselines are included.

Survey baseline processing uses carrier phase observations and satellite ephemerides to compute the position of one receiver relative to another (Schwarz and Sideris, 1993; Merry, 1995). The carrier phase observables are derived from measuring the difference in phase between the received signal from the satellite and the signal generated by the receiver's oscillator. The difference in phase is also referred to as the carrier beat phase. The carrier phase measurements between the transmitting antennae of the satellites and the receiver

antennae are however corrupted by the errors and biases affecting the GPS signals. These errors and biases propagate into the computed position. A further nuisance in the phase measurements is the integer ambiguity-the number of whole cycles of the carrier waves between the satellite and the receiver. This parameter requires that there be a change in the satellite geometry during the observation session so it can be separated from the baseline components. It is responsible in part for the long observations required by static GPS surveying. Integer ambiguity is detailed in section 2.5.

Differential carrier phase observations reduce the effects of orbit and propagation media errors to a very large extent. In fact, this technique yields sub centimetre accuracy. However in dealing with very long baselines, such as the ones in this project, these errors must be reduced even further. The following sections look at the various errors affecting GPS measurements and available remedies.

## 2.1 ORBITS

The applications of GPS depend substantially on knowing the satellite orbits (Hofmann-Wellenhof et al., 1997). The WGS-84 earth gravity model forms the basis of GPS orbit prediction. However, the earth's gravity field is not known perfectly and the effects of other perturbing forces cannot be computed exactly. Otherwise it would be possible to predict satellite orbits far into the future with very little error (Merry, 1995). In reality the predicted orbits degrade rapidly with time due to the unpredictable variations of solar radiation pressure and the earth's albedo. Consequently, the satellites have to be tracked continuously, with the fresh observations serving to improve the initial estimate of orbit. Orbital information is either transmitted by the satellite as part of the navigation message or can be obtained after the event, from specialised agencies such as the IGS.

### 2.1.1 Broadcast Orbits

These orbits are a prediction of the time changing positions of the satellites through space. Their computation is a two step process that begins with the calculation of a reference ephemeris. Permanent tracking stations at Colorado Springs, Diego Garcia, Ascension, Kwajalein and Hawaii collect observations using the GPS satellites. The known coordinates of these stations and the previous week's observations of pseudo-range data are used together

with the WGS-84 gravity model to compute an initial estimate of each satellite's orbit (Merry, 1995).

In the second step, pseudo-range and Doppler measurements are used to apply corrections to the reference ephemeris in an online mode. Satellite clock corrections are computed as a by-product. The refined orbits are extrapolated over the next 26 hours and reformatted in a compact quasi-keplerian form. These quasi-keplerian elements, the satellite clock errors and the satellite health status are uploaded to each satellite at least once per day (D'Arcy-Evans, 1991; Merry, 1995).

The estimated accuracy of the broadcast ephemerides is 5-10 m (Merry, 1995; Hofmann-Wellenhof et al., 1997). However, that accuracy range is intentionally downgraded to around 30-40 m through the policy of Selective Availability (SA). SA is a US Department of Defense (DoD) tool that is designed to restrict accurate positioning with GPS, to the US and its allies only. SA involves both dithering of the satellite clock and introducing slowly varying orbit biases into the broadcast orbital parameters. The recourse for civilian users, who are denied access to the coded corrections, is to use GPS differentially. This reduces the effect of SA considerably since it is common across receiver-satellite pairs at any epoch.

Under SA, the estimated maximum relative error due to orbit bias is 2 ppm. These orbit biases are overall insignificant for differential GPS and can be safely ignored for most survey applications using carrier beat phase observations (Merry, 1995). However geodetic and geodynamical applications require that these biases be reduced even further. Accuracy of better than 2 ppm can be achieved by using the IGS precise orbits. With the IGS orbits the effect of orbit bias on differential positioning should be reduced to less than 0.01 ppm (Merry, 1995).

### 2.1.2 Precise Orbits

The Naval surface Warfare Centre (NSWC) together with the Defense Mapping Agency (DMA) generate the official precise orbits about two months after the event (Hofmann-Wellenhof et al., 1997; Beutler et al., 1998). The precise ephemeris is computed from tracking the satellite to get the actual path. In addition to the five permanent tracking stations data from other stations in Australia, Ecuador, Argentina, England and Behrein are used to

compute the precise ephemeris. These orbits are available upon request from the US National Geodetic Surveys (NGS) and the US Coast Guard (Beutler et al., 1998). There is however a subscription charge for this service.

The most accurate orbital information is that provided by the IGS, with a delay of about two weeks (Hofmann-Wellenhof et al., 1997; Beutler et al., 1998). The IGS is a federation of government agencies and Universities around the world. Its paramount objective is to support, through the provision of GPS data products, geodetic and geophysical research activities. Its Central Bureau is housed at the Jet Propulsion Laboratory in California. IGS precise orbits of the GPS satellites and raw GPS data from the tracking stations are among the products available at their Internet FTP site. The raw GPS data are provided in the Receiver Independent Exchange format (RINEX), while the orbit files are in the Standard Product 3 (SP3) format. The RINEX format allows the exchange of GPS data across receivers and processing software from different manufacturers.

IGS precise orbits have estimated accuracy of 10-20 cm (Beutler et al., 1998). They are therefore ideal for geodetic and geodynamical applications. The optimal processing algorithm for this project used IGS precise orbits. Working with IGS orbits and observations from one or more tracking stations (as well as the precise IGS coordinates of the tracking sites), guarantees that the results of a GPS survey refer to the ITRF (Beutler et al., 1998).

## 2.2 TROPOSPHERIC REFRACTION

Orbit biases are no longer considered an error source of great concern due to the availability of IGS precise ephemerides. Presently propagation delays of the GPS signals due to the neutral atmosphere are considered the ultimate accuracy limiting factor for geodetic positioning with GPS. The neutral atmosphere comprises the troposphere, tropopause and the stratosphere. The troposphere contains neutral atoms and molecules that affect signal propagation. Atoms and molecules in the stratosphere also exist in sufficient quantities to affect signal propagation. However, since the bulk of the neutral atmosphere lies within the troposphere, the whole entity is referred to by the misnomer 'troposphere' (Brunner and Welsch, 1993; Langley, 1996).

The troposphere's nondispersive nature for radio frequencies delays the arrival of the carrier phase and carrier modulation (of both the L1 and L2 signals) by the same amount (Leick, 1995). The propagation of GPS signals through the troposphere is thus frequency independent. The disadvantage however is that an elimination of the tropospheric refraction by dual frequency methods is not possible (Hofmann-Wellenhof et al., 1997). Since the tropospheric delay cannot be measured directly using the GPS signals themselves, geodesists resort to modelling it. Two kinds of tropospheric biases can be distinguished (Bernese Software User Manual, version 4.0). These are:

- Relative troposphere biases caused by the unmodelled effects of tropospheric refraction at one end of the baseline relative to the other
- Absolute troposphere biases caused by the unmodelled effects of tropospheric refraction common to both endpoints of a baseline

Relative troposphere biases primarily produce biased station heights whereas absolute troposphere biases produce scale biases of the estimated baseline lengths. For local and regional campaigns relative troposphere errors are much more important and difficult to model. Absolute troposphere biases on the other hand are very similar to the biases caused by the ionosphere. The main difference between the two effects is that tropospheric refraction occurs in the lower levels of the atmosphere (up to 40 km above the earth) whereas ionospheric refraction occurs within 40-1000 km above the earth (Merry, 1995). The ionosphere is discussed in subsection 2.3.

Troposphere biases are orders of magnitude above the noise level of the phase observable. Thus, their influence must be reduced to make full use of the accuracy of the observable (Bernese Software User Manual, version 4.0).

### 2.2.1 Troposphere Modelling

The amount of the tropospheric refraction depends on the meteorological conditions and the path length through the troposphere (Seeber, 1993). Hence signals from satellites at low elevation angles pass through more troposphere than those from satellites at higher elevation angles. On the shortest path through the troposphere-the zenith direction, the effect increases the measured range by about 2.3 m (Brunner and Welsch, 1993). The delay increases rapidly

towards the horizon and reaches about 13 m for a zenith angle of 80°. The bulk of the error (90%) can be eliminated using a model such the one given in equation (2.1). The model uses standard values of temperature, pressure and humidity. Unfortunately, these models break down near the horizon and most receivers restrict their measurements to zenith angles of less than 80° (Leick, 1995).

Carrier phase measurements can only be used differentially and they largely eliminate the effect of tropospheric refraction. However, for geodetic positioning using carrier phases, the tropospheric effect may be a severe accuracy limitation, more so for the heights (Sjöberg et al., 1993; Brunner and Welsch, 1993). The elimination of the tropospheric effect was therefore a critical aspect in this project as tide gauges are essentially heighting devices.

In units of cycles, the tropospheric effect on carrier phase measurements is given by Merry (1995) as:

$$d_{trop} = 11.95 \times 10^{-3} \left[ P + \left( \frac{1255}{T} + 0.05 \right) .e - \tan^2 \theta \right] .\sec \theta \qquad (2.1)$$

Where:

P = Atmospheric pressure

e = Partial water vapour in millibars

T = Temperature in Kelvin at the receiver and

$\theta$ = Zenith angle of the satellite.

Troposphere modelling can be achieved either by using surface meteorological data or using standardised values of P, T and e. Merry (1995) and Seeber (1993) recommend the use of standard values on short baselines and surface measurements on longer baselines (greater than 20 km). However, surface meteorological data are often not representative of the upper atmospheric conditions above the sites (Sjöberg et al., 1993). Therefore the use of a standard model will suffice for most applications. No meteorological data were recorded for this project.

A series of models have been developed to reduce the tropospheric effect. These include the Saastamoinen, Hopfield, Goad and Goodman (Modified Hopfield) and Black models. Most GPS processing software provide these models.

### 2.2.2 Tropospheric Zenith delay

Tropospheric delay of the signal from a satellite at zenith-directly above the receiver is minimized. It reaches a maximum at, or near the horizon. Tropospheric delay cannot be predicted correctly in its totality, so geodesists resort to estimating it. This is notwithstanding accurate surface measurements of pressure, temperature and relative humidity. The problem is an accurate profile of the highly variable water vapour cannot be represented for all times and places empirically.

Based on the assumption that the neutral atmosphere is both horizontally stratified and azimuthally symmetrical, the tropospheric delay can be modelled in two parts. These are the delay experienced in the zenith direction and the scaling of that delay to the one experienced at the raypath's zenith angle (Collins and Langley, 1999). The raypath's zenith angle is also referred to as the mapping function. Total tropospheric delay is a function of the delays in the zenith direction, as well as their corresponding mapping functions. Tropospheric delay is of course caused by atmospheric gases in hydrostatic equilibrium and those that are not. Gases not in hydrostatic equilibrium are primarily water vapour. The mapping functions are usually described as functions of the satellite elevation angle- the complement of the zenith angle.

This customary formulation of tropospheric delay precludes the existence of gradients in the atmosphere as it assumes horizontal stratification and azimuthal symmetry. Researchers have developed a variety of algorithms over the years aimed at empirically modelling the tropospheric delay with varying degrees of accuracy. Unfortunately, these models can rarely predict the true delay with accuracy better than a few percent (Collins and Langley, 1999).

The delay's hydrostatic component in the zenith direction can be determined at the millimetre level. However, the highly variable nature of the atmospheric water vapour degrades the accuracy of the wet delay prediction to the centimetre level. This occurs because the hydrostatic delay in the zenith direction is a function of the total surface pressure only. This represents the total weight of the column of air above the user, under conditions of

hydrostatic equilibrium. Analogously, the zenith-wet delay is a function of the total precipitable water. This is the amount of water vapour present in the column of air above the user. Tropospheric delay models express these two parameters in various ways. The most common method describes the wet delay through a combination of surface parameters and some kind of water vapour lapse rate. This water vapour lapse rate is commonly known as the lambda parameter. Not all models explicitly parameterise the wet delay as such, but they often do so implicitly (Collins and Langley, 1999).

Unlike the hydrostatic delay, no simple physical laws govern the distribution of water vapour in the lower atmosphere. Hence, a precise definition and evaluation of the lambda parameter is to employ a technique that attempts to sample the whole atmospheric column. The ideal instruments for this task are a radiosonde or a radiometer. These instruments are not perfect and are generally not available to most GPS users. As such, the lambda parameter can only be represented empirically. Consequently, it will always be associated with some error in the determination of the wet zenith delay. It is often possible to improve tropospheric delay modelling by estimating a zenith delay correction from the GPS data itself. The software used to process this project's data had the capacity to estimate a zenith delay correction.

The technique becomes more effective over long baselines. This is because the weather conditions at either end can be significantly different, so that the unmodelled effects do not cancel out in double differencing. At the same time, the increased separation allows two parameters, one from each station, to be estimated. Over shorter to medium baselines, only one parameter can be estimated because of mathematical correlations of the partial derivatives (P. Collins, personal communication, 1999).

## 2.3 IONOSPHERIC REFRACTION

The ionosphere, extending in various layers from about 40-1000 km above the earth, is a dispersive medium with respect to the GPS radio signal (Merry, 1995; Hofmann-Wellenhof et al., 1997). Gas molecules in the ionosphere are ionized by solar radiation in sufficient quantities to affect signal propagation (Langley, 1997). The Pseudo-Random Noise (PRN) codes used in pseudo-range measurements are modulations superimposed on the carrier signal. As such, a group velocity governs them, whereas a phase velocity governs carrier phases. The consequence of the different velocities is that, a group delay and a phase advance

occurs in the ionosphere. Therefore, code pseudo-ranges are measured too long and phase ranges are measured too short compared to the geometric distance between the satellite and the receiver. The error is negative for the carrier phases and positive for pseudo-ranges. However, the numerical values are the same in both cases (Merry, 1995; Leick, 1995).

Following Merry (1995), the apparent decrease in the carrier phase measurement (or increase in the pseudo-range) is given by the expression:

$$d_{ion} \approx \frac{40.3N_T}{f^2}.\sec\theta \qquad (2.2)$$

Where, f is the carrier frequency in Hz, θ is the zenith angle of the satellite and NT is the average electron density in the direction of zenith. Unfortunately NT is highly variable and depends on the amount of solar radiation present (Merry, 1995). It is also affected by sunspot activity, which is currently moving from a minimum to a maximum in its 10-11 year cycle. So ionospheric conditions are mostly benign right now but will worsen in about two years as the cycle nears its peak (Langley, 1997).

Ionospheric refraction generally induces scale biases in the computed baselines. Its effect must therefore be reduced or altogether eliminated to attain maximum accuracy with GPS.

### 2.3.1 Ionosphere Modelling

The GPS broadcast message includes parameters of an ionospheric correction model. This broadcast model can remove about 50% root mean square (RMS) of the ionospheric effect (Langley, 1997). Single frequency measurements typically depend on the elimination of the ionospheric effect by way of the broadcast model or as common mode errors in double differencing. Differencing between observations made by simultaneously observing receivers removes that part of the ionospheric range error common to the measurements at both stations. The remaining residual ionospheric effect results because the signals received at the two stations passed through the ionosphere at slightly different elevation angles. The Total Electron Content (TEC) along the two signal paths is slightly different even if the vertical ionospheric profile is the same at the two stations (Langley, 1996). The main result of this effect in differential positioning is a baseline shortening that is proportional to both the TEC

and the baseline length. The net effect is that scale and orientation biases will propagate into the computed relative coordinates.

### 2.3.2 Ionosphere-Free Observable

The primary purpose of the second frequency in GPS satellites is to neutralize the effect of the ionosphere on signal propagation (Leick, 1995; Hofmann-Wellenhof et al., 1997). Dual frequency methods may be applied to find a combination in which the ionospheric refraction cancels out. Such a combination is termed the ionosphere-free observable and may be derived for both code ranges and carrier phases. This approach takes advantage of the frequency dependency of the ionospheric effect. However, the problem with pseudo-ranges is that there is no C/A code modulation on the L2 frequency. Consequently, only the US Military and their allies (P-code users) can determine this correction. Civilian users are denied access to the P-code and are subsequently condemned to using the broadcast model. Ionospheric refraction is nonetheless highly coherent spatially and differential pseudo-ranging reduces its effect to a few parts per million of the baseline length (Merry, 1995).

Presently it is possible to reconstruct both the L1 and L2 carriers without knowledge of the P-code. Thus, civilian users can use this approach to eliminate the ionospheric effect on carrier phase measurements. Merry (1995) gives the dual frequency correction for carrier phases, in units of cycles as:

$$d\Phi_{ion}(L_1) = \frac{f_2^2}{f_2^2 - f_1^2}\left[\Phi(L_1) - \Phi(L_2).\frac{f_1}{f_2} - N(L_1) + N(L_2).\frac{f_1}{f_2}\right] \qquad (2.3)$$

Where $\Phi(L1)$ and $\Phi(L2)$ are the carrier phase measurements on f1 and f2 frequencies respectively. N(L1) and N(L2) are the corresponding integer ambiguities. Integer ambiguity is discussed in section 2.5. In practice N(L1) and N(L2) cannot be determined, but as long as the phase measurements are continuous, they remain constant (Langley, 1996).

The ionosphere-free linear combination of L1 and L2 carriers is denoted as the L1c or L3 observable. Merry (1995) gives the expression:

$$\Phi(L_3) = \Phi(L_1) - \frac{f_2}{f_1}.\Phi(L_2) \tag{2.4}$$

The major advantage of the L3 is of course the elimination of ionospheric refraction. It however has the significant disadvantage of resolving the ambiguities as non-integers (Hofmann-Wellenhof et al., 1997). Some processing software allow several passes through the data. As such, the ionosphere may be corrected for on one pass and the integers fixed on the L1 in another pass. The software used by this project had such a provision.

## 2.4 ANTENNAE

### 2.4.1 Antenna Phase Centre Variations

The antenna phase centre is the point at which the GPS signal appears to be received. It is to this point that the measurements and the positions in GPS refer (Leick, 1995; Merry, 1995). A GPS geodetic solution for a baseline fundamentally provides the vector between the phase centres of the antennae at either end of the baseline. To relate this vector to physical points on the ground, the exact location of the phase centre of each antenna relative to those points must be known. Standard GPS positioning procedures reduce all GPS observations from the antenna phase centre to the reference point by way of the measured vertical antenna height (Stewart, 1998). The antenna phase centre for the most part, does not exactly coincide with the geometric antenna centre. The offset between the two centres depends on the elevation, azimuth and intensity of the satellite signal. Further, L1 and L2 carrier frequencies also have different offsets. This offset must be set apart from the antenna phase centre variation. Ultimately, the precision of an antenna should be based on the antenna phase centre variation and not the offset (Hofmann-Wellenhof et al., 1997). A constant offset should however be determined and taken into account.

A good antenna design must ensure an unambiguous phase centre. Unfortunately, the requirements for good antenna design are often in conflict. As such, a compromise has to be made between high gain, multipath reduction and unambiguous phase centre (Merry, 1995). Phase centre variations may be caused by an antenna pattern that is not azimuthally symmetric. In this case, antenna phase centre will be different for satellites at different azimuth. Fortunately, this effect and that of a constant offset may be reduced for differential

positioning by always using identical antennae, orientated to the same direction. The elevation dependency of the antenna phase centre variation is especially troublesome for the height determination with GPS. The remedy to this lies in calibrating the antenna against a standard or reference antenna. Details of antenna calibration appear in subsection 2.4.2.

Using same make antennae, orientated to the same direction through out the observation session should ensure constant biases that are instrument specific. These would then be eligible for elimination, over short lines, in the differencing process. However, baselines using mixed antennae, more so for large-scale projects, are inevitable. Differencing unfortunately does not cancel the relative offset shift of the antenna phase centre in such cases. In the absence of corrections for these phase centre variations, the measured baseline will be between the average phase centres of the two antennae. These average phase centre locations are a weighted average of all the individual phase centres for each of the measurements included in the solution. The consequence of this is the correlation of the station height with elevation cutoff. This is especially noticeable for baselines using mixed antennae. Such baselines tend to show increased sensitivity to elevation cutoff angle and the distribution of observations within a solution (Mader, 1999).

On long baselines, high precision requires the estimation of the tropospheric scale height along with the baseline components. This parameter is highly correlated with height and its estimation depends on the variation of the phase residuals with elevation. This variation may include an effect that arises from the antenna in addition to that from the troposphere. As a consequence, the scale height parameter and the height can be significantly in error (Mader, 1999). The determination of these antenna phase centre variations and their incorporation into post-processing solutions is therefore an essential component of precise baseline resolution with GPS.

### 2.4.2 Antenna calibration

The worldwide array of permanent and continuously operating GPS receivers allows users to incorporate reference network data into local or regional network solutions. The IGS network of tracking stations is a prime example of a reference network. In using these reference sites for geodetic positioning, users may face the problem of mixed antennae. The antenna type at the reference site may be different from the user's antenna. Where different type antennae are

used to measure baselines, antenna phase centre modelling may become necessary if high precision is to be realised (Stewart, 1998).

Antenna calibration is a procedure that uses field measurements to determine the relative phase centre position and phase variations of a series of test antennae. The calibration is done with respect to a reference antenna. The antenna widely used as a reference, is the type T Dorne-Margolin choke ring antenna. It is also the antenna that is used with the Turbo-Rogue receivers throughout the global network of the IGS. Phase centre errors are particularly important for applications requiring high resolution in the height component. These include, tide gauge monitoring and GPS geoid determination. This project is the first of a series that are intended to monitor the nine major tide gauges around South Africa's coastline. As such high resolution in the heights was cardinal.

Specialized agencies such as NASA and NOAA in the US, have determined antenna calibration tables for the most commonly used antennae. For the antenna used in this project, the Ashtech L1/L2 L-Shaped Notches, the two agencies unfortunately disagree on the L1-L2 offset. NASA on one hand shows a nominal offset of 3 mm while NOAA shows an offset of 7.5 mm on the other. Except for this difference, the NASA and NOAA antenna calibration tables are identical.

### 2.4.3 Calibration tests

Mader (1999) provides a detailed description of how the calibration tests are carried out by the NGS at their Corbin facility in Virginia. The test range consists of two stable 15 cm diameter concrete piers rising about 1.8 m above ground. On top of these piers are permanently attached antenna-mounting plates. The piers are 5 m apart, lie in a north-south line and are located in a grassy field. Levelling data show that the south (test antenna) pier is 3.4 mm taller than the north (reference antenna) pier.

A Dorne-Margolin choke ring antenna, identical to the reference antenna, is placed on the test pier. This is to determine the location of the test antenna's L1 and L2 phase centres on this pier. These positions are then used as the a priori positions for the L1 and L2 phase centres of the test antennae. The displacements that are found from the test antenna solutions then give the test antenna phase centre locations relative to the reference antenna. Further reading on

calibration tests and antenna calibration tables are also available on the NGS web site (http://www.ngs.noaa.gov).

### 2.4.4 Multipath

Satellite signals may arrive at the receiver's antenna via multiple paths as a result of signal reflection. Multipath, as the resulting error is termed, distorts the C/A code and P-code modulations as well as carrier phase observations. Although multipath signals have the same emission time at the satellite, they arrive with code and carrier phase offsets due to the reflection differences along their paths (Leick, 1995). The multipath signals, which are delayed, tend to interfere with the direct signals, which arrive first at the antenna. This culminates in a measurement error as the receiver processes the composition signal anyway. The impact of multipath on GPS measurements depends on a variety of factors. These include the strength and delay of the reflected signal compared to the direct signal and the attenuation characteristics of the antenna.

The effect of multipath can neither be reduced nor eliminated, even by differencing (Merry, 1995). The remedies to multipath lie in site selection and antenna design. As much as possible, the antenna must be located far from any reflective surfaces. Further, the antenna should by design, have a reduced response near the horizon to avoid multipath. It also ought to have an absorbent ground plane or choke ring to cutout multipath signals. The effect of multipath can reach 10 m for pseudo-ranges and should not exceed 5 cm for carrier phase observations (Merry, 1995).

All ITRF tracking sites have choke ring antennae while the Ashtech receivers used by this project do not. As a precaution, the tide gauge sites were chosen so as to reduce multipath.

## 2.5 INTEGER AMBIGUITY

At the first measurement, the GPS receiver can tell what fractional part of the incoming cycle it is looking at. Therefore, the receiver can determine the fractional part of the first cycle. It cannot however tell how many whole cycles lay between it and the satellite at the time that first cycle left the satellite. Hence, the initial phase measurement made when a GPS receiver first locks onto a GPS signal is ambiguous by an integer number of cycles (Langley, 1995).

This ambiguity remains constant, as long as lock on the GPS signal is maintained and can be established when the carrier phase data are processed. The cycle ambiguity is different for each satellite-receiver combination and a new cycle ambiguity is created every time a break in satellite tracking occurs. Such a break in the continuous satellite tracking is termed a cycle slip. Cycle slips are not necessarily a bad thing, provided the baseline processor can detect and repair them in its computations.

Differencing double differenced carrier phase observations over time forms what are termed 'triple differences'. These triple differences are a robust technique for identifying and repairing cycle slips. A cycle slip will appear as a spike in the residuals from a triple difference solution. This can then be traced to a particular satellite-receiver pair and all subsequent observations corrected for the effect of this slip. Once the data is cleaned in this manner, double difference observations are formed and processed (Merry, 1995).

The long observations associated with static GPS surveying are such that a change in the satellite geometry is allowed for during the observation session. This is in order that the cycle ambiguity can be separated from the baseline components. Ambiguities constrained to their correct integer values provide precise ranges between the satellite and the receiver. This yields relative positions that are accurate to a few millimetres. However, the algorithms used to determine, by least squares, the most probable values of the unknowns can only work with real numbers. The ambiguities are however integers and the result should reflect this. The first solution nonetheless provides real values for the integers. The accuracy of the final result will be improved if the integers are fixed. A grave consequence is that the resulting baseline components may be in significant error if the wrong integers are chosen (D'Arcy-Evans, 1991).

Ambiguity resolution becomes more difficult with increasing distance between the receiver and the reference receiver. This is attributed to the increased effects of the atmosphere and orbit errors over longer distances. Hence, the distance at which ambiguity resolution becomes difficult is dependent on the magnitude of these errors. This distance may be increased significantly if these errors are reduced (D'Arcy-Evans, 1991).

The use of precise orbits and correcting for the atmosphere increases the likelihood of constraining the ambiguities to their correct integer values on long baselines. A variety of

search methods to find the most probable combination of integers have been developed and applied. These include the general search and confidence interval methods described by Merry (1995).

## 2.6 REVIEW OF PREVIOUS RESEARCH

This part of the thesis highlights a collection of works by other researchers that had some influence on this project. It exposes their motivations, experiences, results and conclusions with a view of applying their recommendations here (where applicable).

### 2.6.1 Global Absolute Sea Level: The Hawaiian Network

Carter et al., (1987) describe the work begun by NOAA on a pilot absolute sea level network in Hawaii. Tide gauge stations on the islands of Hawaii, Maui, Oahu and Kauai have been upgraded to next generation water level measurement systems (NGWLMS). A regular program of monitoring the stability of each tide gauge in the International Earth Rotation Service (IERS) conventional terrestrial reference system was begun. The two primary IERS stations located in Hawaii are the VLBI observatory at Kokee Par, Kauai and the SLR station at Haleakala, Maui. During March and April 1987, as well as April 1988, geodetic surveys using GPS were performed at the tide gauge stations. The quest was to determine the positions of the tide gauges relative to the two (IERS affiliated) Hawaiian observatories. The inter-station distances ranged from about 10 to 350 km. Height differences were as large as 3050 m.

In the data processing, root mean square scatter of repeated measurements on the longest lines was computed. The results yielded a RMS scatter of approximately 1 centimetre in latitude, 2-3 cm in longitude and 5-6 cm in height. These were excellent results considering the GPS satellite constellation was only partially completed then. A second independent method of monitoring changes in heights of stations was being tested at the Kauai, Oahu and Maui sites. This method measures changes in absolute gravity. The first observations, made in October 1987 had uncertainties of about 2-3 cm in height.

### 2.6.2 Baltic Sea Level Project with GPS

Sjöberg and Ming (1993) outline a GPS campaign that was undertaken to unify the national height systems of countries surrounding the Baltic sea. Parties from Denmark, Finland, Germany, Poland and Sweden carried out GPS measurements at 26 tide gauges along the Baltic sea. Eight VLBI and SLR fiducial stations were incorporated into the network with baseline lengths ranging from 230 km to 1600 km. The VLBI and SLR fiducial sites were observed during the whole two weeks campaign period, while the tide gauges were observed for six days each. The observations were made using up to 19 single-and, in general, dual frequency Ashtech and Trimble GPS receivers.

The observations were processed in the network mode with the Bernese software (version 3.3) using orbit improvement techniques. The Bernese software is capable of estimating station coordinates, ambiguities, orbit parameters, tropospheric zenith correction and ionospheric single layer model. The tide gauge sites were estimated together with orbit, ambiguity, tropospheric and ionospheric parameters. The fiducial station coordinates were however fixed.

All results were obtained using the ionosphere-free observable (L3) for dual frequency receivers and the L1 observable for single-frequency receivers. The scale error introduced by the ionospheric refraction from single frequency data was mitigated by using local models of the ionosphere estimated on the L4 observable. The preliminary results showed average RMS errors of about ± 3 cm in the horizontal and ± 7 cm in the vertical position. These positions were computed relative to the Potsdam SLR station, in the ITRF89 system.

Sjöberg and Ming were not exactly certain they resolved the ambiguities correctly, more so in the auroral zone of their network. With reference to Rothacher (1992), they stated that it is better not to resolve ambiguities when uncertain. Otherwise biases will be introduced in the solution for coordinates due to wrong ambiguities. Subsequently, the solutions presented here had ambiguities not resolved to integers. Furthermore, a standard atmosphere model (Saastamoinen) was used to correct for tropospheric refraction in the data processing. This was despite the availability of meteorological data for the campaign. Sjöberg's earlier works prompted this choice. Sjöberg (1988) and Sjöberg et al., (1991) showed that using surface meteorological data does not improve results of data processing. The main reason would be,

surface meteorological values are not often representative of the true upper atmospheric conditions above the site.

The GPS derived results were transformed to geoid heights using the levelled heights. Thereafter, an absolute comparison with the gravimetric geoid heights from a least squares modification of Stoke's formula (LSML), modified Molodensky and the NKG-89 was made. This resulted in a standard deviation of the difference of ± 7 cm to ± 9 cm, for the NKG-89 model and ± 9 cm to ± 30 cm for LSML and modified Molodensky models. The Swedish height system was found to be about 8-37 cm higher than those of other Baltic countries for the NKG-89 model are.

### 2.6.3 GPS Monitoring of Vertical Land Movements in the UK

Ashkenazi et al., (1998) give details of the development and application of high precision GPS techniques to the monitoring of vertical land movements in the United Kingdom (UK). GPS measurements at UK tide gauges have been going on at the Institute of Engineering Surveying and Space Geodesy (IESSG) since the late eighties. The drive is to distinguish between true sea level variations and vertical land movements at the tide gauge sites. Hence, to monitor changes in 'absolute' mean sea level, the rates of any vertical land movements must be determined and removed from the tide gauge records.

The initial projects were based on the use of episodic GPS campaigns. However, this project used a combination of a small number of continuously operating GPS receivers and episodic GPS measurements. The tide gauge sites were selected on the basis that they had at least 20 years of data in the Permanent Service for Mean Sea Level (PSMSL) archive. Alternatively, the tide gauge sites had to be a part of the Global Sea Level Observing System (GLOSS).

Tide gauge GPS stations (TGGS) were established at each tide gauge in addition to the TGBM. TGBMs serve as a reference for mean sea level in the tide gauge records. The TGGSs have been located as close as possible to the tide gauge, but in locations suitable for GPS measurements. These TGGSs are also installed in bedrock or a substantial concrete structure, such as a pier or sea wall piled down to bedrock to ensure stability. A total of nine episodic campaigns were undertaken between 1991 and 1996. For each of these, simultaneous GPS measurements were made at the selected tide gauges and a number of fiducial stations in

Europe. These fiducial stations are continuously operating GPS receivers (COGR) that are part of the International GPS Service for Geodynamics (IGS) network. The observations extended from 8 hours per day, for six consecutive days, to a maximum of 24 hours per day, for six consecutive days. Through these high precision GPS measurements, the heights of the TGGSs were determined in the ITRF. Local precise levelling connections were made to link the TGGSs to the TGBMs.

Data from the episodic campaigns that included observations to one or more of the sixteen UK tide gauges were combined into a single data set. Different type receivers and antennae were used in the nine campaigns. This is typical for a series of observations carried out over a period as long as five years. Improvements in receiver technology and limited availability of large numbers of similar GPS receivers (for use in campaigns of this magnitude) prompt mixing of equipment. Processing of the combined data set was carried out using the IESSG in-house developed GPS analysis software. The GPS data from UK91 and UK92 campaigns were processed with regional orbit improvements carried out as part of a fiducial network adjustment. The GPS data from latter campaigns were processed with IGS precise orbits. In both cases the ITRF stations at Onsala, Wettzell and Madrid were constrained at some stage. Their ITRF94 coordinates were projected to the observational epoch using the ITRF94 velocity field. For all campaigns, the data were processed using the L1/L2 ionosphere-free double difference observable. The integer ambiguities were not fixed, however. Furthermore, a common set of systematic error models was applied throughout the processing. These were corrections for earth body tides, ocean tide loading, antenna phase centre variations and tropospheric delay.

The preliminary results indicated that the time-averaged mean heights of some of the TGGSs were determined to a precision (internal consistency) of 2-3 mm; but when compared to an external standard the accuracy was 10 mm or better. The major assumption was that negligible vertical land movement took place over the five-year period. Further research into vertical land movements in the UK is presently on going (R. .Bingley, personal communication, 1999).

# Chapter 3

# METHODOLOGY

## 3.1 INTRODUCTION

This stage of the thesis discusses how the various biases and errors highlighted in chapter 2 are mitigated or altogether eliminated. Data processing entails data editing, cycle slip detection and repair, as well as ambiguity resolution for subsequent baseline and station computation. Typically, the observations, which are simply carrier phases, are reformed into linear combinations of the raw measurements for mathematical convenience and robustness. The mathematical models of these measurements are based upon combining the raw measurements between receivers and satellites. These measurements are formed into various combinations of L1 and L2 carrier phases and pseudoranges. Each of these combinations exhibits unique properties that help in solving, modelling or reducing the effects of different parameters. These include the ionosphere, troposphere and multipath. The postprocessor uses least square algorithms to solve for the integer ambiguities and the unknown receiver position. In doing so, it uses one or more of these measurement combinations.

## 3.2 DATA SOURCES

After each field campaign, the observed data were downloaded onto laptop computers and backed up on stiffy diskettes. Eventually, all the field data (in Ashtech format) were copied onto a single desktop computer. Some files had inevitable breaks in them, mainly due to power losses during the data collection. Where these breaks were less than an hour long, the Ashtech program Filetool, was used to combine such data files. The data were then converted to the RINEX format using the program Ashtorin. The use of software alien to the Ashtech format was deemed inevitable, given the project requirements. Hence the subsequent conversion of the data to the RINEX format. However, contrary to the RINEX convention, the antenna heights given in the data files were the height of the L1 phase centre above the reference marks. Consequently, the antenna heights were changed by subtracting 0.064 m in conformity with the RINEX convention that antenna heights refer to the antenna reference point (ARP). The RINEX ARP is the bottom of the antenna mount. 0.064 m was the

micrometer reading for the difference between the L1 phase centre and the ARP for the Ashtech antennae used here. This is illustrated in figure 2.

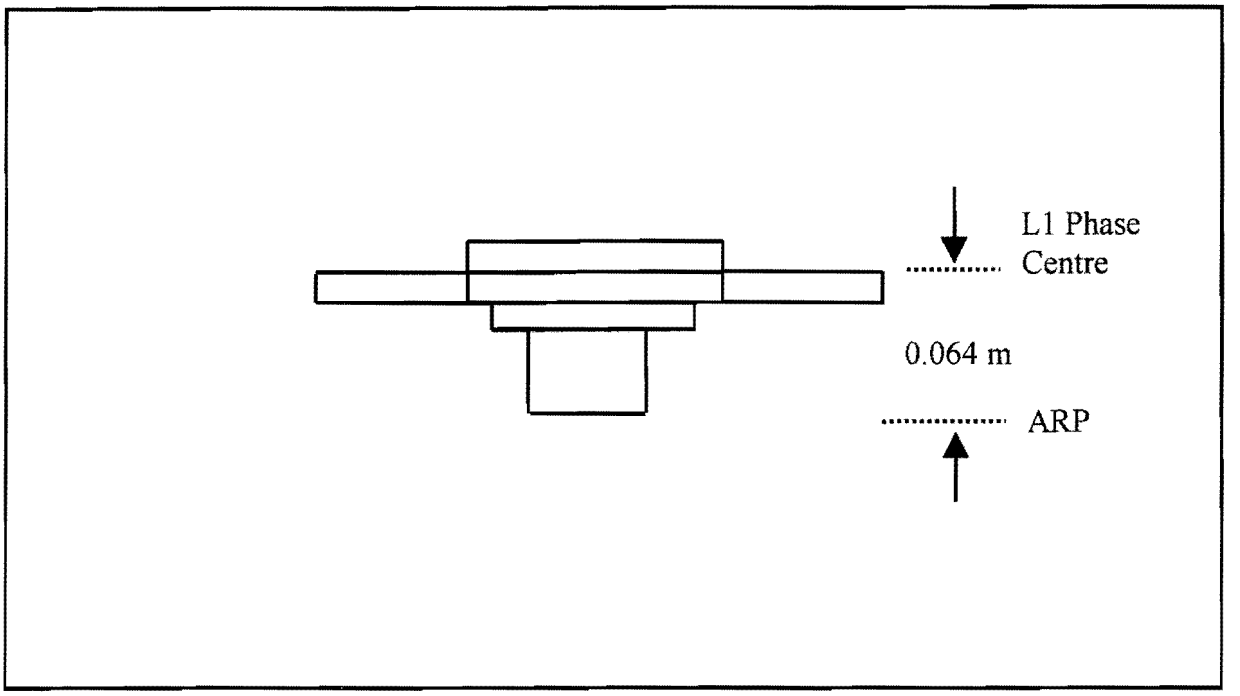


**Figure 2:** Difference between the L1 phase centre and the ARP for the Ashtech antenna geodetic L1/L2 L (Rev. B)

RINEX data for the IGS stations HARK, HRAO and SUTH were downloaded off the Crustal Dynamics Data Information System (CDDIS) FTP site. The corresponding ITRF97, epoch 1997.0 coordinates of these fiducial stations were obtained from the IGS web site. These were then projected to the ITRF97 at epoch 1998.0 using their respective velocity vectors. This simply served to have the ITRF frame at an epoch corresponding to the period of the observations. Table 1 shows the ITRF97 station positions at epoch 1997.0 with their respective velocity vectors. Table 2 on the other hand shows the ITRF97 station positions at epoch 1998.0. It further supplies their corresponding ellipsoidal equivalents. Precise ephemerides covering the three campaigns were downloaded from the IGS Central Bureau FTP site. These are stored and transmitted in a compressed form. Fortunately, the IGS also provides compress and decompress utilities together with the download. Once decompressed, the downloaded binary files convert to American Standard Code of Information Interchange

(ASCII) files in the Standard Product 3 (SP3) format. Certain software has the capability to work with ephemeris data in the SP3 format while others require further conversions.

**Table 1:** ITRF97 Station Positions at epoch 1997.0 and Velocities

| Domes NB | Site Name | Tech. ID | X/Vx | Y/Vy | Z/Vz |
|---|---|---|---|---|---|
| | | | m/m/y | | |
| 30302M004 | Hartebeesthoek | GPS HRAO | 5085352.503<br>.0001 | 2668395.679<br>.0209 | -2768731.702<br>.0140 |
| 30302M007 | Hartebeesthoek | GPS HARK | 5084625.317<br>.0001 | 2670366.236<br>.0209 | -2768494.568<br>.0140 |
| 30314M002 | Sutherland | GPS SUTH | 5041274.814<br>.0030 | 1916054.004<br>.0141 | -3397076.087<br>.0085 |
| 30314M001 | Sutherland | SLR SSLR | 5041543.397<br>.0030 | 1915353.113<br>.0141 | -3396942.332<br>.0085 |

**Table 2:** ITRF97 Station Positions at epoch 1998.0

| Domes NB | Site Name | Tech. ID | X/φ | Y/λ | Z/h |
|---|---|---|---|---|---|
| | | | m/ ° ′ ″ | | m |
| 30302M004 | Hartebeesthoek | GPS HRAO | 5085352.503<br>-25 53 24.38254 | 2668395.700<br>27 41 13.12495 | -2768731.688<br>1414.196 |
| 30302M007 | Hartebeesthoek | GPS HARK | 5084625.317<br>-25 53 13.59275 | 2670366.257<br>27 42 27.92825 | -2768494.554<br>1555.412 |
| 30314M002 | Sutherland | GPS SUTH | 5041274.817<br>-32 22 48.76298 | 1916054.018<br>20 48 37.66102 | -3397076.079<br>1799.773 |
| 30314M001 | Sutherland | SLR SSLR | 5041543.400<br>-32 22 45.06042 | 1915353.127<br>20 48 08.95413 | -3396942.324<br>1729.919 |

## 3.3 SOFTWARE SELECTION

The baselines in this GPS survey were up to 1132 km in length. Over such expanses, high precision may be attained through the use of a specialist software package. These specialist software are however not user friendly, and require a thorough understanding of the GPS signals and error behaviour. Their advantage is that they allow the user access to the code and to estimate all nuisance parameters, including orbits. Unfortunately, none were readily available to this project. Either the software itself was too expensive or a PC running windows (as operated by this campaign) was not its ideal platform. Most of these packages run under UNIX on a workstation.

Software that was immediately available comprised three commercial packages. The first was Ashtech's GPPS (provided with the receivers) and its windows version-Prism. While this package proved to be robust and reliable for short baselines, it lacked many of the features desirable for processing longer lines. The second package was the windows based Geogenius software loaned from their South African agents-Geodetic systems. Some initial processing was carried out using this package (Merry, 1999). However, the results fell short of this project's requirement of a 1-2 cm height accuracy. The third package, Trimble's GPSurvey version 2.30, was borrowed from Optron (Pty) Ltd. GPSurvey exhibited a number of features that made it more suited to meeting the project requirement. This report describes the results of processing the tide gauge survey data using Trimble's GPSurvey.

GPSurvey exhibited the following desirable traits with regard to this project's requirements:

- Direct import of RINEX data files
- Ability to import precise ephemerides (a format conversion is however necessary)
- Ability to use antenna calibration tables with separate offsets for the L1 and L2 frequencies
- Troposphere and zenith delay correction modelling
- Ionosphere free processing

Desirable features not available in GPSurvey include:

- Session mode data processing (only baseline mode possible)
- Corrections for earth tides, ocean tide loading and crustal motion

## 3.4 PREPROCESSING

Preparing the project data for subsequent processing proved to be an intensive and painstaking process. By design, all observations should have lasted 24-hour periods. However, some files did not meet this requirement. The main cause of this, as indicated earlier, was power losses during some of the observations. For instance, the power box on the jetty at Saldanha bay was shared with a tugboat. Whenever the tugboat left the jetty, all power to the box was cut off. A backup battery was available except the receiver appeared to have drained it before switching to mains power. The net effect was that the data recorded for that site had a number of significant gaps. A power loss was also experienced at Sutherland on the last day of the third campaign. That resulted in the shortening of the session length for the vector SSLR-ELTG. Fortunately, SUTH became available during that time and thus provided alternative cover to ELTG. It was subsequently used in preference to SSLR as the link to ELTG. Simon's bay is a military dockyard and due to some misunderstanding with security personnel, the receiver there was removed at some point during the observations. This resulted in a loss of several hours of data. Further hours of data were lost at the same site when a severe rainstorm caused the power transform to short out. Several smaller breaks in power occurred at other sites. The data recording rate for all sites was 30 seconds in unison with the rate of the Turbo Rogue receivers at the IGS sites. This was also the intended-processing rate for all vectors in the network. Unfortunately, the operator of the Ashtech receiver at Durban started off with a 20-second rate. Upon realising this mistake, the rate was later changed to 30 seconds. The overall implication was the common epoch for vectors into DNTG was 60 seconds for this data set.

There was no alternative but to process the entire network at a 30-second rate with a switch to 60 seconds at DNTG. As indicated earlier, data files with breaks less than an hour long were combined using Filetool. Where the breaks exceeded an hour, the data file with the longest span was adopted. GPSurvey is designed to handle both kinematic and static data. Thus its setup includes a feature that automatically detects the receiver type and mode of data collection. This unfortunately proved to be a nuisance as it identified data files with slight jumps as kinematic stop and go files. These jumps were lines in the observation file with similar information except one was an incomplete replica of the other. The portion of the file before the jump was wrongly viewed as a rover-kinematic file. While that after, was labelled a static file. As a remedy to this, a text editor was employed to remove the replicated but

incomplete line of information. Thereafter, the software correctly labelled all data files-static. Mismatched file labels were also corrected using the text editor. The tide gauge data were uploaded into GPSurvey once all corrections were made. Data editing to detect and repair cycle slips, outlier detection, as well as data thinning form part of the main processor in GPSurvey. Details of the main processor appear in subsection 3.5.1.

GPSurvey program documentation for the version 2.30 indicates that SP3 format precise orbit files can be directly imported. However, a further conversion was required, it turned out. A DOS conversion program 'SP3EF18' had to be used to convert the orbit files from SP3 to EF18 format. This program is particularly sensitive to naming conventions. A great deal of time was expended before successful conversions were made. Other concerns were the differences in start to end times of the observation files as opposed to those for precise orbit files. Fortunately, GPSurvey automatically extracts the required precise orbit cover from adjoining orbit files.

## 3.5 DATA PROCESSING

GPSurvey comprises a series of modules that handle GPS data at the various stages of data processing. With particular regard to this project, the modules used were the Project Manager, GPLoad, Check-in, Wave, Trimnet-Plus, Network Map and Utilities. The Project Manager is responsible for creating and managing the various projects. It also updates, edits, saves, deletes, archives and restores projects. The project is the fundamental unit within GPSurvey and all functions are built around this concept. Thus the first step in all the data processing was the creation of a project. This was followed by the upload of the data sets into the project. The GPLoad and Check-in modules were employed in this task. The GPLoad module has a RINEX interface and allowed the upload of all the project data into GPSurvey. Check-in was used with user interaction to assign data to project databases. User interaction served as a double check for any discrepancies in the data. The integrity of the data files was reinvestigated and alterations made where necessary. Then baseline processing would follow. The Wave module is the baseline processing entity within GPSurvey. Its processing rationale is discussed in the next subsection. Trimnet-Plus is an Adjustment package and it was used to adjust networks of the processed baselines. Network Map is a graphics display module and provided screen displays of the stations and baselines. Utilities is a multifunction module that provides access to the reference and adjusted coordinates among other things.

### 3.5.1 Wave Baseline Processing

Once the project's data integrity was reaffirmed and fiducial station coordinates entered in data Check-in, baseline processing followed. The baseline processor uses both carrier-phase and code observations to produce precise three-dimensional vectors (GPS baselines) between survey stations. A typical data processing session in Wave begins with code data processing. Code pseudoranges are used to estimate the coordinates of each endpoint of a line before an initial baseline vector can be computed. In addition to the three-dimensional positions, the receiver clock offsets are obtained. Phase data processing then follows, with the raw phases being combined into double and triple differences. Receiver-satellite double differences result when simultaneous observations from two receivers are made to two satellites. More precisely, between receiver single differences are formed for each of the two satellites and these two differences are differenced again to form the double difference. This differencing technique effectively eliminates satellite and receiver clock errors while orbit and refraction errors are considerably reduced. A schematic representation of the double difference is shown in figure 3. Equation 3.1 (Merry 1995) shows the double difference terms.

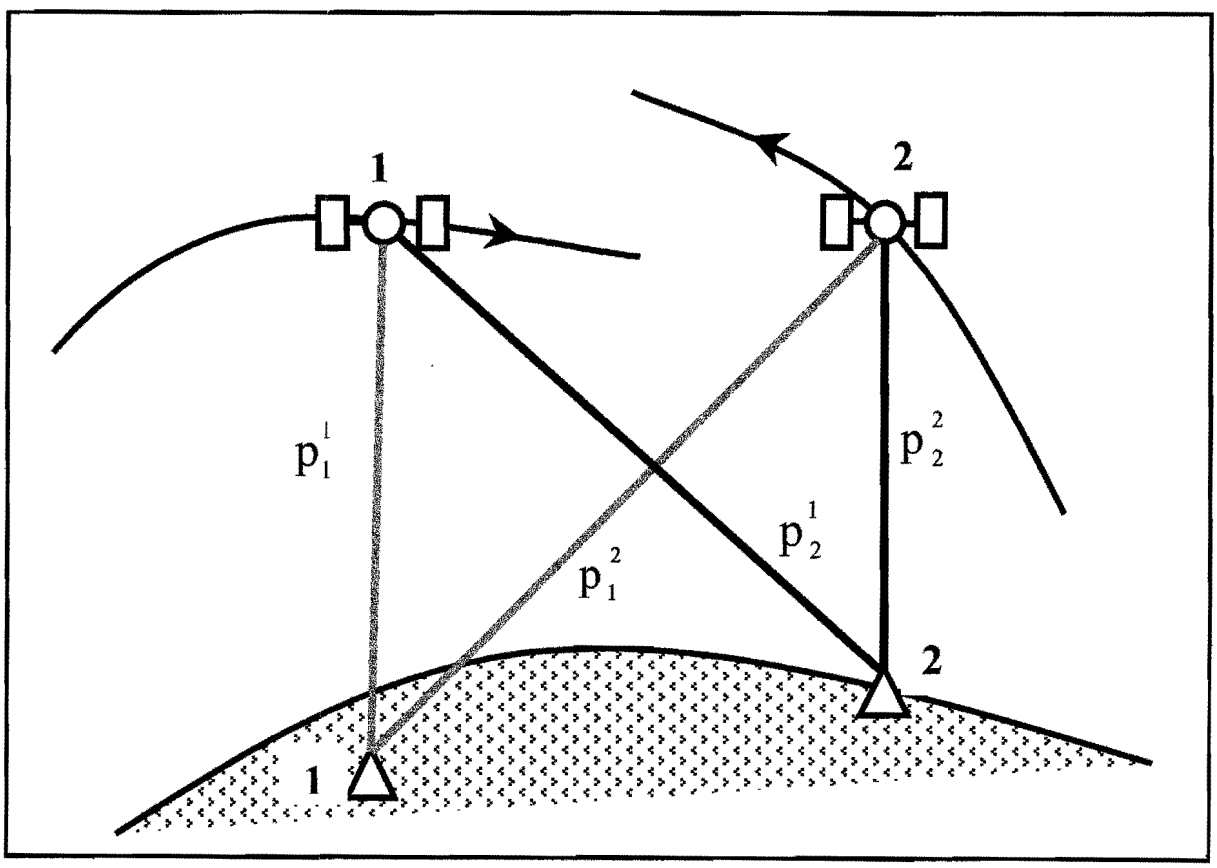


**Figure 3**: Receiver-Satellite double difference

$$\lambda.\Delta\Phi\ {}^{21}_{21} + \Delta^2 d_{ion} - \Delta^2 d_{trop} = \Delta p^{21}_{21} - \lambda.\Delta N^{21}_{21} \qquad (3.1)$$

The term $\lambda.\Delta\Phi^{21}_{21}$ is the wavelength '$\lambda$' multiplied by the double differenced carrier beat phase. $\Delta^2 d_{ion}$ and $\Delta^2 d_{trop}$ are the double differenced ionospheric and tropospheric refraction terms respectively. $\Delta p^{21}_{21}$ contains two satellite positions (known from the navigation message) and the two unknown receiver positions. The last term in equation 3.1 contains four cycle ambiguities but the double difference of these ambiguities can be treated as a single unknown. Wave uses triple differences (as do most other baseline processors) to detect and repair cycle slips. A triple difference is formed when a receiver-satellite double difference is differenced over time. This approach eliminates all nuisance parameters as the integer ambiguities disappear (cancel out) in differencing between epochs. Figure 4 illustrates the triple difference while the triple difference terms appear in equation 3.2.

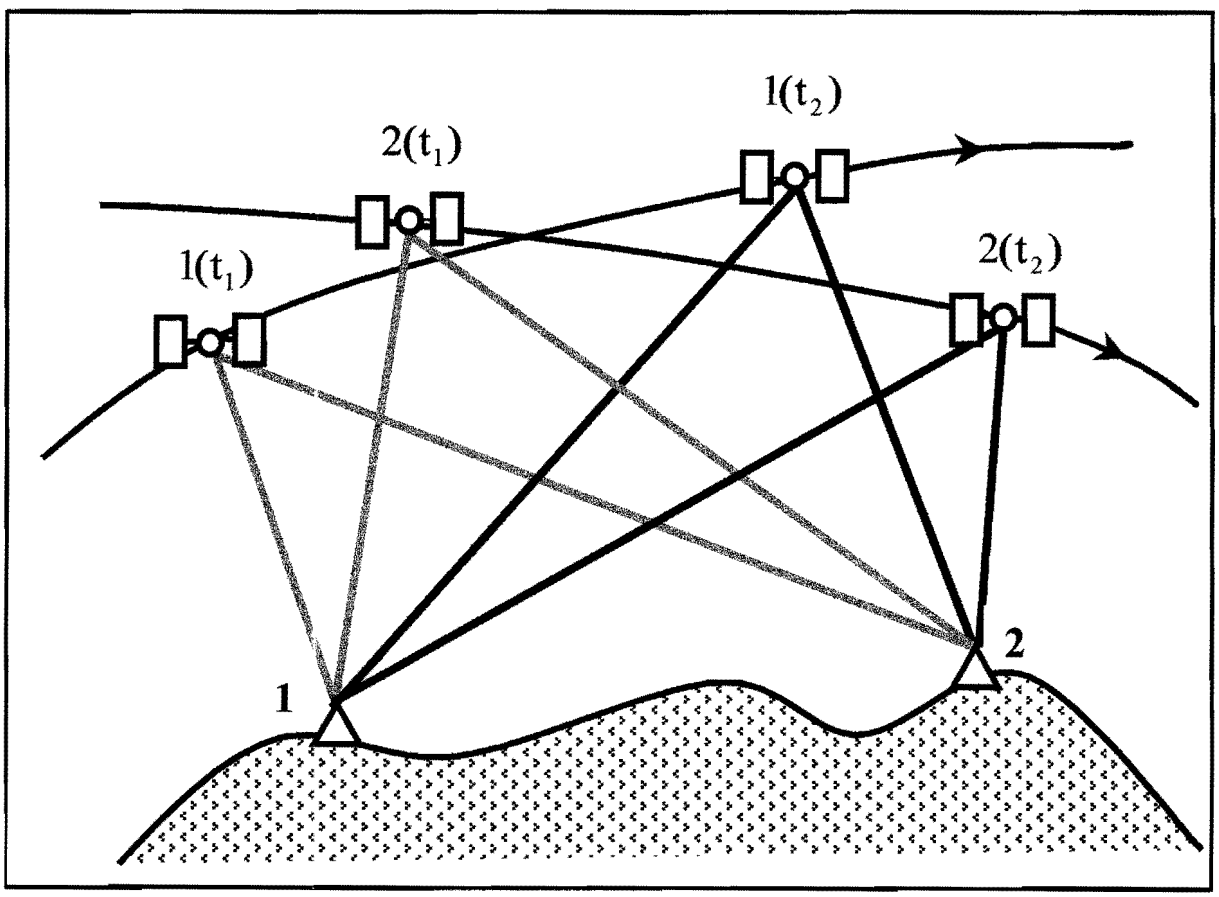


**Figure 4:** The Triple Difference

$$\lambda.\Delta\Phi_{21}^{21}(t_2 - t_1) + \Delta^3 d_{ion} - \Delta^3 d_{trop} = \Delta p_{21}^{21}(t_2 - t_1) \qquad (3.2)$$

Equation 3.2 stays valid only if there is continuous counting of the cycles from $t_1$ to $t_2$. If any cycle slips occur, then an additional cycle ambiguity must be computed. Cycle slips are mapped as individual outliers in the computed triple difference residuals. Individual outliers can usually be detected and removed or corrected. The resulting cycle slip free or nearly so observations are then used in the double difference solution.

In addition to the L1 and L2, Wave provides combined dual frequency phases in the form of the ionosphere-free (L1c), wide lane and narrow lane signals. The L1c effectively eliminates the ionospheric effect and its explicit details appear in subsection 2.3.2. The wide lane observable has a wavelength of approximately 86 cm, derived from subtracting the L1 and L2 carrier waves (L1-L2). Its long wavelength makes it easier to find the integer ambiguities. Adding the carrier phase observables (L1+L2) on the other hand creates the narrow lane carrier phase. The effective wavelength of the narrow lane is about 11 cm and it is very effective in cancelling out ionospheric effects. These observables by themselves are inadequate for high precision GPS data processing. High precision GPS demands among other requirements that the final solution be ionosphere-free and fixed in terms of the ambiguities. This is more so for long baselines. The L1c quite rightly eliminates the ionospheric effect but it does not fix the integers. Conversely, the wide lane is effective in fixing the integers on long baselines, but it is susceptible to the amount of noise in the data. Fortunately, Wave can be configured to use the wide lane to resolve L1 integers in a solution that also corrects for ionospheric refraction. The advantage of this option is that ambiguities can be constrained to integers. This results in a greater degree of freedom and hence greater precision in the solution.

### 3.5.2 Process Set-up

Wave provides both automatic processing and flexible controls for advanced processing. It first examines the data to be processed and then makes an intelligent decision about default values to be used. The latter option was taken and Wave was configured in all processing

sessions for this project. The following options were selected in order to investigate the effects of the various nuisance parameters en route to the most accurate solution.

**Processing variations:**

- Broadcast L1c:

Broadcast orbits, corrections for the ionosphere, troposphere and antenna phase centre variations (using GPSurvey antenna calibration table- A700288.pct, in appendix A).

- Broadcast L1:

Broadcast orbits, corrections for the troposphere, antenna phase centre variations (using A700288.pct), but no correction for the ionosphere.

- Broadcast $L1c_{(-trop)}$:

Broadcast orbits, corrections for the ionosphere, antenna phase centre variations (A700288.pct), excluding corrections for the troposphere.

- Broadcast $L1c_{(-Ant)}$:

Broadcast orbits, plus corrections for the troposphere and ionosphere, but no antenna phase centre variations correction.

- Precise L1c:

IGS precise orbits, corrections for the ionosphere and troposphere, plus antenna phase centre variation correction (using GPSurvey's A700288.pct table).

- Precise $L1c_{(NOAA)}$:

IGS precise orbits, corrections for the ionosphere and troposphere as well as antenna phase centre variation correction. Except the GPSurvey table A700288.pct was replaced by one from NOAA. See appendix A, for the differences between the two tables.

In order to assess the precision and accuracy of the tide gauge network in figure 1, the following comparisons were investigated:

- L1c/L1:

To analyse the ionospheric effect and the amount of scale bias it introduced into the computed baseline components.

- $L1c/L1c_{(-trop)}$:

To investigate and analyse the amount of bias the troposphere induces on the station heights and scale bias of the computed baselines.

- L1c/L1c$_{(-Ant)}$:

To analyse the amount of bias induced into station heights by antenna phase centre variations.

- L1c/Precise L1c:

To analyse the amount of improvement in baseline results due to precise orbits as opposed to broadcast orbits.

- Precise L1c/L1c$_{(NOAA)}$:

To investigate and analyse results of processing using the two different antenna calibration tables (A700288.pct versus NOAA table).

In all the processing variations above, an elevation cutoff angle of 15° (differing from the 10° used in the field) was selected. This effectively cut off all data from satellites below a line 15° above the horizon. More data would have been available for processing at the initial 10° mask. Unfortunately, GPS signals at such low angles travel significantly longer paths through the atmosphere. That makes these GPS signals more susceptible to more deflection in the ionosphere and troposphere. A 30-second decimation rate was applied throughout the network but for two lines into Durban. These two lines used a 60-second rate as this particular Durban data was recorded at 20 then 30 seconds. Where tropospheric refraction modelling or corrections were applied, standard meteorological parameters were used. The reason for this choice is given in subsection 2.2.1. Furthermore, tropospheric zenith delay was estimated using an interval of two hours. Process set-ups effecting ionospheric refraction corrections used the ionosphere-free (L1c) approach. Ultimately, correcting for the ionospheric effect gave access to the L1 ionosphere-free fixed integer option. However, selecting this option is not in itself a guarantee that the ambiguities will be resolved to their integer values. This is reaffirmed by some of the processing results (see subsection 3.5.4).

### 3.5.3 Quality Control

Wave, as with most GPS software, provides statistics that allow the user to discern the quality of the processed baselines. The most significant of these are the ratio and reference variance tests. The reference variance is an indicator of how well the observed data for a particular

baseline fit into the computed solution. The observed data being the actual carrier phase measurements. The software makes initial estimates for error within the baseline solutions. If the actual errors found within the baseline solution equalled the estimated errors, the variance would equal 1.0. A value greater than 1.0 would indicate that the actual errors were greater than those estimated for the solution. Consequently, values of variance lower than 1.0 would indicate better baseline solutions. If the reference variance is much greater than unity, there may well be a problem with the solution. High numbers more often than not result from noisy data, significant multipath, unmodelled systematic errors and wrongly fixed integers (Wave software user's guide, 1995).

Fixed integer solutions resulting from an integer search have ratio displayed with their results. The ratio is a measure of how well the software feels that it arrived at the correct solution for the baseline. The software has a number of possible solutions with different combinations for the solution of the integer ambiguities. It determines a number of solutions, then computes how well each solution fits the data collected by the receiver. In actual fact, it computes the variance of each of the solutions. Each of these solutions is then ranked according to the computed variances. Ranking begins with the lowest variance set as the best, then the second lowest as the second best and so on. The solution ratio represents the ratio of the variance of the second best candidate fixed solution to the variance of the best candidate fixed solution (Wave software user's guide, 1995; Meade, 1998). A higher ratio represents a greater difference between the best and second best solutions. As default, the baseline processor requires that the best solution be at least 1.5 times better than the second best. Only then does it accept the solution as a valid fixed solution. If there is no fixed solution with ratio at least 1.5, the processor gives a float solution (does not resolve ambiguities as integers).

The Wave user's manual recommends that the ratio and variance figures be looked at together. Baselines with a low ratio and high variance are highly suspect. There is a possibility on such lines that the wrong ambiguity candidates were chosen. It may be necessary to reprocess such baselines or reobserve them altogether, for longer periods. If a baseline solution shows a high ratio and high variance, the fixed solution may well be correct. However, there may also be unmodelled errors distorting the solution. It is difficult to specify absolute ranges of acceptable ratios and variances. This is because each of these indicators is a function of the total amount of observations in the raw GPS data files. In this regard, the final decision about the validity of baseline results should only be made after considering

independent loop closures and network adjustment results. A loop closure is a quick way of checking questionable baselines. Each baseline comprises three components; dx, dy and dz that are defined in the earth-centred, earth fixed cartesian coordinate system. In a loop closure, baselines between points are added together until the loop returns to the point of origin. The algebraic sum of these vectors should be near zero. If it is more than several centimetres, there is likely a bad baseline or baselines in the loop.

### 3.5.4 Results

The results described here refer to the Wave baseline processing prior to the network adjustment. These results appear in their entirety as appendix B of this report. The Wave processor could not fix the ambiguities as integers for all process set-ups using broadcast orbits. The exceptions to this rule were the shorter baselines where the effects of unmodelled systematic errors cancelled out in the double differencing process. The baselines in figure 1 range from slightly less than a kilometre (SSLR-SUTH, 760 m), to 1132 km (HARK-PNTG) in length. The increased effects of the atmosphere and orbit bias make it difficult to resolve the ambiguities over longer distances.

In analysing the results of this project, subscripts were used to symbolise corrections that were not being effected and otherwise. For example, the subscript '-trop' (in $L1c_{(-trop)}$) was adopted to signify that the troposphere was not corrected for. Similarly, subscripts '-Ant and NOAA' symbolise the absence of antenna calibration and the use of NOAA antenna tables respectively. Processing GPS data without correcting for tropospheric refraction is not normally done. It was done here purely for the purpose of analysing the amount of error it produces in the computed baseline solution.

Results obtained from broadcast L1c and $L1c_{(-Ant)}$, while mostly exhibiting ionosphere-free float solutions, showed some relatively low variance figures. The general trend showed an increase in the variance with increased distances between stations. This may be attributed mainly to the increased effect of orbit bias over longer distances. Processing on the L1 and $L1c_{(-trop)}$ on the other hand resulted in variances that were way too high. This is because, other than orbit biases, these set-ups did not account for the ionosphere and troposphere respectively. The variances in these two set-ups reached as high as a thousand, more so for

broadcast L1. Overall, process variations using broadcast orbits resulted in poorly computed baselines. This was expected and such work merely served to show the effects of the various errors on the final results. Precise L1c and $L1c_{(NOAA)}$, provided ionosphere-free fixed solutions on all but the shorter lines which were L1 fixed. The computed ratios and variances for precise L1c and $L1c_{(NOAA)}$ were generally acceptable as they showed high ratios with correspondingly low variances. Some outliers were however present despite using precise orbits and correcting for the atmosphere. For instance the baselines MBTG-PETG, MBTG-SBTG, PNTG-SATG, SSLR-SATG and SUTH-PETG showed relatively high variances for $L1c_{(NOAA)}$. This can be attributed to shorter spans of data owing to power loses at some sites (SATG and SBTG) as well as high occurrences of multipath. Furthermore systematic errors due to crustal motion, earth and ocean tide loading could not be corrected for as GPSurvey lacks the capability to do so. These baselines were however adopted together with the rest for further scrutinisation.

Independent loop closures and root mean square height misclosures were considered next. As indicated earlier the processing variations using broadcast orbits were primarily formulated to show the extent of the effects of the various nuisance parameters. Consequently, their results were useless for the most part; in as far as meeting this project's objective was concerned. The use of broadcast orbits resulted in some triangular loop closures that were well over several centimetres. This was especially so for the projects not effecting corrections for the atmosphere (broadcast $L1/L1c_{(-trop)}$). Particular attention was however given to the projects that used precise ephemerides. For these, loop closures were computed for all the triangles shown in figure 1. Of the 22 vector miclosures, the largest amounted to 0.097 m for both precise L1c and $L1c_{(NOAA)}$, over a total distance of 1218 km. This corresponds to a relative error of 0.08 ppm. This is a great result considering that the desired accuracy in heights was 1-2 cm. At 0.08 ppm, this relative error falls well below the 1 ppm relative error limit that commercial software are designed to provide (Merry, 1999).

Root Mean Square (RMS) height misclosures were also computed for all the process variations listed in subsection 3.5.2. The RMS height misclosures were worked out on the basis of the observed height differences between end points of baselines making up a triangular loop. RMS height misclosure for each processing variation was computed as:

$$\text{RMS Height misclosure} = \sqrt{\frac{1}{n}\sum v^2} \qquad 3.3$$

Where n = number of sample

v = observed height misclosure per triangular loop

This computation was aimed at quantifying the amount of influence exerted by atmosphere, orbit bias and antenna phase centre variations on the computed station heights. The bar chart in figure 5 shows the comparison of RMS height misclosures from one process set-up to the next. The actual height misclosures per triangular loop appear in appendix C of this report. In the ideal set-ups (precise L1c and $L1c_{(NOAA)}$), the RMS height misclosure was approximately 3 cm and around 5 cm for broadcast L1c. This ultimately shows that choosing precise ephemerides over broadcast orbits improved the RMS height misclosure by a factor of around 1.5. Ionospheric and tropospheric refraction are major factors limiting the accuracy when processing GPS carrier phase observations. This is especially so for height and scale errors. The solutions of ellipsoidal heights without tropospheric refraction corrections gave a RMS height misclosure of approximately 28 cm. This was the largest RMS height misclosure, and resounding proof of the need to correct for the troposphere when accurate heights with GPS are sought. By comparison to broadcast L1c, a six-fold deterioration in the RMS height misclosure occurred when tropospheric refraction correction was disabled. The solution for ellipsoidal heights without ionospheric refraction corrections on the other hand gave a RMS height misclosure of around 23 cm. This was five times worse than RMS height misclosure for broadcast L1c.

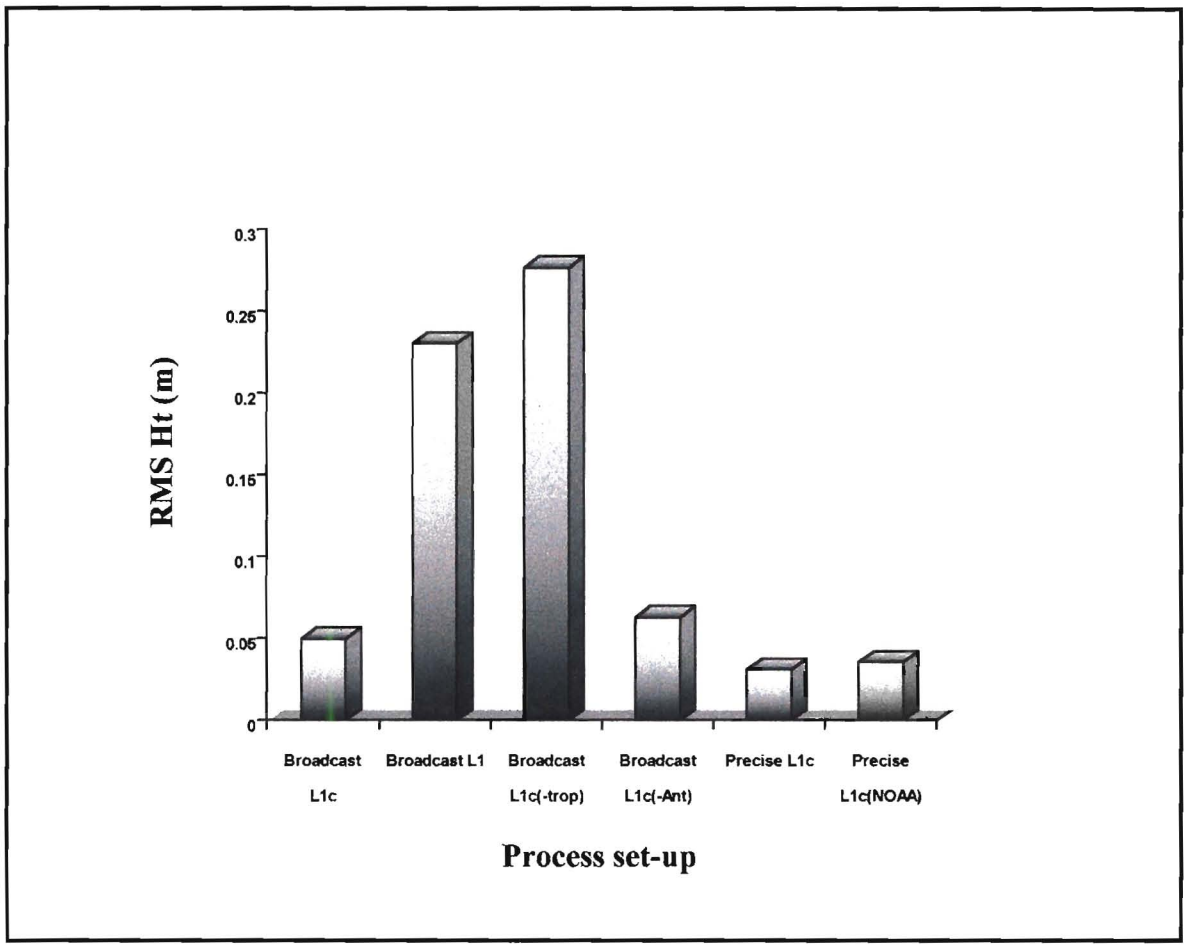


**Figure 5:** RMS Height Misclosure for all processing Variations

# Chapter 4

# NETWORK ADJUSTMENT

## 4.1 INTRODUCTION

Network adjustment is a process that combines survey measurements and determines their relative quality, or strength of fit within the survey network. It provides rigorous mathematical techniques for investigating the accuracy and precision of the observations in a survey network (GPSurvey software user's guide, 1995). Furthermore, it gives unique co-ordinates for each point.

It is inadequate to only compute the GPS vectors and accept them as the final results of the survey. Standard practice demands that these GPS vectors be checked against one another within a network context. This serves to determine if any gross blunders or systematic errors exist in the measurements. As a prime example, erroneous antenna heights will not adversely affect the GPS baseline processing. However, baselines so computed will not fit with other vectors in the network because of the incorrect antenna height values. The network adjustment serves to expose these and other discrepancies.

The baselines produced by Wave and their corresponding covariance matrices were imported into the Trimnet adjustment package. Minimally and fully constrained least squares network adjustments were then carried out. The purpose of the minimally constrained adjustment was to detect the internal precision and consistency of the field observations. The fully constrained network adjustment was then carried out to merge the network in figure 1 into existing fixed control. The reference frame (ITRF) was imposed at the network adjustment stage by fixing or tightly constraining the coordinates of the control stations to define origin (Bock, 1996). In the minimally constrained adjustment, only the coordinates of the point HRAO were held fixed. The fully constrained network adjustment on the other hand, held the points HRAO and SUTH fixed. The coordinates used for both these points were their ITRF97 coordinates, updated to the observational epoch 1998.0 using the ITRF97 velocity field (see tables 1 and 2). Besides HRAO and SUTH, the points HARK and SSLR also had their coordinates published in the ITRF97. These points are however, very close to HRAO and

SUTH respectively. Thus there seemed little point in holding all four points fixed. HARK is only about 2 km from HRAO and its antenna is hoisted on top of a 9 m pole. This raised concerns about the stability of that point. The separation between SSLR and SUTH is less than a kilometre. Besides that, the coordinates of SSLR were determined using only two months worth of SLR data from 1994. Preliminary processing results from Zimba and Merry (1999) also showed that HRAO and SUTH were the better choice for fiducial stations

## 4.2 TRIMNET QUALITY CONTROL

Trimnet's theory of adjustment is based on least square techniques. The program converts the measured GPS vectors from cartesian coordinate differences to azimuth, distance and height difference and then adjusts them in a three-dimensional network adjustment.

The standard error of unit weight (S.E) is the a posteriori indication of the accuracy of the adjusted network. S.E is referred to as the network reference factor in GPSurvey terminology. In high precision surveying it is uncommon for the S.E to be equal or less than 1.0. When it is less than 1.0, then the predicted observational errors were over-estimated. Hence, the network would exceed the precision predicted for it in such a scenario. Conversely, when S.E exceeds 1.0, then part or all of the predicted errors were underestimated (Trimnet Software User's Manual, 1992). In a healthy network (without major blunders or bad vectors), S.E is normally less than 10 on the first run.

The predicted observational errors may be considered probably valid even though S.E exceeds 1.0, provided the S.E passes a probability test called the Chi-square test. The actual subject of the Chi-square test is to reject or accept the hypothesis that the predicted errors have been accurately estimated. When trouble-shooting an inflated S.E, it may be unclear at first which observations or predicted errors with larger-than-predicted residuals are acceptable and otherwise. Classically, inflated S.E are attributed to the presence of systematic errors that are notoriously difficult to isolate. A least squares statistical test designed to aid in identifying observations or predicted errors which are likely candidates for rejection is the Tau test.

In addition to S.E, Trimnet provides errors ellipses and histograms of standardised residuals as auxiliary checks on the quality of the adjusted network. The error ellipses pertain to position. The histograms of standardised residuals give a general overview of how closely the computed residuals conform to the distribution expected of random systems. These histograms are presented as separate horizontal and vertical plots with one final plot combining the two. The critical Tau value (1.0) is also displayed on the histograms as two vertical magenta lines, one on either side of the zero centre line. For each observation another empirical value is computed by dividing the computed residual for the observation by the propagated standard error of the residual. If the empirical value exceeds the critical Tau value, then the observation is flagged as a candidate for rejection. Such candidates are called outliers, as they lie outside the Tau lines in the histogram. The recommended procedure (one followed by this project) when disabling outliers is, one at a time. Then readjust until all outliers have been removed from the network. If the Tau value is greater than 1.0 for any given observation, then that observation is flagged for rejection. Rejection candidates are also flagged with dashed lines separating them from other observations.

All processing variations listed in subsection 3.5.2, except for broadcast L1 and $L1c_{(-trop)}$, had S.E values greater than 10 on the first run. These networks were scrutinised for major blunders and bad vectors but all seemed to be in order. Particular attention was given to the ideal processing set-ups that used precise orbits as the others contained induced systematic errors. A check on their error ellipses and histograms of standardised residuals showed that the baselines were generally acceptable. The inflated values of S.E may be attributed in part to the absence of corrections for crustal motion, earth and ocean tide loading. The network in figure 1 comprised mostly very long baselines and GPSurvey proved to be not entirely ideal for processing this project's data. Furthermore, despite applying corrections for the atmosphere, residual errors due to refraction must have still existed. The statistics of all processing variations were improved by applying a weighting strategy globally. Thereafter, S.E approached unity. Where absolutely necessary some baselines were reprocessed or altogether replaced.

The overall accuracy of the networks was evaluated on the basis of the residuals of the adjusted vectors and standard errors of the adjusted coordinates.

## 4.3 ADJUSTMENT RESULTS

In line with this project's main objective, only the optimal processing results from the six variations are presented here. The rest of the results are summarised in section 4.5. Optimal processing results were obtained from $L1c_{(NOAA)}$. This solution used IGS precise orbits, corrected for the atmosphere and antenna phase centre variations. The antenna calibration table used (as suggested by the subscript 'NOAA') was the updated NOAA table for the Ashtech L1/L2 Rev. B, L-shaped notches antenna.

A total of 32 vectors linking 14 points were included in the network adjustment. Initially a minimally constrained network adjustment holding HRAO fixed to its ITRF97 (1998.0) coordinates was carried out. The resulting standard errors for the heights at the tide gauge sites ranged from 24 mm at MBTG to 37 mm at SATG. The height residuals for the 32 vectors ranged from zero to 61 mm. The largest residual occurred on the baseline SSLR-HARK that is 983 km long. Over this distance the residual translates into a relative error of 0.06 ppm. However, in a relative sense the largest residual was the 6 mm on the baseline TBTG-UCTN which amounted to 0.9 ppm over 6.4 km. Table 3 shows the coordinates and standard errors of all the points included in the network after the minimally constrained network adjustment.

**Table 3:** Final positions - ITRF97(1998.0) reference frame, WGS84 ellipsoid. Network constrained at HRAO (Precise $L1c_{(NOAA)}$).

| Site Code | Latitude ° ′ ″ | Longitude ° ′ ″ | Height (metres) | $\sigma_\phi$ | $\sigma_\lambda$ | $\sigma_h$ |
|---|---|---|---|---|---|---|
| | | | | (metres) | | |
| DNTG | -29 52 27.37082 | 031 03 03.53386 | 31.150 | 0.004 | 0.004 | 0.025 |
| ELTG | -33 01 37.80770 | 027 54 52.91190 | 32.818 | 0.005 | 0.003 | 0.026 |
| HARK | -25 53 13.59275 | 027 42 27.92815 | 1555.406 | 0.001 | 0.001 | 0.009 |
| HRAO | -25 53 24.38254 | 027 41 13.12495 | 1414.196 | 0.000 | 0.000 | 0.000 |
| MBTG | -34 10 46.60641 | 022 08 49.71029 | 33.396 | 0.004 | 0.004 | 0.024 |
| PETG | -33 57 35.28049 | 025 37 45.48751 | 31.640 | 0.005 | 0.004 | 0.033 |
| PNTG | -29 15 24.64192 | 016 52 02.52021 | 34.981 | 0.005 | 0.006 | 0.034 |
| RBTG | -28 47 45.33570 | 032 04 42.47814 | 28.168 | 0.004 | 0.005 | 0.026 |
| SATG | -33 01 24.77145 | 017 57 37.55722 | 33.191 | 0.006 | 0.005 | 0.037 |
| SBTG | -34 11 17.45526 | 018 26 22.64512 | 33.418 | 0.004 | 0.004 | 0.025 |
| SSLR | -32 22 45.06013 | 020 48 08.95351 | 1729.859 | 0.003 | 0.003 | 0.019 |
| SUTH | -32 22 48.76327 | 020 48 37.66045 | 1799.754 | 0.003 | 0.003 | 0.018 |
| TBTG | -33 54 19.88009 | 018 26 00.55237 | 33.058 | 0.004 | 0.004 | 0.028 |
| UCTN | -33 57 30.64337 | 018 27 36.68648 | 165.481 | 0.005 | 0.005 | 0.032 |

In the fully constrained network adjustment, HRAO and SUTH fiducial stations were held fixed to their ITRF97 epoch 1998.0 coordinates. SUTH is closer to the Western Cape tide gauges than HRAO. Thus, the fixation of SUTH as a control point caused the standard errors of the heights at MBTG and SATG to improve to 17 mm and 33 mm respectively. However, in accordance with expectations, some residuals increased in magnitude due to greater constraints. The largest height residual was now the 64 mm on the line HRAO-SSLR (982 km). Table 4 shows the coordinates and standard errors of all the 14 points after the fully constrained network adjustment. The large residuals on vectors between Hartebeesthoek and Sutherland indicate that the GPS data were not entirely consistent with the coordinates of the fixed points.

**Table 4:** Final positions - ITRF97(1998.0) reference frame, WGS84 ellipsoid. Network constrained at HRAO and SUTH (Precise $L1c_{(NOAA)}$).

| Site Code | Latitude ° ′ ″ | Longitude ° ′ ″ | Height (metres) | $\sigma_\phi$ | $\sigma_\lambda$ | $\sigma_h$ |
|---|---|---|---|---|---|---|
| | | | | (metres) | | |
| DNTG | -29 52 27.37052 | 031 03 03.53373 | 31.152 | 0.005 | 0.004 | 0.025 |
| ELTG | -33 01 37.80727 | 027 54 52.91203 | 32.823 | 0.005 | 0.003 | 0.026 |
| HARK | -25 53 13.59275 | 027 42 27.92815 | 1555.409 | 0.001 | 0.001 | 0.009 |
| HRAO | -25 53 24.38254 | 027 41 13.12495 | 1414.196 | 0.000 | 0.000 | 0.000 |
| MBTG | -34 10 46.60599 | 022 08 49.71081 | 33.414 | 0.003 | 0.002 | 0.017 |
| PETG | -33 57 35.28003 | 025 37 45.48782 | 31.649 | 0.005 | 0.005 | 0.032 |
| PNTG | -29 15 24.64190 | 016 52 02.52097 | 34.994 | 0.005 | 0.006 | 0.032 |
| RBTG | -28 47 45.33546 | 032 04 42.47793 | 28.169 | 0.004 | 0.005 | 0.026 |
| SATG | -33 01 24.77116 | 017 57 37.55799 | 33.208 | 0.005 | 0.004 | 0.033 |
| SBTG | -34 11 17.45490 | 018 26 22.64589 | 33.436 | 0.003 | 0.003 | 0.019 |
| SSLR | -32 22 45.05984 | 020 48 08.95408 | 1729.877 | 0.001 | 0.001 | 0.009 |
| SUTH | -32 22 48.76298 | 020 48 37.66102 | 1799.773 | 0.000 | 0.000 | 0.000 |
| TBTG | -33 54 19.87974 | 018 26 00.55313 | 33.076 | 0.003 | 0.003 | 0.022 |
| UCTN | -33 57 30.64301 | 018 27 36.68724 | 165.499 | 0.004 | 0.004 | 0.028 |

## 4.4 COMPARISONS

The same data were used in both adjustments. The only difference being, other than HRAO, the coordinates of SUTH were also fixed to their ITRF97 (1998.0) values in the second adjustment. The discrepancy in the height of SUTH between the two adjustments was 19 mm. The discrepancies in position were even smaller, with a latitude difference of 10 mm and a longitude difference of 15 mm. Similar but smaller height discrepancies were noted for the tide gauge stations. The height discrepancy even fell below 10 mm on the south and east coasts. It was as little as a millimetre for RBTG and 2 mm for DNTG. Considering the precision of the coordinates and that of the measurements, the 19 mm discrepancy at SUTH is not significant at the $2\sigma$ (95 %) confidence level.

The horizontal discrepancies of SUTH between the two adjustments (10 mm in $\phi$ and 15 mm in $\lambda$) are not consistent with the standard deviations (3 mm in $\phi$ and $\lambda$) computed by Trimnet. This disparity can be attributed to the accuracy of the fixed point HRAO. Both HRAO and SUTH have positional accuracy of the order of 10-15 mm in their ITRF97 published positions (http://lareg.ensg.ign.fr/ITRF/ITRF97). Thus the coordinate standard deviations of the fixed point tended to manifest themselves in the adjustment results despite HRAO's sigmas being set to zero.

## 4.5 RESULTS SUMMARY

This section presents a condensed form of the Trimnet processing results for the tide gauge sites for all the processing variations listed in 3.5.2. Only the minimally constrained adjustment results are presented here. This is because the main objective was to show how the results from the various processing variations compare to one another. The results from the fully constrained network adjustment showed a similar trend relative to the minimally constrained adjustment. The only differences being that the standard errors improved slightly in moving from minimum to full constraints. Correspondingly, the residuals deteriorated in the fully constrained network adjustment owing to greater constraints. The general trend in both the minimally and fully constrained adjustments was a marked deterioration of standard errors and residuals with increased systematic errors. Table 5 shows the ranges of height standard errors and residuals at the tide gauges (for all processing set-ups).

The effects of systematic errors such as orbit bias, atmospheric refraction and antenna phase centre variations propagate into the computed position. The troposphere and ionosphere are especially notorious for limiting the accuracy of the height component and introducing scale errors respectively. As shown in table 5, tropospheric refraction correction can eliminate a systematic height bias and thus improve height estimation almost two fold. Similarly, correcting for the ionosphere improves height estimation by a factor of about three. The effects of systematic errors on this project's results are discussed in finer details in the next chapter.

**Table 5:** Height Standard errors and Residuals for all processing set-ups (for the minimally constrained network adjustment).

| **Processing set-up** | **Standard error** $\sigma_h$ **(mm)** | **Residuals (mm)** |
|---|---|---|
| **Broadcast L1c:** Broadcast orbits and all corrections | 42-59 | 0-79 |
| **Broadcast L1:** Broadcast orbits minus ionosphere | 132-189 | 0-499 |
| **Broadcast L1c** $_{(-trop)}$**:** Broadcast orbits minus troposphere | 82-105 | 0-650 |
| **Broadcast L1c** $_{(-Ant)}$**:** Broadcast orbits minus antenna calibration | 40-55 | 1-107 |
| **Precise L1c:** Precise orbits and GPSurvey antenna table | 24-39 | 0-54 |
| **Precise L1c** $_{(NOAA)}$**:** Precise orbits and NOAA antenna table | 24-37 | 0-61 |

## 4.6 FURTHER ADJUSTMENT OF PRECISE L1c $_{(NOAA)}$

In order to validate the adjustment results obtained with Trimnet, the vectors output from GPSurvey were re-adjusted independently using the Columbus package (version 1.03). Columbus is a one-, two- and three-dimensional geodetic network adjustment, network pre-analysis and coordinate transformation software package (Columbus user manual, 1996). It is a versatile package and will allow the user to extract GPS baseline data from selected GPS receiver manufacturers' post-processing software. It can handle GPS data from Ashtech, Leica, Motorola and Trimble. It extracts GPS baseline data from the output files produced by the various post-processing software and writes these to an ASCII (text) file which it can load directly. A further provision is that the output data (the coordinate differences and covariances) can easily be uploaded into Columbus via input menus. This feature was utilized in the upload of the baselines produced by Wave and their corresponding covariance matrices into the Columbus adjustment package. Minimally and fully constrained network adjustments were subsequently carried out.

## 4.7 RESULTS AND COMPARISONS

In the minimally constrained adjustment (with only HRAO fixed) the resulting standard errors for the heights ranged from 22 mm at MBTG to 35 mm at SATG. This result compare very well with that obtained with Trimnet. The standard errors for the heights from Columbus were 2 mm better than Trimnet's for both points (MBTG and SATG). The average difference in standard errors of the heights between Columbus and Trimnet results was 2 mm (see table 6). The precision estimates obtained with Columbus were better than Trimnet's.

Overall, the average discrepancy in latitude, longitude and height at the tide gauges (between the two minimal adjustments in Columbus and Trimnet) were 4 mm, 3 mm and 5 mm, respectively. Details of discrepancy at each tide gauge reference station appear in table 6.

**Table 6:** Comparison of results between the minimally constrained network adjustments from Trimnet and Columbus

| Station | Discrepancies between Trimnet and Columbus results | | | |
|---|---|---|---|---|
| | $\Delta\sigma_h$ (m) | $\Delta\phi$ (m) | $\Delta\lambda$ (m) | $\Delta h$ (m) |
| DNTG | 0.002 | 0.001 | 0.000 | 0.004 |
| ELTG | 0.002 | 0.004 | 0.004 | 0.013 |
| MBTG | 0.002 | 0.003 | 0.004 | 0.000 |
| PETG | 0.004 | 0.002 | 0.005 | 0.019 |
| PNTG | 0.003 | 0.008 | 0.001 | 0.000 |
| RBTG | 0.002 | 0.002 | 0.000 | 0.004 |
| SATG | 0.002 | 0.006 | 0.003 | 0.009 |
| SBTG | 0.001 | 0.005 | 0.005 | 0.003 |
| TBTG | 0.002 | 0.006 | 0.004 | 0.001 |
| UCTN | 0.002 | 0.005 | 0.004 | 0.001 |
| **MEAN** | **0.002** | **0.004** | **0.003** | **0.005** |

The fully constrained network adjustment with Columbus yielded standard errors for the heights ranging from 18 mm at MBTG to 36 mm at SATG. Here too (as with the Trimnet results) the fixation of SUTH as a control point improved the standard errors of western Cape tide gauges. By comparison to Trimnet results, the standard errors of heights at MBTG and SATG deteriorated by 1 mm and 3 mm, respectively. Generally, the standard errors of the heights derived with Columbus were on average 1 mm worse than Trimnet's. The mean discrepancy in latitude, longitude and height between Columbus and Trimnet results for the fully constrained adjustments were 4 mm, 2 mm and 12mm, respectively. For actual discrepancies at each tide gauge station see table 7.

The results obtained from Columbus clearly agree with and validate the results from Trimnet. Full lists of coordinates and their corresponding standard errors from the

minimally and fully constrained adjustments with Columbus appear in tables E.13 and E.14 in appendix E.

**Table 7:** Comparison of results between the fully constrained network adjustments from Trimnet and Columbus

| Station | Discrepancies between Trimnet and Columbus results | | | |
|---|---|---|---|---|
| | $\Delta\sigma_h$ (m) | $\Delta\phi$ (m) | $\Delta\lambda$ (m) | $\Delta h$ (m) |
| DNTG | 0.002 | 0.007 | 0.003 | 0.007 |
| ELTG | 0.000 | 0.008 | 0.002 | 0.027 |
| MBTG | 0.001 | 0.002 | 0.002 | 0.005 |
| PETG | 0.001 | 0.005 | 0.000 | 0.034 |
| PNTG | 0.001 | 0.001 | 0.005 | 0.013 |
| RBTG | 0.001 | 0.005 | 0.006 | 0.007 |
| SATG | 0.003 | 0.002 | 0.002 | 0.016 |
| SBTG | 0.002 | 0.004 | 0.001 | 0.001 |
| TBTG | 0.002 | 0.004 | 0.001 | 0.005 |
| UCTN | 0.002 | 0.003 | 0.002 | 0.003 |
| **MEAN** | **0.001** | **0.004** | **0.002** | **0.012** |

# Chapter 5

# RESULTS AND ANALYSIS

## 5.1 INTRODUCTION

This section analyses the magnitude by which corrections for the various nuisance parameters eliminate systematic biases in the solution for coordinates. This was achieved by comparing results from the different processing set-ups listed in 3.5.2. For example, atmospheric refraction was analysed by comparing results from a set-up applying all corrections to set-ups not correcting for the atmosphere. Similarly, the influence of orbit bias was investigated by comparing results from processing with broadcast orbits to processing with precise orbits. The effects of antenna phase centre variations were investigated in two ways. The first compared results from processing with antenna tables to results from processing without antenna calibration tables. The second comparison, besides analysing phase centre variations also looked at the effect of using different calibration tables for the same antenna type. The basis of all comparisons was the minimally adjusted coordinates of each processing variation.

## 5.2 THE IONOSPHERIC REFRACTION EFFECT

The ionosphere has a tendency of inducing scale biases into the computed and adjusted results when it is unmodelled. Since a phase velocity governs carrier phases as they propagate through the ionosphere, a phase advance occurs. Consequently, phase measurements are measured too short compared to the geometric distance between satellite and receiver (in the ionosphere). This results in a negative error whose numerical value is given by equation 2.2 (Leick, 1995; Merry, 1995).

The ionospheric effect was thoroughly analysed by comparing results from processing this project's data with and without ionospheric refraction correction. This was achieved by initially processing the data on the L1 ionospherically free double difference observable. Thereafter, the same data was reprocessed on the L1-without however correcting for the ionosphere. Both sets of results were later subjected to a network adjustment holding HRAO fixed. The resultant adjusted coordinates were then used to compute a scale factor between

the two sets of results. The scale factor was initially computed using XForm (version 4.1) as part of the datum transformation parameters between the two sets of coordinates. XForm is essentially a transformation package that compares two sets of coordinates before working out transformation parameters between them to enable a best fit. Besides the scale factor, XForm also works out translations and rotations. The procedure followed in this investigation initially worked out translations and scale factor. Thereafter, a computation of translations, scale factor and rotations followed. The reason rotations were left out of the initial computation is that rotations are directly linked to the shifts. Thus including rotations tends to increase these shifts and their respective accuracy. Ionospheric scale bias was also analysed on the basis of computed baseline lengths obtained from processing with and without ionospheric refraction correction. The discrepancies in baseline lengths were translated into a scale factor signifying the ionospheric refraction error. Baselines less than 50 km long were not considered in this analysis as these would only lead to an erroneous scale factor. Over short separations ionospheric refraction is highly spatially coherent and is considerably mitigated by the double differencing technique. Hence, large scale errors on rather short lines may be attributed to error sources other than the ionosphere. For instance, an antenna centred slightly off the actual reference mark may contribute to a relatively large scale error.

Further to all of the above, RMS ellipsoidal height discrepancy was computed. The standard errors of both sets of coordinates were also compared. This was done to illustrate the magnitude by which ionospheric refraction correction improved the precision of the computed ellipsoidal heights. Additional analysis was carried out to determine whether the effect of ionospheric refraction on the computed heights was:

- A scale error
- A function of distance from the fixed point (HRAO)
- A function of the height differences between the fixed point and the tide gauge stations
- A function of the inter-station height differences

A series of graphs were plotted to aid in finding solutions to the scenarios described above.

### 5.2.1 Translations and Scale factor

The adjusted coordinates obtained from processing with and without ionosphere correction were imported into XForm to determine the datum transformation parameters. Translations and scale factor was determined first. The source datum coordinates used in the transformation were the adjusted coordinates without ionospheric refraction correction. Conversely, the target datum coordinates were the adjusted coordinates of the processing variation that corrected for the ionosphere. The resulting translations and scale factor are shown in table 8.

**Table 8:** Translations and Scale factor due to ionospheric refraction

| | |
|---|---|
| **X-shift:** | -2.348 ± 0.206 metres |
| **Y-shift:** | -1.224 ± 0.091 metres |
| **Z-shift:** | 1.236 ± 0.138 metres |
| **Scale factor:** | 1.0000004 ± 0.0000000 |
| | 0.4318 ppm ± 0.0411 ppm |
| **RMS Error:** | 0.0888 metres |

The input coordinates, datum transformation parameters and residuals appear in greater detail in appendix D. The computed shifts (see table 8) were relatively small although the X-shift was approximately two times larger than the Y- and Z-shift. The X-shift is greatest because in South Africa X is correlated with height (this is illustrated in the table on page 99 giving XYZ and $\phi\lambda h$ residuals). The scale factor was found to be less than half a part per million at 0.4318 ppm. This is a relatively low value.

### 5.2.2 Translations, Scale and Rotations

The computation of datum transformation parameters for the comparison between L1c/L1 was extended to include rotations. Again XForm was used and the resulting translations, scale factor and rotations are shown in table 9.

**Table 9:** Translations, Scale factor and Rotations due to ionospheric refraction

| | |
|---|---|
| **X-shift:** | -1.047 ± 0.343 metres |
| **Y-shift:** | -1.984 ± 0.248 metres |
| **Z-shift:** | 2.697 ± 0.406 metres |
| **Scale factor:** | 1.0000004 ± 0.0000000 |
| | 0.4318 ppm ± 0.0332 ppm |
| **X-rotation:** | -0.00608 ± 0.00750 seconds |
| **Y-rotation:** | -0.06323 ± 0.01492 seconds |
| **Z-rotation:** | -0.02748 ± 0.00914 seconds |
| **RMS Error:** | 0.0716 metres |

The complete set of results for these datum transformation parameters is listed in appendix D. The introduction of rotations increased the magnitude of the shifts and their respective accuracy. This was expected as the rotations are directly correlated to the shifts and tend to increase the values of the shifts and their corresponding accuracy. As with the results in 5.2.1, the shifts were relatively minor although the Z-shift was comparatively larger than the other two. The scale factor stayed unchanged at 0.4318 ppm. The rotations in all directions were relatively small and only measured as fractions of seconds. The Y-rotation was however, relatively large in comparison to the X- and Z-rotations. RMS error decreased to 0.0716 m following the inclusion of rotations.

### 5.2.3 Scale factor from L1c/L1 Distance Discrepancies

Further to the analysis with XForm, the discrepancies in baseline lengths between L1c and L1 were converted into a scale factor representing ionospheric refraction error. The scale factor per baseline was computed by dividing each baseline's discrepancy by its length measured to the nearest hundredth of a metre. Thereafter, average scale factor for the entire network was worked out (see table 10). Average scale factor due to ionospheric refraction was computed as 0.4702 ppm. This figure compared relatively well with the scale factor computed by XForm. In fact, the difference between the two scale factors was a meagre 0.04 ppm, which is quite insignificant. The scatter of scale factor about baseline lengths is shown in figure 6.

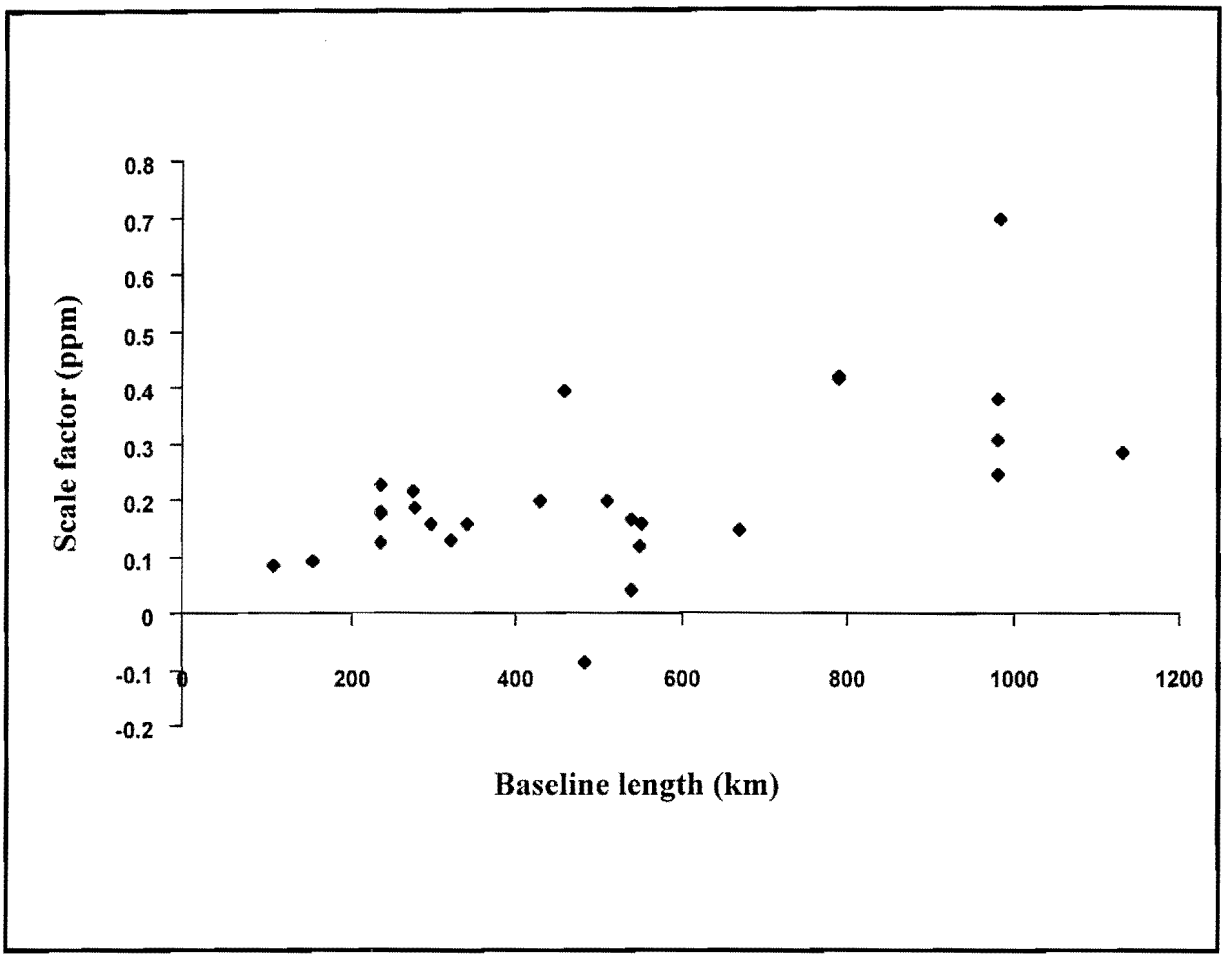


**Figure 6:** Scale factor scatter about baseline length

Table 10 below shows particular baseline details that were used to compute scale factor for each baseline.

**Table 10:** Scale factor from L1c/L1 Distance Discrepancies

| BASELINE | L1c DISTANCE (m) | L1 DISTANCE (m) | DISCREPANCY (L1c-L1) (m) | SCALE FACTOR (ppm) | DISTANCE (km) |
|---|---|---|---|---|---|
| DNTG-ELTG | 459278.272 | 459277.880 | 0.392 | 0.853472676 | 459.3 |
| DNTG-HARK | 550825.253 | 550825.136 | 0.117 | 0.212418301 | 550.8 |
| DNTG-HRAO | 551773.672 | 551773.514 | 0.158 | 0.286335629 | 551.8 |
| ENTG-HRAO | 790988.360 | 790987.947 | 0.413 | 0.522123894 | 791.0 |
| HARK-ELTG | 791275.305 | 791274.888 | 0.417 | 0.526980917 | 791.3 |
| HARK-PNTG | 1131787.599 | 1131787.316 | 0.283 | 0.250044177 | 1131.8 |
| HARK-RBTG | 539216.567 | 539216.527 | 0.040 | 0.074183976 | 539.2 |
| HARK-SUTH | 982843.347 | 982843.041 | 0.306 | 0.311355311 | 982.8 |
| HRAO-RBTG | 540656.058 | 540655.893 | 0.165 | 0.305159978 | 540.7 |
| MBTG-PETG | 322310.539 | 322310.411 | 0.128 | 0.397145516 | 322.3 |
| MBTG-SBTG | 341721.872 | 341721.715 | 0.157 | 0.459467369 | 341.7 |
| PETG-ELTG | 236211.130 | 236210.953 | 0.177 | 0.749364945 | 236.2 |
| PNTG-SATG | 430345.147 | 430344.951 | 0.196 | 0.455496165 | 430.3 |
| RBTG-DNTG | 155702.018 | 155701.928 | 0.090 | 0.578034682 | 155.7 |
| SSLR-HARK | 983283.970 | 983283.275 | 0.695 | 0.706803620 | 983.3 |
| SSLR-HRAO | 981652.174 | 981651.932 | 0.242 | 0.246536267 | 981.6 |
| SSLR-MBTG | 235741.315 | 235741.088 | 0.227 | 0.963088672 | 235.7 |
| SSLR-MBTG | 235741.291 | 235741.167 | 0.124 | 0.526092490 | 235.7 |
| SSLR-PNTG | 511324.744 | 511324.548 | 0.196 | 0.383336593 | 511.3 |
| SSLR-SATG | 275916.002 | 275915.789 | 0.213 | 0.772018847 | 275.9 |
| SSLR-SBTG | 297828.677 | 297828.519 | 0.158 | 0.530557421 | 297.8 |
| SSLR-TBTG | 278416.700 | 278416.514 | 0.186 | 0.668103448 | 278.4 |
| SUTH-ELTG | 669636.058 | 669635.913 | 0.145 | 0.216547192 | 669.6 |
| SUTH-HRAO | 981212.321 | 981211.943 | 0.378 | 0.385242560 | 981.2 |
| SUTH-MBTG | 235252.124 | 235251.951 | 0.173 | 0.735544218 | 235.2 |
| SUTH-PETG | 482295.332 | 482295.421 | -0.089 | -0.184532449 | 482.3 |
| TBTG-SATG | 107250.986 | 107250.904 | 0.082 | 0.764925373 | 107.2 |
| | | AVERAGE | 0.214 | 0.470216585 | |

### 5.2.4 Comparison of Height errors between L1c and L1

The solutions for ellipsoidal heights obtained from the minimally constrained network adjustments of broadcast L1c and L1 were compared. The following analyses used L1-L1c heights to arrive at height discrepancies, as broadcast L1 heights were estimated higher than broadcast L1c heights. The average difference in height was found to be 142 mm and the RMS height discrepancy was 194 mm. The maximum height shift was the 460 mm at DNTG. Furthermore, a comparison of the standard errors of heights for the L1c and L1 was made.

The results of this comparison showed that applying a correction for the ionosphere improved the precision of the heights by about three times. A similar improvement was noticed for the horizontal positions. Figure 7 below shows a graphic representation of how the L1c standard errors of heights compared to those for the L1.

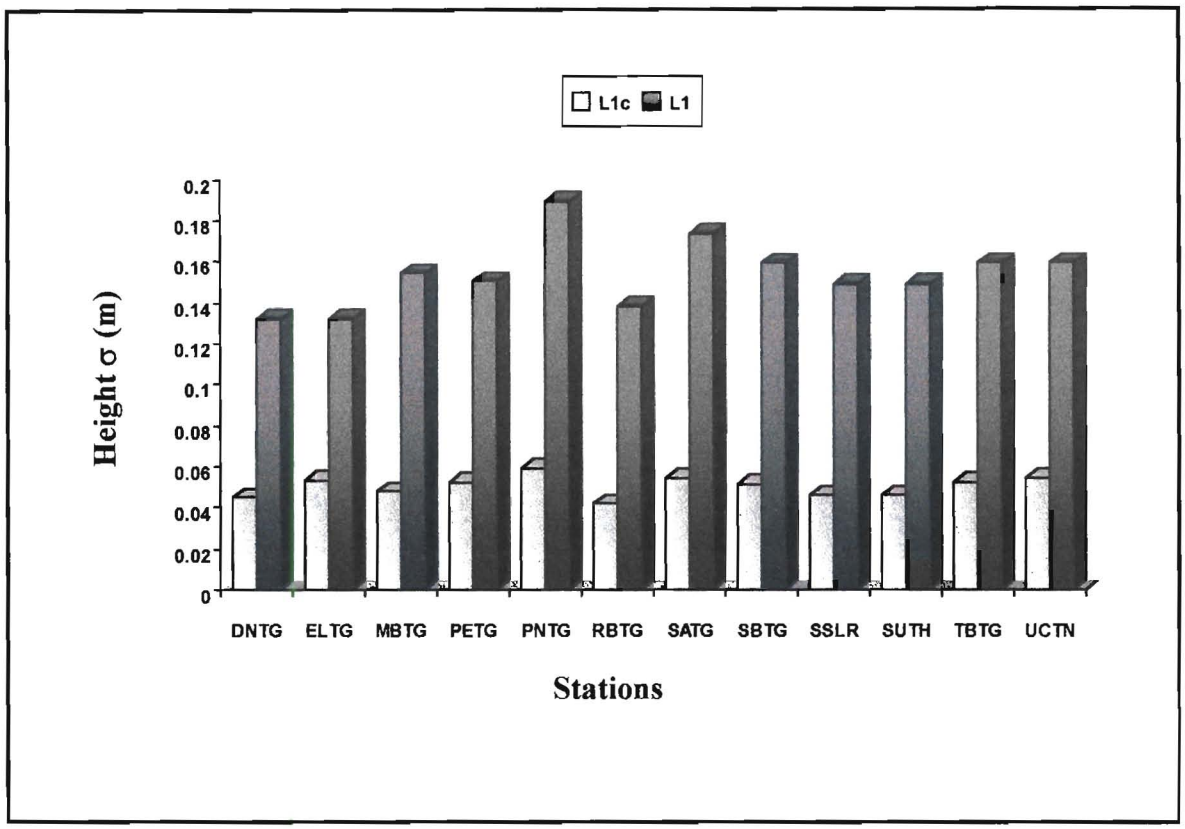


**Figure 7:** Standard errors of heights for broadcast L1c/L1

HRAO was not included as it was held fixed in the network adjustment. HARK on the other hand was excluded because it is too close to HRAO for ionospheric refraction to register its effect there. The standard error of height at HARK was rather over optimistic under the circumstances as it was almost devoid of any refraction errors.

### 5.2.5 Correlation analysis

The discrepancies in height between broadcast L1 and L1c were plotted against distance from the fixed point (HRAO) to the tide gauge sites. This was to determine whether the effect of the ionosphere on the estimated heights was a function of the distance from the fixed point. Figure 8 is an illustration in aid of this analysis.

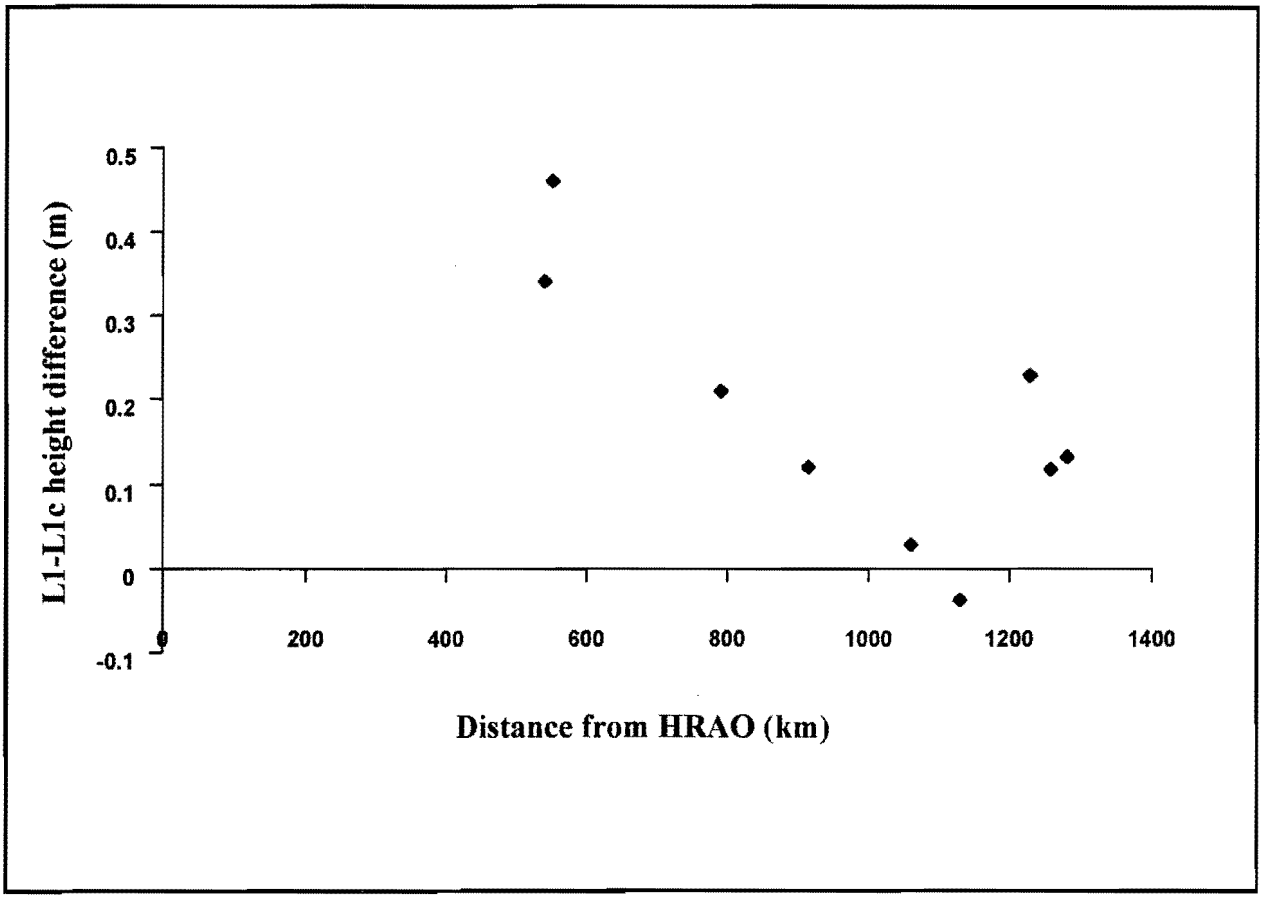


**Figure 8:** Discrepancies in height (L1-L1c) versus distance from fixed point

The graph in figure 8 shows that the ionosphere does not appear to introduce a scale error in heights, contrary to its effect on baseline lengths. What the graph depicts is a negative correlation between the L1-L1c height discrepancies and distance from the fixed point to the tide gauges. The correlation coefficient of these two variables was computed and found to be -0.553. This indicated a moderate negative correlation between the L1-L1c height discrepancies with distance from HRAO to the tide gauge stations. Figure 8 clearly supports this observation in that the L1-L1c height discrepancies tended to decrease with increased distance from HRAO. What then are the implications of this observation? and why should the ionospheric refraction effect on heights be smaller over longer distances. Unfortunately, most literature on the ionosphere is silent about how the height error is propagated with increased distance between survey stations. This thesis recommends a research topic in the future that will investigate the ionospheric effect on heights in relation to distance from the fixed point.

The proportion of a perfect linear relationship that two variables have is indicated by the square of their correlation coefficient (Alreck and Settle, 1995). The square of the correlation coefficient is called the coefficient of determination. In the instance above the coefficient of determination was found to be 0.31. This means that the two variables were 31% as closely related as they would have been if they were perfectly associated with one another.

Height differences between HRAO (the fixed point) and the tide gauge stations were also computed. These were subsequently plotted against the L1-L1c height discrepancies. This was to ascertain whether the height discrepancies were a function of height differences between the fixed point and the tide gauges. Figure 9 below shows how the L1-L1c height discrepancies related to the height differences between HRAO and the Tide gauge stations.

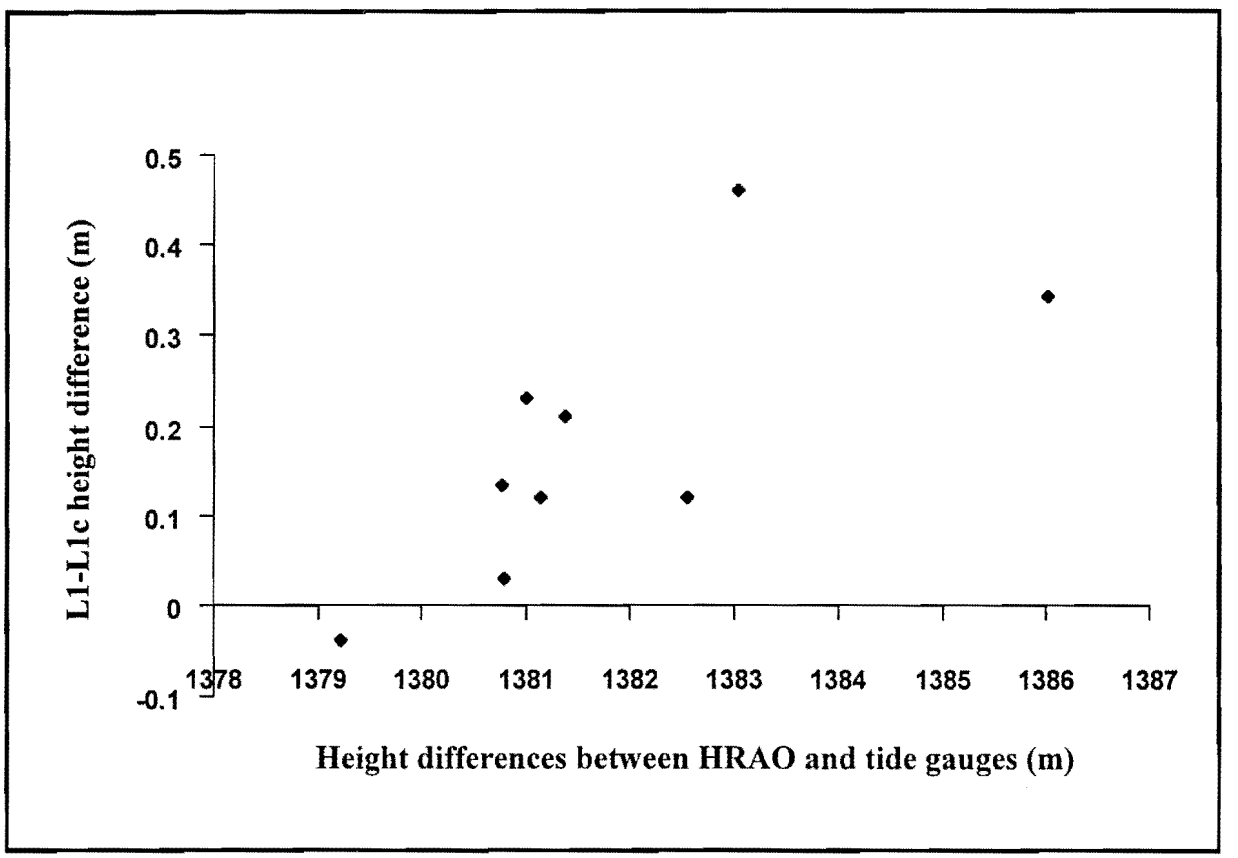


**Figure 9:** L1-L1c Height discrepancies versus height differences between HRAO and tide gauge stations

With reference to figure 9, the correlation between the L1-L1c height discrepancies and the HRAO-tide gauge height differences was a strong positive one. This was reaffirmed by the computed correlation coefficient for the two entities. This was found to be 0.732, thus

implying a strong positive correlation. The coefficient of determination was computed as 0.536. Hence, these two variables were 54% as closely related as they would have been if they were perfectly associated with one another.

Lastly, the inter-station height differences were computed. This was to investigate the degree of correlation between inter-station height differences with L1-L1c inter-station height discrepancies. Subtracting the L1-L1c height discrepancy of one station from the next gave the inter-station height discrepancies. For example, the L1-L1c height discrepancy for Durban (DNTG) was 0.460 m and 0.341 m for Richard's bay (RBTG). It follows therefore that the inter-station height discrepancy for the baseline RBTG-DNTG is -0.119 m.

A weak negative correlation was observed between the inter-station height differences and L1-L1c inter-station height discrepancies. In line with this observation a correlation coefficient of -0.367 was obtained. This worked out into a coefficient of determination of 0.135. Therefore, the two variables were only 13% as closely related as they would have been if they were perfectly associated with one another.

## 5.3 THE TROPOSPHERIC REFRACTION EFFECT

The troposphere has earned the reputation of being the most notorious error source in present day geodetic positioning with GPS. Orbit biases are no longer considered an error source of great concern with the availability of IGS precise orbits.

In a relative sense, tropospheric refraction primarily produces biased station heights and produces scale biases of the estimated baseline lengths in an absolute sense. Height biases in excess of one metre are obtained when the tropospheric effect is unmodelled (Collins and Langley, 1999). Furthermore, the tropospheric effect worsens with increased distance between the stations. This made tropospheric refraction a major concern in the processing carried out in this project as the baselines were up to 1132 km long. As was the case with the ionosphere, the tropospheric effect was analysed by way of comparisons. Results obtained from processing with tropospheric refraction correction (broadcast L1c) were compared to those obtained without such a correction (broadcast $L1c_{(-trop)}$ ). Processing GPS data without correcting for the troposphere is not normally done. It was done here purely for the purpose of analysis. The basis of the comparison was the minimally adjusted coordinates of

broadcast L1c and L1c$_{(-trop)}$. These sets of coordinates were imported into XForm for the computation of datum transformation parameters. Further to the analysis with XForm, the RMS ellipsoidal height discrepancy was computed. The standard errors of heights of both sets of coordinates were also compared. Finally, additional analysis was carried out to investigate the correlation of the height errors with the following:

- Distance from the fixed point (HRAO)
- HRAO-tide gauge station height differences and
- Inter-station height differences

### 5.3.1 Translations and Scale factor

The minimally adjusted coordinates of broadcast L1c and broadcast L1c$_{(-trop)}$ were imported into XForm. In the first instance, translations and scale factor were computed. The results obtained for the translations and scale factor are given in table 11. The entire set of results for datum transformation parameters for L1c/ L1c$_{(-trop)}$ appears in appendix D.

**Table 11:** Translations and Scale factor due to tropospheric refraction

| | |
|---|---|
| **X-shift:** | 5.335 ± 0.780 metres |
| **Y-shift:** | 2.821 ± 0.346 metres |
| **Z-shift:** | -2.869 ± 0.523 metres |
| **Scale factor:** | 0.9999988 ± 0.0000002 |
| | -1.1535 ppm ± 0.1558 ppm |
| **RMS Error:** | 0.3365 metres |

The resulting shifts (see table 11) were relatively small, even though the X-shift was about twice the size of the Y- and Z-shifts. The scale factor was -1.1535 ppm, which was quite significant in comparison to the scale factor obtained for the ionospheric effect. Tropospheric zenith delay estimation and antenna phase centre variations correction are tied into the tropospheric refraction correction. As such these errors become more pronounced in the

absence of a correction for tropospheric refraction. The net effect is that the tropospheric scale height parameter and the height will be in significant error.

### 5.3.2 Translations, Scale and Rotations

Rotations were added to the computations of datum transformation parameters for the comparison between L1c/ $L1c_{(-trop)}$. Table 12 below is a summary of the results obtained while the entire set of results for this computation appears in appendix D.

**Table 12:** Translations, Scale and Rotations due to tropospheric refraction

| | |
|---|---|
| **X-shift:** | 9.168 ± 1.502 metres |
| **Y-shift:** | 1.608 ± 1.088 metres |
| **Z-shift:** | 2.106 ± 1.777 metres |
| **Scale factor:** | 0.9999988 ± 0.0000001 |
| | -1.1535 ppm ± 0.1452 ppm |
| **X-rotation:** | 0.03721 ± 0.03283 seconds |
| **Y-rotation:** | -0.19030 ± 0.06534 seconds |
| **Z-rotation:** | -0.07507 ± 0.04003 seconds |
| **RMS Error:** | 0.3136 metres |

The inclusion of rotations once again increased the magnitude of the shifts and their corresponding accuracy. The shifts were however still relatively small, although the X-shift was significantly larger than the other two. The scale factor stayed unchanged at -1.1535 ppm. The rotations were relatively small and were only fractions of seconds. The Y-rotation was comparatively larger than the X- and Z-rotations. The RMS error was 0.3136 m, after the inclusion of rotations. This represents a 13 cm decrease from the RMS error computed in 5.3.1.

### 5.3.3 Comparison of Height errors between broadcast L1c and L1c $_{(-trop)}$

The solution for ellipsoidal heights obtained from the minimally constrained network adjustments of L1c and L1c $_{(-trop)}$ were compared. The computation of height discrepancies used L1c $_{(-trop)}$-L1c heights throughout this analysis as broadcast L1c $_{(-trop)}$ heights were estimated higher than broadcast L1c heights. The average difference in ellipsoidal height was 81 cm and the RMS height discrepancy was 97 cm. The maximum height shift was the 139 cm at DNTG. These discrepancies were quite large and clearly indicated the importance of correcting for tropospheric refraction where accurate heights are sought. A comparison of the standard errors of heights for the L1c and L1c $_{(-trop)}$ was also made. The results of that comparison revealed that applying a correction for the troposphere improved the precision estimates of ellipsoidal heights by about two fold. A figurative representation of the comparison of standard errors of heights for L1c/ L1c $_{(-trop)}$ is given in figure 10. HRAO was again not included in this analysis because it was held fixed. HARK was left out on account of its proximity to HRAO. Its standard errors in both height and position were clearly devoid of refraction errors due to the short inter-station distance between it and HRAO.

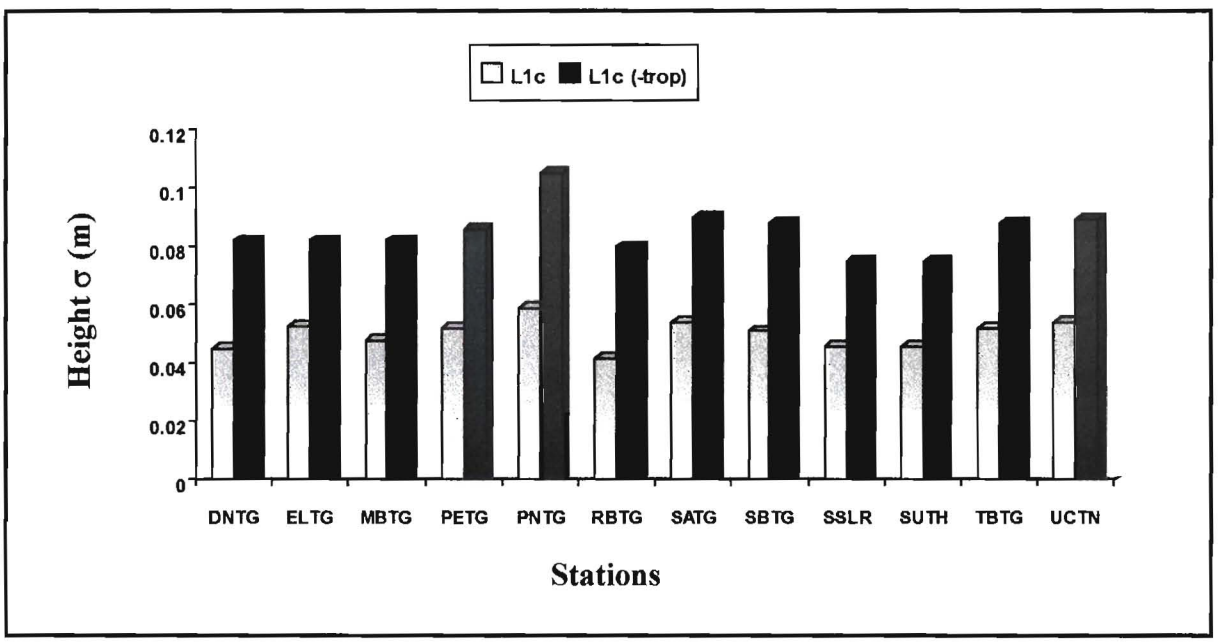


**Figure 10:** Standard errors of heights for broadcast L1c/ L1c $_{(-trop)}$

### 5.3.4 Correlation analysis

Height discrepancies between broadcast $L1c_{(-trop)}$ and L1c were plotted against distance from the fixed point (HRAO) to the tide gauge stations. This was to investigate whether the effect of the troposphere on the estimated heights was a function of distance from the fixed point. Figure 11 depicts a scatter plot of $L1c_{(-trop)}$-L1c height discrepancies versus the distance from HRAO to the tide gauge stations.

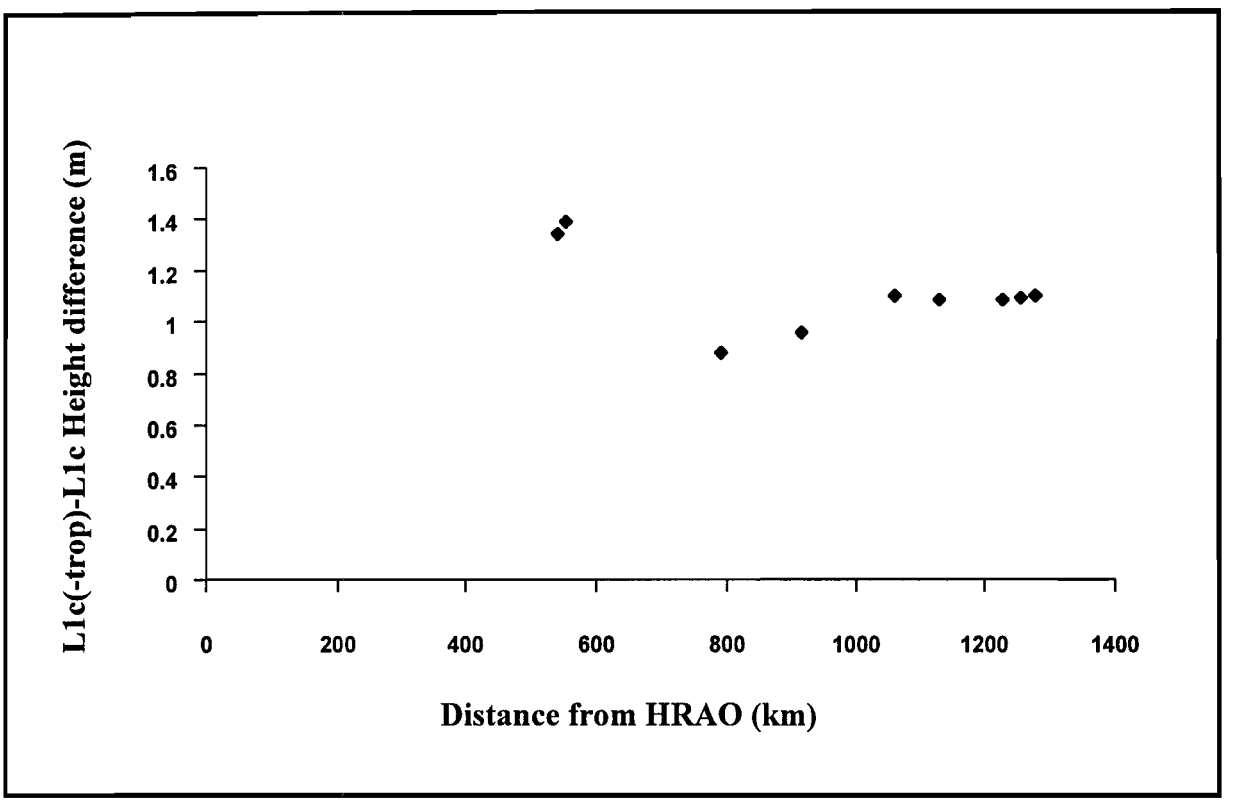


**Figure 11:** $L1c_{(-trop)}$-L1c height discrepancies versus the distance from HRAO to the tide gauge stations.

A correlation coefficient was computed to show how much the two variables moved together. The two variables being the broadcast $L1c_{(-trop)}$-L1c height discrepancies and the HRAO-tide gauge station distances. Furthermore, the coefficient of determination (described in 5.2.5) was also computed to show the proportion of a perfect linear relationship that the two variables had.

A correlation coefficient of -0.497 was computed indicating a relatively weak negative correlation between the two variables. Consequently, the coefficient of determination was 0.247. Therefore, the two variables were 25% as closely related as they would have been if they were perfectly associated with one another.

It was interesting to note that this result suggested that the height discrepancies tended to decrease with increased distance from the HRAO. This thesis did not attempt to account for this relationship as it was beyond its scope. However, the investigation and analysis of this relationship is strongly recommended for future research.

The relationship between $L1c_{(-trop)}$-L1c height discrepancies and the height differences between HRAO and the tide gauge stations was investigated next. A scatter plot showing these two variables is depicted in figure 12.

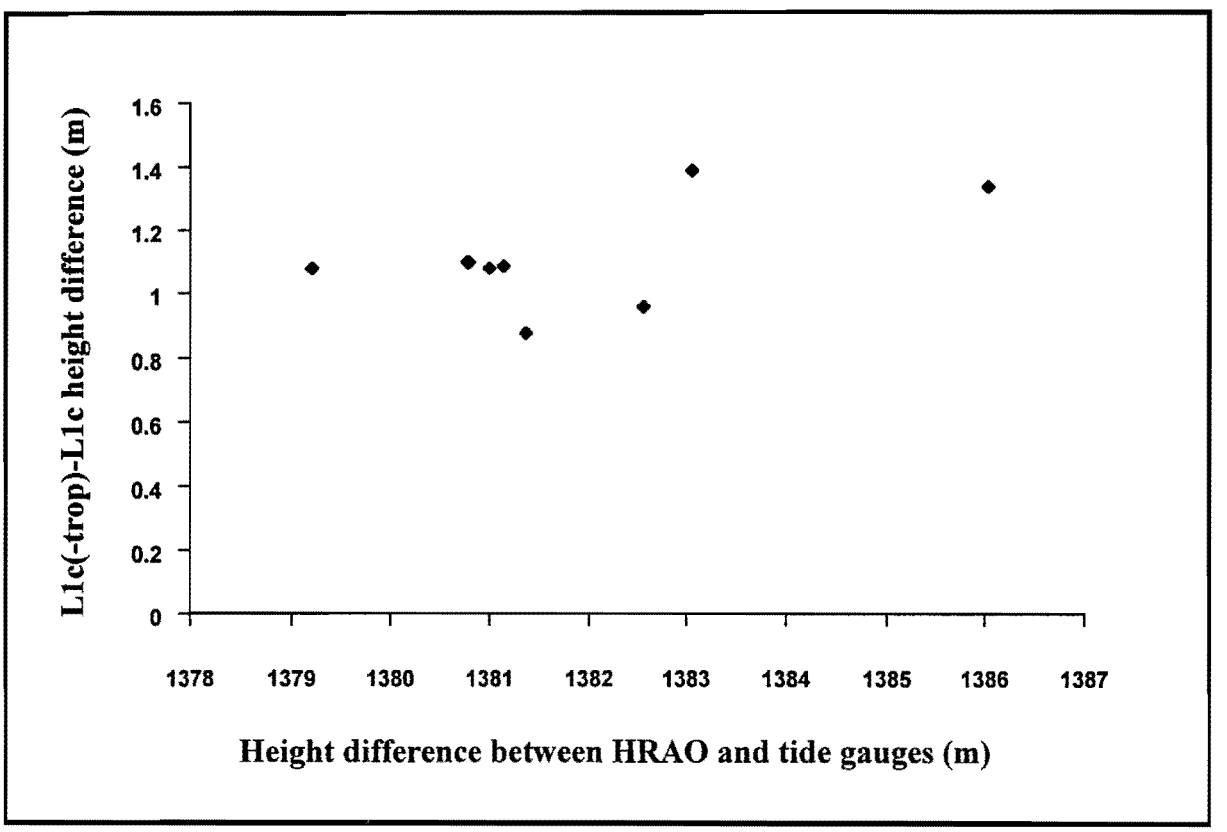


**Figure 12:** $L1c_{(-trop)}$-L1c height discrepancies versus the height differences between HRAO and the tide gauge stations.

The purpose of this analysis was to measure the strength and direction of the relationship between the two variables. The $L1c_{(-trop)}$-L1c height discrepancies and the height differences between HRAO and the tide gauge stations were the two variables in this instance. Looking at figure 12 a fairly linear relationship between the two variables can be noted. This is supported by the computed correlation coefficient of 0.666. At this magnitude the correlation coefficient corresponds to a fairly strong positive correlation. The square of the correlation coefficient (the coefficient of determination) was computed as 0.444. Hence, the two variables above were 44% as closely related as they might have been if they were perfectly associated with one another.

Finally, the inter-station height differences were pitted against the $L1c_{(-trop)}$-L1c inter-station height discrepancies. A correlation coefficient of 0.227 was computed following the analysis. Therefore, there was a weak positive correlation between inter-station height differences and $L1c_{(-trop)}$-L1c inter-station height discrepancies. A coefficient of determination of 0.051 was obtained. It follows therefore that the two variables were only 5% as closely related as they might have been if they were perfectly correlated.

## 5.4 EFFECTS OF ANTENNA PHASE CENTRE VARIATIONS

The solutions of ellipsoidal heights with and without antenna calibration were compared in this analysis. The effects of antenna phase centre variations are clearly set out in subsection 2.4.1 of this thesis. The intention here was to investigate the extent to which phase centre variations affected this project's processing results. To this end, the minimally adjusted coordinates of $L1c_{(-Ant)}$ were compared to those of L1c. L1c corrected for antenna phase centre variations using GPSurvey's inbuilt antenna calibration table for antenna used by this project. $L1c_{(-Ant)}$ as suggested by the subscript '-Ant', disabled antenna phase centre variations corrections. Antenna phase centre variation is an important factor limiting the accuracy of carrier phase derived GPS heights.

### 5.4.1 Comparison of Height errors between broadcast L1c and $L1c_{(-Ant)}$

The following analysis used $L1c_{(-Ant)}$-L1c heights to compute height discrepancies since broadcast $L1c_{(-Ant)}$ heights were estimated higher than broadcast L1c heights. In comparing the two sets of results (L1c/$L1c_{(-Ant)}$), an average difference in height of 45 mm was determined. The RMS height discrepancy was found to be 55 mm, while the maximum height shift was the 74 mm at SATG. These discrepancies are well within the expected precision of the differences between these two sets of results. An inspection of the standard errors of positions between these sets of results revealed a millimetre's difference for the worst case scenario. This is quite insignificant. The standard errors of the heights differed by a wider margin, but there too the largest difference was only 1 cm. Overall, the consistency of the corrected data (L1c) was marginally worse than that of the uncorrected data, with standard errors of the heights on average 14% larger. Nevertheless, the corrected data should give the more reliable results. This is because the correction takes into account the systematic vertical bias between the Ashtech and Dorne Margolin antennae. This bias introduces a significant shift in the heights.

### 5.4.2 Correlation analysis

A correlation analysis was done to measure the strengths and direction of the relationships described in the following paragraphs.

The relationship between broadcast $L1c_{(-Ant)}$-L1c height discrepancies and the distance from the fixed point (HRAO) to the tide gauge stations was analysed first. To this end a correlation coefficient was computed for these two variables. This was found to be 0.953 indicating a very strong positive correlation. From the coefficient of determination (0.908), the two variables were 91% as closely related as they would have been if they were perfectly correlated. The strong positive correlation between the two variables can be attributed to the long baselines and the use of mixed antennae. Ignoring antenna

corrections on long baselines can cause errors in the tropospheric scale bias parameter, which is modelled by the software (see section 2.4.1).

Secondly, the relationship between $L1c_{(-Ant)}$-L1c height discrepancies and the height differences between HRAO and the tide gauge stations was analysed. Following the analysis a correlation coefficient of -0.717 was obtained. Therefore, the relationship between the two variables was a strong negative correlation. With a coefficient of determination of 0.514, only 51% of the variance in the two entities were shared between them.

Finally, the relationship between inter-station height differences and the $L1c_{(-Ant)}$-L1c inter-station height discrepancies was investigated. The results gave a correlation coefficient of -0.261 for these two variables. Therefore, there was a very weak negative correlation between the inter-station height differences and the $L1c_{(-Ant)}$-L1c inter-station height discrepancies. A coefficient of determination of 0.068 indicated that only 7% of the variance in the two variables were shared between them.

### 5.4.3 Antenna calibration table swap

In furtherance of the investigation into the effects of antenna phase centre variations, the effect of swapping antenna tables was taken into consideration. The minimally adjusted coordinates of precise L1c were compared to those of precise $L1c_{(NOAA)}$. Precise L1c processed data using GPSurvey's inbuilt antenna calibration table for the Ashtech L1/L2 L-Shaped notches antenna used by this project. $L1c_{(NOAA)}$ on the other hand used the updated antenna calibration table for the same type antenna, as calibrated by NOAA. The NOAA calibration table of 1996 is currently the latest update for the Ashtech L1/L2 L-Shape notches antenna. Remarkable differences between the NOAA and GPSurvey tables were noticed (see appendices A.1 and A.2). For example, the L1/L2 nominal offsets as well as the azimuth and elevation corrections were all dissimilar for the two tables. However, the primary objective was to find out how each of these tables would enhance the quality of this project's heights.

Comparing the solutions of ellipsoidal heights obtained from precise L1c and $L1c_{(NOAA)}$ resulted in an average height difference of 15 mm. The RMS height discrepancy was found to be 17 mm, while the maximum height shift was 33 mm at PETG. These discrepancies were consistent with the expected precision for the differences between these two sets of results. The precision estimates of heights at the tide gauges (relative to HRAO) ranged from about 24 mm to 39 mm for both results. The standard errors of the positions were identical for the most part in both precise L1c and $L1c_{(NOAA)}$. Where differences in standard errors of positions did occur, these were no more than a millimetre. A similar trend emerged for the height standard errors with the largest difference being the 3 mm at RBTG. Figure 13

illustrates the comparison of standard errors of heights for precise L1c and $L1c_{(NOAA)}$. Looking at figure 13, it becomes apparent that the NOAA table was the better of the two tables. Hence it's subsequent use in the optimal processing algorithm for this project.

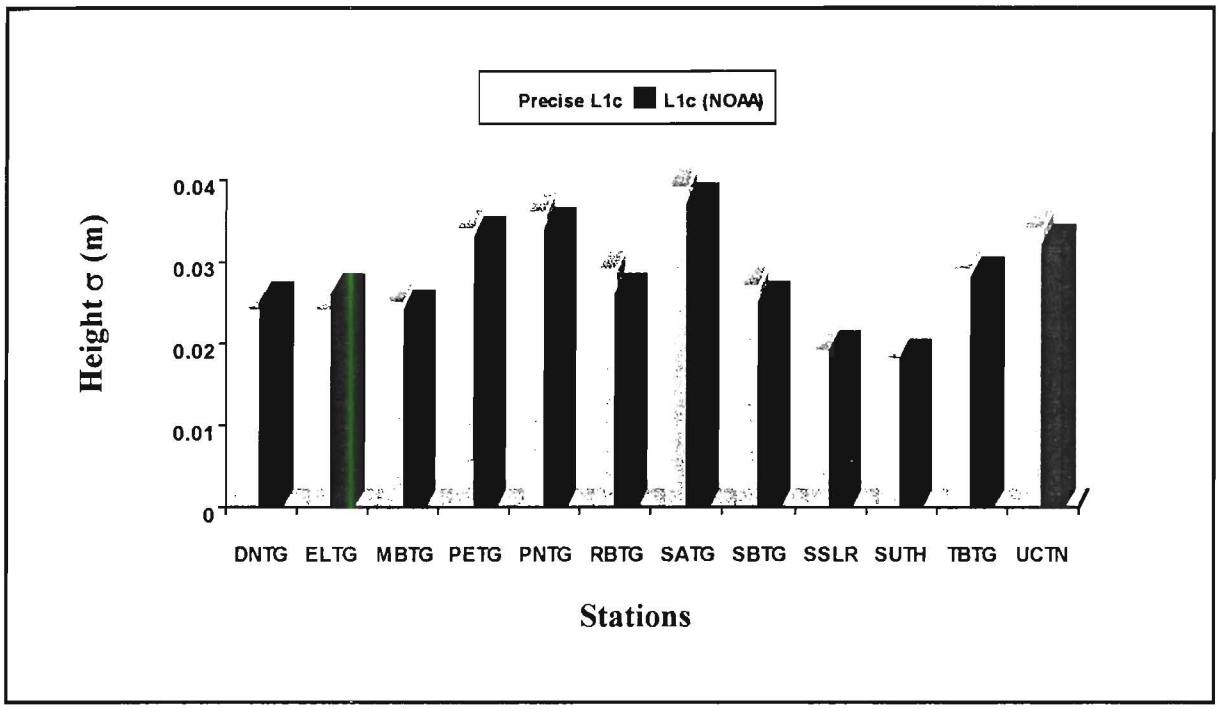


**Figure 13:** Standard errors of heights for preciseL1c/ $L1c_{(NOAA)}$

## 5.5 THE EFFECTS OF ORBITS

This section examines the benefits derived from using precise orbits as opposed to broadcast orbits. Broadcast L1c was analysed in contrast to precise L1c, using their respective minimally adjusted coordinates. By definition, broadcast orbits are predicted time changing positions of satellite through space. The estimated accuracy of the broadcast ephemerides is 5-10 m (Hofmann-Wellenhof et al., 1997). Unfortunately, that accuracy range is intentionally downgraded to around 30-40 m through the policy of Selective Availability (SA). Precise orbits in total contrast are computed from tracking the satellites to get actual paths. IGS precise orbits have estimated accuracy of 10-20 cm (Beutler et al., 1998). Bearing that in mind, greater accuracy would be attained using precise orbits.

### 5.5.1 Comparison of Height errors between broadcast L1c and precise L1c

Broadcast L1c heights were estimated higher than precise L1c heights. Consequently, broadcast L1c heights minus precise L1c heights gave the height discrepancies. The comparison of results from broadcast L1c and precise L1c yielded an average height difference of 1 mm. The RMS height discrepancy was computed as 22 mm, with a maximum height shift of 35 mm at PNTG (furthest from HRAO). These discrepancies were quite consistent with the expected precision for the differences between these two sets of results. The standard errors of the heights for broadcast L1c were approximately twice as large as those for precise L1c. Clearly, precise orbits improved the precision of the ellipsoidal heights by about two times (see figure 14 below).

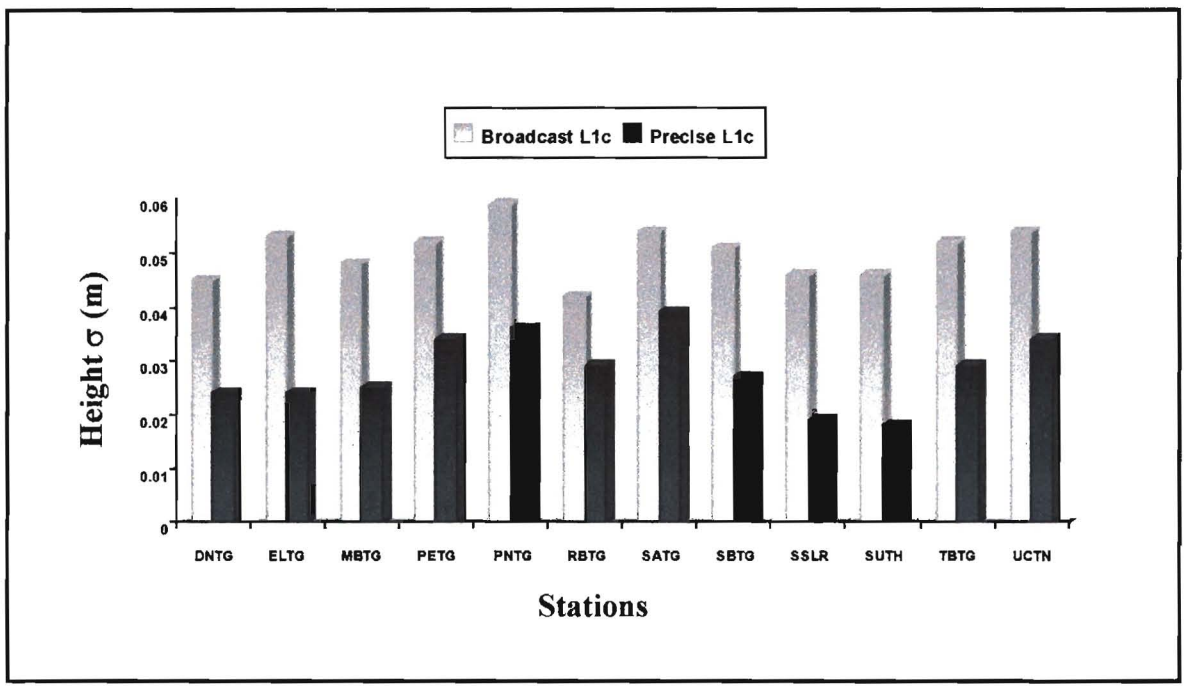


**Figure 14:** Standard errors of heights for broadcast L1c and precise L1c

### 5.5.2 Correlation analysis

The discrepancies in height between broadcast L1c and precise L1c were pitted against distance from the fixed point (HRAO) to the tide gauge stations. This was done to measure the degree of linear relationship between these two variables. A correlation coefficient of 0.386 was computed. This symbolised a relatively weak positive correlation between the two

variables. Further analysis gave a coefficient of determination of 0.149. Therefore, the two variables were only 15% as closely related as they might have been if they were perfectly correlated.

The relationship between broadcast L1c and precise L1c height discrepancies and the height differences between HRAO and the tide gauges was considered next. In the correlation analysis a correlation coefficient of -0.256 was computed for these two variables. This implied that the two variables had a weak negative correlation. Furthermore, the coefficient of determination was computed as 0.065. Hence, the two variables were only 6% as closely related as they might have been if they were perfectly associated with one another.

Finally, the computed inter-station height differences were pitted against the broadcast L1c and precise L1c inter-station height discrepancies. As a result of this analysis a correlation coefficient of -0.429 was obtained. This corresponds to a relatively weak negative correlation for the two variables. The coefficient of determination was calculated as 0.184. Consequently, the two variables were only 18% as closely related as they would have been if they were perfectly correlated.

# Chapter 6

# DISCUSSION AND RECOMMENDATIONS

## 6.1 DISCUSSION

The results presented in this thesis render the high precision GPS data processing for the survey of South African tide gauges a successful campaign. The coordinates of the nine tide gauges have been computed in the ITRF97 reference frame at the observational epoch 1998.0. The preferred (most accurate) results were obtained using the optimal processing algorithm-precise $L1c_{(NOAA)}$, following a fully constrained network adjustment. These coordinates and their corresponding standard errors are given in table 4. Heighting accuracy of 2-3 cm was achieved at the tide gauges using the L1-ionosphere free fixed integers observable and IGS precise orbits. SUTH is closer to the Western Cape tide gauges than HRAO. Thus, its inclusion as a fixed point in the full network adjustment improved the precision estimates of the heights of Western Cape tide gauges. Large residuals obtained on vectors between Hartebeesthoek and Sutherland indicate that the GPS data were not entirely consistent with the coordinates of the fixed points. Applying corrections for the various biases and errors improved the precision of the heights as follows:

- Ionospheric refraction correction improved the precision of the heights by as much as three times
- Correcting for tropospheric refraction improved the precision of the heights about two fold
- Correcting for antenna phase centre variations did introduce significant changes in height of up to 7 cm, even though it did not improve the consistency of the network
- Finally, using precise orbits in preference to broadcast orbits, improved the precision of the heights by about two times

There appeared to be no major problems with the data, although the power outages did reduce the amount of data available. Despite that, the processed baselines (precise L1c and $L1c_{(NOAA)}$) proved to be statistically precise. The computed baseline ratios and variances in precise L1c and $L1c_{(NOAA)}$ showed the desired trend of high ratios and correspondingly low

variances. Furthermore, precise ephemerides provided RMS height misclosure of about 3 cm, with loop closures well below the 1 ppm relative error limit expected of commercial software. Bearing in mind that the software used was not entirely ideal for this application, it has nonetheless performed well, providing relative accuracy better than 0.1 ppm.

## 6.2 RECOMMENDATIONS

A great deal more could be done with the available data set to improve results. GPSurvey did produce relatively good results. However, it is likely that even better results would have been obtained had a specialist software package been used instead. Specialist software have the capability of modelling earth tides, ocean tide loading and crustal motion in addition to the corrections available in GPSurvey. Efforts to acquire one such package are currently underway.

Ideally, permanent continuously operating GPS receivers (COGR) with choke ring antennae should be located at all tide gauge sites. This is presently an unfeasible venture in the South African context given the expensive nature of geodetic quality GPS receivers. Financial and other limitations restricted the observations (with only three receivers) to single 24 hour sessions. However, should sufficient funds become available, it would be desirable to repeat this survey with some alterations. These would include the procurement of sufficient identical receivers to occupy all sites simultaneously for a minimum period of three days.

Future plans for a further IGS or other permanent continuously operating GPS receiver should consider a location close to the south-east coast. A COGR station somewhere midway on a straight line between Sutherland (SUTH) and Durban (DNTG) would be an excellent choice. Such a station would provide strong control for the tide gauges on the south-east and eastern coasts of South Africa.

Finally, in the interest of future research or any subsequent re-evaluation of this thesis, the adjusted coordinates of all processing variations appear in appendix E.

# REFERENCES

Alreck, P.L and Settle, R.B (1995): *The Survey Research Handbook,* Irwin McGraw-Hill.

Aquino, M.H.O; Bingley, R.M; Dodson, A.H; and Penna, N.T (1999): A National Network of Continuously Operating GPS Receivers for the UK. Proceedings IUGG-99, Birmingham, July 1999.

Ashkenazi, V; Baker, T; Bingley, R; Dodson, A; and Penna, N (1998): GPS Monitoring of Vertical Land Movements in the UK. Proceedings, ION GPS-98, Nashville, Sept. 1998.

Ashkenazi, V; Basker, G; Davison, M; Dodson, A; Ffoulkes-Jones, G; Moore, T; and Westrop, J. (1988):Levelling of Tide Gauges Using GPS. Chapman Conference on GPS measurements for Geodynamics, September 1988, Ft. Lauderdale, Florida, USA. 1-7.

Bevis, M (1998): Draft Report: Continuous GPS positioning of tide gauges. IGS/PSMSL Technical Committee on CGPS positioning of tide gauges.

Beutler, G; Hein, G.W; Melbourne, G.W; and Seeber, G (Eds) (1995): GPS Trends in Precise Terrestrial, Airborne, and Spaceborne Applications. Symposium No. 115, Boulder, CO., USA, July 3-4, 1995.

Beutler, G; Kouba, J; Neilan, R.E; Rothacher, M; and Springer, T (1998): The International GPS Service (IGS): an interdisciplinary service in support of Earth sciences. Proceedings, 32nd COSPAR Scientific Assembly, Nagoya, Japan, July 1998.

Blewitt, G and Gregorius, T (1998): The Effect of Weather Fronts on GPS Measurements, *GPS WORLD,* Vol. 9, No. 5, 52-60.

Brundrit, G.B (1995): Trends of Southern African Sea Level: Statistical Analysis and Interpretation, *South African Journal of Marine Science,* Vol. 16, 9-17.

Brunner, F.K, and Welsch, W.M. (1993): Effect of the Troposphere on GPS Measurements. *GPS WORLD,* Vol. 4, No. 1, 42-51.

Carter, W.E; Chin, M; Diamante, J; Mackay, J.R; Peter, G; and Scherer, W. (1988): Global Absolute Sea Level: The Hawaiian Network, *Marine Geodesy,* Vol. 12, 247-257.

Cazenave, A; Cretaux, J.F; Dominh, K; Le Provost, C; Ponchaut, F; and Soudarin, L (1999): Sea Level changes from Topex-Poseidon altimetry and tide gauges and vertical crustal motions from DORIS. *Geophysical Research letters,* Vol. 26, No. 14, 2077-2080, July 15, 1999.

Clark, N (1996): Investigation into the use of GPS for the measurement of Long Baselines. Final year Thesis, Dept. of Geomatics, University of Cape Town.

Cochlovius-Gouws, A.C (1992): Preplanning GPS Session Lengths for Cadastral Surveying in South Africa. MSc. Thesis, Dept. of Geomatics, University of Cape Town.

Combrinck, W.L (1996): Antenna Axis Offset and Intersection Determination using GPS. MSc. (ApplSc) Thesis, Dept of Geomatics, University of Cape Town.

Collins, J; Hofmann-Wellenhof, B; and Lichtenegger, H (1997): *GPS Theory and Practice*, Springer-Verlag Wien, New York.

Collins, P and Langley, B.R (1999): Tropospheric Delay-Prediction for the WAAS User. *GPS WORLD*, 07/99, 52-58.

Columbus Software User's Manual (1996): Best-Fit Computing, Beaverton, Oregon.

Craig, A (1996): A GPS Derived Control Network for UCT campus. Final year Thesis, Dept. of Geomatics, University of Cape Town.

D'Arcy-Evans, J.F (1991): GPS Simulation Studies for Monitoring Vertical Crustal Motions in Lesotho. MSc. Thesis, Dept. of Geomatics, University of Cape Town.

Deakin, R.E (1996): The Geoid, What's it got to do with me? *The Australian Surveyor*, Vol.41, No.4, 294-304.

Fulton, D.E; Neilan, R.E; and Zumberge, J.F (Eds.) (1996): *International GPS Service for Geodynamics*. 1996 Annual Report. IGS Central Bureau, JPL, California.

Gagnon, P and Nassar, M (1973): The Methods of Least Squares: Interval Estimation and Hypothesis testing, Dept. of Surveying Engineering, The University of New Brunswick, Frederiction, N.B.

GPS Surveying General Reference (1994): Trimble Navigation Ltd., Sunnyvale, California.

GPSurvey Software User's Guide (1995): Trimble Navigation Ltd., Sunnyvale, California.

Joselyn, J.A (1999): Eye on the Ionosphere. *GPS Solutions* Vol. 3, No. 1, 79-81.

Kaplan, E.D (1996): *Understanding GPS Principles & Applications*, Artech House, Inc.

Kleusberg, A and Teunissen, P.J.G, (Eds.) (1996): *GPS for Geodesy*: Lecture Notes in Earth Sciences, Springer-Verlag, Berlin.

Krynski, J, and Swiatek, A. (1997): A Regional Precise GPS Network in South Africa. Presented at The Congress for South African Surveyors, 97.

Langley, B.R (1995): A GPS Glossary, *GPS WORLD,* 10/95, 61-63.

Langley, B.R (1996): Propagation of the GPS Signals. *GPS for Geodesy*: Lecture Notes in Earth Sciences, spronger-Verlag, Berlin.

Langley, B.R (1997): The GPS Error Budget, *GPS WORLD,* Vol. 8, No. 3, 51-56.

Langley, B.R (1998): A Primer on GPS Antennas, *GPS WORLD,* Vol. 9, No. 7, 50-54.

Leick, A. (1995): *GPS Satellite Surveying.* Second edition, John Wiley & Sons, Inc., New York.

Ma, C and MacMillan, D.S (1997): Atmospheric gradients and the VLBI terrestrial and celestial reference frames. *Geophysical Research letters,* Vol. 24, No. 4, 453-456, Feb. 15, 1997.

Ma, C and MacMillan, D.S (1998): Using Meteorological Data Assimilation Models in Computing Tropospheric Delays at Microwave Frequencies. *Phys. Chem. Earth,* Vol. 23, No. 1, 97-102, 1998.

Ma, C and MacMillan, D.S (1999): Improving the modelling of Atmospheric Delay Using Meteorological Data Assimilation Models. Proceedings IUGG-99, Birmingham, July 21, 1999.

Mader, G.L (Ed) (1991): Permanent Satellite Tracking Networks for Geodesy and Geodynamics. International Association of Geodesy Symposia. Symposium No. 109, Vienna.

Mader, G.L (1999): GPS Antenna Calibration at the National Geodetic Survey. *GPS Solutions,* Vol. 3. No. 1, 50-58.

Meade, M.E (1998): CORS-A National Asset, *Point of Beginning,* Vol. 23, No. 11, 14-21.

Mendenhall, W (1967): *Introduction to Probability and Statistics,* Wadsworth Publishing Company, Inc. Belmont, California.

Merry, C.L (1989): Recent Variations in Mean Sea Level in southern Africa. Proceedings International Association of Geodesy Symposia, Edinburgh, 1989.

Merry, C.L (1995): *Introduction to the Global Positioning System.* Fourth edition, Dept. of Geomatics, University of Cape Town.

Merry, C.L (1999): Preliminary processing of the 1997/1998 South African tide gauge GPS survey. Internal Report G-22, Dept. of Geomatics, University of Cape Town.

Mertikas, S.P (Ed) (1992): Global Positioning Systems in Geosciences. Proceedings of the International Workshop on Global Positioning Systems in Geosciences, Technical University of Crete, Chania Greece, 8-10 June 1992.

Morris, M.D (Ed) (1991): *Errors in Practical Measurements in Surveying, Engineering and Technology.* Landmark enterprises 10324 Newton Way, Rancho Cardova, California.

Nerem, R.S; Schenewerk, M.S; and vanDam, T.M (1999): Gauging the Tides: Monitoring Subsidence around Chesapeake Bay, *GPS WORLD,* Vol. 10, No. 5, 34-41.

Pan, M. and Sjöberg, L.E (1993): Baltic Sea Level Project With GPS, *Bulletin Geodesique,* Vol.67, 51-59.

Pugh, D.T (1987): The Global Sea-Level Observing System, *The Hydrographic Journal,* No. 45, 5-8.

Reilly, J.P (1998): Adjustment of Geodetic Networks, Part 3. *The GPS Observer,* Point of Beginning, July 1998.

Schwarz, K.P, and Sideris, M.G. (1993): Heights and GPS, *GPS WORLD,* 02/93, 50-56.

Seeber, G (1993): *Satellite Geodesy,* Walter de Gruyter & Co., Berlin.

Sickle, Van, J (1996): *GPS for Land Surveyors,* Ann Arbor Press, Inc.

Spiegel, M.R (1972): Schaum's Outline series: *Theory and problems of Statistics.* McGraw-Hill Book company, New York.

Tolkatchev, A (1996): Global Sea Level Observing System (GLOSS), *Marine Geodesy,* Vol. 19, No. 1, 21-62.

Trimnet Software User's Manual (1992): Trimble Navigation Ltd., Sunnyvale, California.

Wanninger, L. (1993): Effects of Equatorial Ionosphere on GPS. *GPS WORLD*, 07/93, 48-54.

Wave Software User's Guide (1995): Trimble Navigation Ltd., Sunnyvale, California

Werner, G. (1994): RINEX: The Receiver Independent Exchange Format. *GPS WORLD,* 07/94, 48-52.

Woodworth, P.L (1997): Introduction to the Workshop on Methods of Monitoring sea level: GPS and tide gauge benchmark monitoring, GPS altimeter calibration. Proceedings, Workshop on Methods for Monitoring Sea Level, Pasadena, California.

Zimba, R and Merry, C.L (1999): Further processing of the 1997/1998 South African tide gauge GPS survey. University of Cape Town, Department of Geomatics, Internal Report G-23, April 1999.

# Appendices

## Appendix A: Antenna calibration tables

**A.1:** GPSurvey antenna calibration table

**A700288.PCT** **ASHTECH L1/L2, REV.B**
**'L-SHAPED NOTCHES'**

;Processor name : WAVE Alpha
;Calibration time : Fri Feb 14 16:41:55 1997
;Reference antenna : Dorne Margolin Model T
;Calibrated antenna : Ashtech Geodetic L1/L2 L
;Model order : 0 x 10

| ;Mean phase centre (mm) | North | East | Up |
|---|---|---|---|
| L1NominalOffset = | -1.9 | 0.4 | 85.2 |
| L2NominalOffset = | -3.1 | 2.8 | 85.6 |

| ;Elevation range (deg) | Start | Stop | Step |
|---|---|---|---|
| ElevationRange = | 5 | 90 | 5 |

;Azimuth step size (deg)
AzimuthStep = 0

;Azimuth/elevation corrections (mm)

AZ=0

**;L1**

2.5 2.2 2.8 3.5 4.0 4.3 4.5 4.6 4.5 4.4
4.2 3.9 3.4 2.8 2.2 1.5 0.7 0.0

**;L2**

-1.7 -1.6 -0.6 0.6 1.8 2.6 3.1 3.3 3.2 3.0
2.7 2.3 2.0 1.6 1.3 0.9 0.5 0.0

**A.2:** NOAA antenna calibration table

**ASH 700228.D ASHTECH L1/L2, REV. B NGS ( 2) 98/06/02**
**'L-SHAPED NOTCHES'**

;Processor name : WAVE Alpha
;Calibration time : Tue Jun 02 16:41:55 1998
;Reference antenna : Dorne Margolin Model T
;Calibrated antenna : Ashtech Geodetic L1/L2 L
;Model order : 0 x 10

| ;Mean phase centre (mm) | North | East | Up |
|---|---|---|---|
| L1NominalOffset = | -3.2 | 0.1 | 84.2 |
| L2NominalOffset = | -1.9 | 4.9 | 76.7 |

| ;Elevation range (deg) | Start | Stop | Step |
|---|---|---|---|
| ElevationRange = | 5 | 90 | 5 |

;Azimuth step size (deg)
AzimuthStep = 0

;Azimuth/elevation corrections (mm)

AZ=0

**;L1**

0.0 -3.9 -1.6 0.1 1.2 1.9 2.3 2.6 2.6 2.6
2.5 2.4 2.2 2.0 1.8 1.4 0.8 0.0

**;L2**

0.0 -1.4 -1.9 -2.1 -2.0 -1.7 -1.4 -1.2 -1.0 -0.9
-1.0 -1.1 -1.3 -1.5 -1.6 -1.5 -1.0 0.0

## Appendix B: Wave processing results

**B.1: L1c-**Broadcast orbits, corrections for troposphere and ionosphere, plus A700288.pct antenna calibration applied.

| From Station Short Name | To Station Short Name | Solution Type | Slope | Ratio | Reference Variance |
|---|---|---|---|---|---|
| DNTG | ELTG | Iono free float | 459278.272 | | 2.270 |
| DNTG | HARK | Iono free float | 550825.253 | | 6.018 |
| DNTG | HRAO | Iono free float | 551773.672 | | 9.745 |
| ELTG | HRAO | Iono free float | 790988.360 | | 17.569 |
| HARK | ELTG | Iono free float | 791275.305 | | 10.928 |
| HARK | PNTG | Iono free float | 1131787.599 | | 5.963 |
| HARK | RBTG | Iono free float | 539216.567 | | 4.044 |
| HARK | SUTH | Iono free float | 982843.347 | | 9.476 |
| HRAO | HARK | L1 fixed | 2113.791 | 13.1 | 1.158 |
| HRAO | RBTG | Iono free float | 540656.058 | | 4.034 |
| MBTG | PETG | Iono free float | 322310.539 | | 3.040 |
| MBTG | SBTG | Iono free float | 341721.872 | | 1.884 |
| PETG | ELTG | Iono free float | 236211.130 | | 2.359 |
| PNTG | SATG | Iono free float | 430345.147 | | 8.461 |
| RBTG | DNTG | Iono free fixed | 155702.018 | 11.0 | 5.410 |
| SBTG | SSLR | Iono free float | 297828.677 | | 3.245 |
| SBTG | TBTG | Iono free fixed | 31358.788 | 22.3 | 0.874 |
| SSLR | HARK | Iono free float | 983283.970 | | 10.661 |
| SSLR | HRAO | Iono free float | 981652.174 | | 16.579 |
| SSLR | MBTG | Iono free float | 235741.315 | | 2.549 |
| SSLR | MBTG | Iono free float | 235741.291 | | 2.175 |
| SSLR | PNTG | Iono free float | 511324.744 | | 8.132 |
| SSLR | SATG | Iono free float | 275916.002 | | 2.460 |
| SSLR | SUTH | L1 fixed | 762.422 | 28.3 | 1.073 |
| SSLR | TBTG | Iono free float | 278416.700 | | 3.179 |
| SUTH | ELTG | Iono free float | 669636.058 | | 1.331 |
| SUTH | HRAO | Iono free float | 981212.321 | | 9.368 |
| SUTH | MBTG | Iono free float | 235252.124 | | 1.572 |
| SUTH | PETG | Iono free float | 482295.332 | | 0.282 |
| TBTG | SATG | Iono free fixed | 107250.986 | 13.5 | 3.317 |
| TBTG | UCTN | Iono free fixed | 6376.676 | 17.8 | 1.553 |
| UCTN | SBTG | Iono free fixed | 25547.206 | 17.6 | 1.560 |

**B.2:** L1-Broadcast orbits, correction for troposphere and A700288.pct antenna calibration applied, but no ionospheric refraction correction.

| From Station Short Name | To Station Short Name | Solution Type | Slope | Ratio | Reference Variance |
|---|---|---|---|---|---|
| DNTG | ELTG | L1 float | 459277.880 | | 54.582 |
| DNTG | HARK | L1 float | 550825.136 | | 1534.533 |
| DNTG | HRAO | L1 float | 551773.514 | | 1771.879 |
| ELTG | HRAO | L1 float | 790987.947 | | 1804.002 |
| HARK | ELTG | L1 float | 791274.888 | | 1200.268 |
| HARK | PNTG | L1 float | 1131787.316 | | 2163.079 |
| HARK | RBTG | L1 float | 539216.527 | | 1412.781 |
| HARK | SUTH | L1 float | 982843.041 | | 4692.776 |
| HRAO | HARK | L1 fixed | 2113.791 | 13.1 | 1.159 |
| HRAO | RBTG | L1 float | 540655.893 | | 1295.115 |
| MBTG | PETG | L1 float | 322310.411 | | 561.033 |
| MBTG | SBTG | L1 float | 341721.715 | | 554.394 |
| PETG | ELTG | L1 float | 236210.953 | | 509.819 |
| PNTG | SATG | L1 float | 430344.951 | | 856.792 |
| RBTG | DNTG | L1 float | 155701.928 | | 761.525 |
| SBTG | TBTG | L1 fixed | 31358.770 | 37.8 | 23.354 |
| SSLR | HARK | L1 float | 983283.275 | | 2638.774 |
| SSLR | HRAO | L1 float | 981651.932 | | 4196.926 |
| SSLR | MBTG | L1 float | 235741.088 | | 989.966 |
| SSLR | MBTG | L1 float | 235741.167 | | 621.104 |
| SSLR | PNTG | L1 float | 511324.548 | | 1617.448 |
| SSLR | SATG | L1 float | 275915.789 | | 980.291 |
| SSLR | SBTG | L1 float | 297828.519 | | 896.829 |
| SSLR | SUTH | L1 fixed | 762.422 | 28.3 | 1.073 |
| SSLR | TBTG | L1 float | 278416.514 | | 512.495 |
| SUTH | ELTG | L1 float | 669635.913 | | 120.028 |
| SUTH | HRAO | L1 float | 981211.943 | | 4661.790 |
| SUTH | MBTG | L1 float | 235251.951 | | 353.647 |
| SUTH | PETG | L1 float | 482295.421 | | 2.301 |
| TBTG | SATG | L1 fixed | 107250.904 | 4.9 | 341.696 |
| TBTG | UCTN | L1 fixed | 6376.673 | 17.7 | 8.160 |
| UCTN | SBTG | L1 fixed | 25547.190 | 29.2 | 19.531 |

**B.3: L1c$_{(-trop)}$** -Broadcast orbits, ionospheric refraction correction and A700288.pct antenna calibration applied, but no correction for the troposphere.

| From Station Short Name | To Station Short Name | Solution Type | Slope | Ratio | Reference Variance |
|---|---|---|---|---|---|
| DNTG | ELTG | Iono free float | 459278.597 | | 190.579 |
| DNTG | HARK | Iono free float | 550825.971 | | 541.344 |
| DNTG | HRAO | Iono free float | 551774.308 | | 1328.094 |
| ELTG | PETG | Iono free float | 236211.464 | | 148.624 |
| HARK | ELTG | Iono free float | 791276.283 | | 603.288 |
| HARK | PNTG | Iono free float | 1131788.284 | | 1038.226 |
| HARK | RBTG | Iono free float | 539217.055 | | 532.629 |
| HARK | SUTH | Iono free float | 982844.270 | | 538.045 |
| HRAO | ELTG | Iono free float | 790989.386 | | 727.281 |
| HRAO | HARK | L1 fixed | 2113.787 | 76.7 | 11.099 |
| HRAO | RBTG | Iono free float | 540656.672 | | 392.232 |
| HRAO | SSLR | Iono free float | 981653.327 | | 559.870 |
| MBTG | PETG | Iono free float | 322311.004 | | 345.092 |
| MBTG | SBTG | Iono free float | 341722.348 | | 319.875 |
| PNTG | SATG | Iono free float | 430345.840 | | 407.791 |
| RBTG | DNTG | Iono free float | 155702.168 | | 45.926 |
| SBTG | SSLR | Iono free float | 297829.022 | | 240.176 |
| SBTG | TBTG | Iono free fixed | 31358.841 | 3.4 | 4.396 |
| SSLR | HARK | Iono free float | 983285.001 | | 595.469 |
| SSLR | MBTG | Iono free float | 235741.652 | | 181.640 |
| SSLR | MBTG | Iono free float | 235741.656 | | 202.384 |
| SSLR | PNTG | Iono free float | 511325.468 | | 380.978 |
| SSLR | SATG | Iono free float | 275916.354 | | 239.116 |
| SSLR | SUTH | L1 fixed | 762.418 | 14.6 | 3.594 |
| SSLR | TBTG | Iono free float | 278417.043 | | 255.021 |
| SUTH | ELTG | Iono free float | 669635.734 | | 135.862 |
| SUTH | HRAO | Iono free float | 981213.274 | | 489.501 |
| SUTH | MBTG | Iono free float | 235252.429 | | 132.768 |
| SUTH | PETG | Iono free float | 482295.914 | | 459.704 |
| TBTG | SATG | Iono free fixed | 107251.168 | 1.7 | 38.583 |
| TBTG | UCTN | Iono free fixed | 6376.685 | 40.6 | 2.881 |
| UCTN | SBTG | Iono free fixed | 25547.246 | 5.1 | 4.161 |

**B.4: $\mathbf{L1c}_{(-\mathrm{Ant})}$** -Broadcast orbits, corrections for troposphere and ionosphere, but no antenna calibration applied.

| From Station Short Name | To Station Short Name | Solution Type | Slope | Ratio | Reference Variance |
|---|---|---|---|---|---|
| DNTG | ELTG | Iono free float | 459278.276 | | 2.298 |
| DNTG | HARK | Iono free float | 550825.254 | | 5.964 |
| DNTG | HRAO | Iono free float | 551773.672 | | 9.690 |
| ELTG | HARK | Iono free float | 791275.298 | | 17.552 |
| ELTG | HRAO | Iono free float | 790988.379 | | 5.245 |
| HARK | PNTG | Iono free float | 1131787.600 | | 6.055 |
| HARK | RBTG | Iono free float | 539216.568 | | 4.021 |
| HARK | SSLR | Iono free float | 983283.976 | | 10.834 |
| HARK | SUTH | Iono free float | 982843.347 | | 9.421 |
| HRAO | HARK | L1 fixed | 2113.791 | 13.1 | 1.157 |
| HRAO | RBTG | Iono free float | 540656.072 | | 3.773 |
| HRAO | SSLR | Iono free float | 981652.108 | | 0.634 |
| MBTG | PETG | Iono free float | 322310.538 | | 3.033 |
| MBTG | SBTG | Iono free float | 341721.872 | | 1.879 |
| PETG | ELTG | Iono free float | 236211.130 | | 2.356 |
| PNTG | SATG | Iono free float | 430345.147 | | 8.482 |
| RBTG | DNTG | Iono free fixed | 155702.018 | 11.0 | 5.401 |
| SBTG | SSLR | Iono free float | 297828.677 | | 3.242 |
| SBTG | TBTG | Iono free fixed | 31358.788 | 22.3 | 0.874 |
| SSLR | MBTG | Iono free float | 235741.316 | | 2.554 |
| SSLR | MBTG | Iono free float | 235741.291 | | 2.175 |
| SSLR | PNTG | Iono free float | 511324.744 | | 8.109 |
| SSLR | SATG | Iono free float | 275916.003 | | 2.450 |
| SSLR | TBTG | Iono free float | 278416.700 | | 3.185 |
| SUTH | ELTG | Iono free float | 669636.140 | | 4.936 |
| SUTH | HRAO | Iono free float | 981212.248 | | 10.718 |
| SUTH | MBTG | Iono free float | 235252.124 | | 1.572 |
| SUTH | PETG | Iono free float | 482295.341 | | 0.282 |
| SUTH | SSLR | L1 float | 762.418 | | 0.891 |
| TBTG | SATG | Iono free fixed | 107250.986 | 13.6 | 3.316 |
| TBTG | UCTN | Iono free fixed | 6376.676 | 17.7 | 1.554 |
| UCTN | SBTG | Iono free fixed | 25547.206 | 17.6 | 1.560 |

**B.5: Precise L1c**-IGS Precise orbits, corrections for troposphere and ionosphere, plus A700288.pct antenna calibration applied.

| From Station Short Name | To Station Short Name | Solution Type | Slope | Ratio | Reference Variance |
|---|---|---|---|---|---|
| DNTG | ELTG | Iono free fixed | 459278.281 | 29.8 | 0.819 |
| DNTG | HARK | Iono free fixed | 550825.253 | 8.7 | 1.741 |
| DNTG | HRAO | Iono free fixed | 551773.700 | 10.5 | 1.005 |
| HARK | ELTG | Iono free fixed | 791275.299 | 29.7 | 1.153 |
| HARK | PNTG | Iono free fixed | 1131787.686 | 5.8 | 2.230 |
| HARK | RBTG | Iono free fixed | 539216.555 | 8.8 | 2.201 |
| HARK | SSLR | Iono free fixed | 983284.025 | 29.4 | 1.514 |
| HARK | SUTH | Iono free fixed | 982843.310 | 20.0 | 0.618 |
| HRAO | ELTG | Iono free fixed | 790988.374 | 5.6 | 1.363 |
| HRAO | HARK | L1 fixed | 2113.791 | 13.1 | 1.150 |
| HRAO | RBTG | Iono free fixed | 540656.040 | 5.3 | 1.503 |
| MBTG | PETG | Iono free fixed | 322310.568 | 5.0 | 14.663 |
| MBTG | SBTG | Iono free fixed | 341721.874 | 3.8 | 19.616 |
| PETG | ELTG | Iono free fixed | 236211.132 | 15.5 | 1.362 |
| PNTG | SATG | Iono free fixed | 430345.168 | 3.3 | 11.144 |
| RBTG | DNTG | Iono free fixed | 155702.019 | 10.5 | 2.482 |
| SBTG | TBTG | Iono free fixed | 31358.789 | 23.9 | 0.797 |
| SSLR | HRAO | Iono free fixed | 981652.166 | 18.0 | 1.953 |
| SSLR | MBTG | Iono free fixed | 235741.328 | 10.7 | 0.687 |
| SSLR | MBTG | Iono free fixed | 235741.321 | 6.1 | 2.018 |
| SSLR | PNTG | Iono free fixed | 511324.750 | 6.4 | 2.731 |
| SSLR | SATG | Iono free fixed | 275916.045 | 16.6 | 10.869 |
| SSLR | SBTG | Iono free fixed | 297828.675 | 6.9 | 0.839 |
| SSLR | SUTH | L1 fixed | 762.422 | 28.3 | 1.067 |
| SSLR | TBTG | Iono free fixed | 278416.693 | 6.0 | 1.285 |
| SUTH | ELTG | Iono free fixed | 669636.133 | 2.1 | 2.530 |
| SUTH | HRAO | Iono free fixed | 981212.282 | 50.9 | 0.555 |
| SUTH | MBTG | Iono free fixed | 235252.154 | 17.1 | 1.124 |
| SUTH | PETG | Iono free fixed | 482295.490 | 7.5 | 9.658 |
| TBTG | SATG | Iono free fixed | 107250.988 | 16.9 | 0.936 |
| TBTG | UCTN | Iono free fixed | 6376.676 | 18.1 | 1.556 |
| UCTN | SBTG | Iono free fixed | 25547.207 | 22.3 | 1.486 |

**B.6: Precise L1c$_{(NOAA)}$**-IGS Precise orbits, corrections for troposphere and ionosphere, but antenna calibration applied with NOAA table.

| From Station Short Name | To Station Short Name | Solution Type | Slope | Ratio | Reference Variance |
|---|---|---|---|---|---|
| DNTG | ELTG | Iono free fixed | 459278.281 | 29.7 | 0.814 |
| DNTG | HARK | Iono free fixed | 550825.250 | 8.9 | 1.700 |
| DNTG | HRAO | Iono free fixed | 551773.692 | 5.2 | 1.621 |
| HARK | ELTG | Iono free fixed | 791275.292 | 30.6 | 1.142 |
| HARK | PNTG | Iono free fixed | 1131787.678 | 5.7 | 2.206 |
| HARK | RBTG | Iono free fixed | 539216.557 | 8.7 | 1.679 |
| HARK | SUTH | Iono free fixed | 982843.313 | 20.2 | 0.614 |
| HRAO | ELTG | Iono free fixed | 790988.366 | 1.8 | 3.668 |
| HRAO | HARK | L1 fixed | 2113.791 | 13.1 | 1.150 |
| HRAO | RBTG | Iono free fixed | 540656.039 | 5.4 | 1.507 |
| HRAO | SSLR | Iono free fixed | 981652.160 | 17.9 | 1.966 |
| MBTG | PETG | Iono free fixed | 322310.567 | 5.0 | 14.666 |
| MBTG | SBTG | Iono free fixed | 341721.910 | 5.3 | 7.733 |
| PETG | ELTG | Iono free fixed | 236211.132 | 15.7 | 1.434 |
| PNTG | SATG | Iono free fixed | 430345.166 | 3.3 | 11.147 |
| RBTG | DNTG | Iono free fixed | 155702.019 | 10.3 | 2.499 |
| SBTG | TBTG | Iono free fixed | 31358.789 | 23.8 | 0.798 |
| SSLR | HARK | Iono free fixed | 983284.029 | 5.7 | 4.642 |
| SSLR | MBTG | Iono free fixed | 235741.328 | 10.5 | 0.661 |
| SSLR | MBTG | Iono free fixed | 235741.324 | 4.0 | 2.068 |
| SSLR | PNTG | Iono free fixed | 511324.749 | 2.6 | 2.730 |
| SSLR | SATG | Iono free fixed | 275916.045 | 16.7 | 10.879 |
| SSLR | SBTG | Iono free fixed | 297828.675 | 8.3 | 0.822 |
| SSLR | SUTH | L1 fixed | 762.422 | 26.5 | 1.097 |
| SSLR | TBTG | Iono free fixed | 278416.706 | 11.8 | 2.382 |
| SUTH | ELTG | Iono free fixed | 669636.125 | 141.1 | 1.404 |
| SUTH | HRAO | Iono free fixed | 981212.282 | 51.0 | 0.555 |
| SUTH | MBTG | Iono free fixed | 235252.152 | 17.7 | 1.103 |
| SUTH | PETG | Iono free fixed | 482295.459 | 13.8 | 4.795 |
| TBTG | SATG | Iono free fixed | 107250.988 | 16.9 | 0.924 |
| TBTG | UCTN | Iono free fixed | 6376.676 | 18.1 | 1.556 |
| UCTN | SBTG | Iono free fixed | 25547.207 | 21.9 | 1.488 |

## Appendix C: RMS Height misclosure

**C.1:** RMS height misclosure for L1c

| Triangle | Obs ht. (m) | Obs ht. (m) | Obs ht. (m) | Delta ht. (m) |
|---|---|---|---|---|
| SSLR-PNTG-SATG | -1694.8738 | -1.7560 | 1696.6625 | 0.0327 |
| TBTG-SATG-SSLR | 0.0955 | 1696.6625 | -1696.7600 | -0.0020 |
| TBTG-SBTG-SSLR | 0.3634 | 1696.4234 | -1696.7600 | 0.0268 |
| SSLR-MBTG-SBTG | -1696.4311 | 0.0166 | 1696.4234 | 0.0089 |
| TBTG-UCTN-SBTG | 132.4164 | -132.0658 | -0.3634 | -0.0128 |
| SSLR-MBTG-SUTH | -1696.3746 | 1766.2888 | -69.8973 | 0.0169 |
| MBTG-PETG-SUTH | -1.7388 | 1767.9723 | -1766.2888 | -0.0553 |
| PETG-ELTG-SUTH | 1.1748 | 1766.6418 | -1767.9723 | -0.1557 |
| SUTH-HRAO-SSLR | -385.5871 | 315.6366 | 69.8973 | -0.0532 |
| RBTG-DNTG-HARK | 2.9804 | 1524.2944 | -1527.2650 | 0.0098 |
| HRAO-ELTG-DNTG | -1381.2988 | -1.7211 | 1383.0602 | 0.0403 |
| HARK-PNTG-SSLR | -1520.4643 | 1694.8738 | -174.4566 | -0.0471 |
| HRAO-RBTG-DNTG | -1386.0286 | 2.9804 | 1383.0602 | 0.0120 |
| HARK-ELTG-SUTH | -1522.5722 | 1766.9836 | -244.3924 | 0.0190 |
| HARK-HRAO-RBTG | -141.2126 | -1386.0286 | 1527.2650 | 0.0238 |
| HARK-HRAO-DNTG | -141.2126 | -1383.0602 | 1524.2944 | 0.0216 |
| HARK-HRAO-ELTG | -141.2126 | -1381.2988 | 1522.5722 | 0.0608 |
| HARK-HRAO-SUTH | -141.2126 | 385.5871 | -244.3924 | -0.0179 |
| HARK-HRAO-SSLR | -141.2126 | 315.6366 | -174.4566 | -0.0326 |
| HARK-ELTG-DNTG | -1522.5722 | -1.7211 | 1524.2944 | 0.0011 |
| SSLR-SUTH-HARK | 69.8973 | -244.3924 | 174.4566 | -0.0385 |
| HRAO-ELTG-SUTH | -1381.2988 | 1766.9836 | -385.5871 | 0.0977 |

**RMS Ht** = 0.0496

**C.2:** RMS height misclosure for L1

| Triangle | Obs ht. (m) | Obs ht. (m) | Obs ht. (m) | Delta ht. (m) |
|---|---|---|---|---|
| SSLR-PNTG-SATG | -1694.9184 | -1.4873 | 1696.3856 | -0.0201 |
| TBTG-SATG-SSLR | 0.1399 | 1696.3856 | -1696.7566 | -0.2311 |
| TBTG-SBTG-SSLR | 0.3762 | 1696.3139 | -1696.7566 | -0.0665 |
| SSLR-MBTG-SBTG | -1696.3817 | 0.0591 | 1696.3139 | -0.0087 |
| TBTG-UCTN-SBTG | 132.4124 | -132.0438 | -0.3762 | -0.0076 |
| SSLR-MBTG-SUTH | -1696.5293 | 1766.3946 | -69.8972 | -0.0319 |
| MBTG-PETG-SUTH | -1.6276 | 1768.5011 | -1766.3946 | 0.4789 |
| PETG-ELTG-SUTH | 1.1868 | 1766.5702 | -1768.5011 | -0.7441 |
| SUTH-HRAO-SSLR | -385.583 | 315.7808 | 69.8972 | 0.0950 |
| RBTG-DNTG-HARK | 3.0899 | 1523.8465 | -1526.9085 | 0.0279 |
| HRAO-ELTG-DNTG | -1380.9652 | -1.6070 | 1382.8525 | 0.2803 |
| HARK-PNTG-SSLR | -1520.4928 | 1694.9184 | -174.6734 | -0.2478 |
| HRAO-RBTG-DNTG | -1385.6825 | 3.0899 | 1382.8525 | 0.2599 |
| HARK-ELTG-SUTH | -1522.1967 | 1766.5705 | -244.3570 | 0.0168 |
| HARK-HRAO-RBTG | -141.2123 | -1385.6825 | 1526.9085 | 0.0137 |
| HARK-HRAO-DNTG | -141.2123 | -1382.8525 | 1523.8465 | -0.2183 |
| HARK-HRAO-ELTG | -141.2123 | -1380.9652 | 1522.1967 | 0.0192 |
| HARK-HRAO-SUTH | -141.2123 | 385.5830 | -244.3570 | 0.0137 |
| HARK-HRAO-SSLR | -141.2123 | 315.7808 | -174.6734 | -0.1049 |
| HARK-ELTG-DNTG | -1522.1967 | -1.6070 | 1523.8465 | 0.0428 |
| SSLR-SUTH-HARK | 69.8972 | -244.3570 | 174.6734 | 0.2136 |
| HRAO-ELTG-SUTH | -1380.9652 | 1766.5705 | -385.5830 | 0.0223 |

**RMS Ht** = 0.2303

**C.3:** RMS height misclosure for $L1c_{(-trop)}$

| Triangle | Obs ht. (m) | Obs ht. (m) | Obs ht. (m) | Delta ht. (m) |
|---|---|---|---|---|
| SSLR-PNTG-SATG | -1693.7327 | -1.9202 | 1695.4029 | -0.2500 |
| TBTG-SATG-SSLR | 0.0954 | 1695.4029 | -1695.4502 | 0.0481 |
| TBTG-SBTG-SSLR | 0.3720 | 1695.0991 | -1695.4502 | 0.0209 |
| SSLR-MBTG-SBTG | -1695.1948 | -0.0394 | 1695.0991 | -0.1351 |
| TBTG-UCTN-SBTG | 132.2970 | -131.9411 | -0.3720 | -0.0161 |
| SSLR-MBTG-SUTH | -1695.1255 | 1764.9835 | -69.8401 | 0.0179 |
| MBTG-PETG-SUTH | -1.8418 | 1766.8684 | -1764.9835 | 0.0431 |
| PETG-ELTG-SUTH | 1.1173 | 1765.5847 | -1766.8684 | -0.1664 |
| SUTH-HRAO-SSLR | -385.4949 | 315.5735 | 69.8401 | -0.0813 |
| RBTG-DNTG-HARK | 3.0625 | 1522.8886 | -1525.5745 | 0.3766 |
| HRAO-ELTG-DNTG | -1380.5477 | -1.8608 | 1381.9519 | -0.4566 |
| HARK-PNTG-SSLR | -1519.5948 | 1693.7327 | -174.3642 | -0.2263 |
| HRAO-RBTG-DNTG | -1384.5492 | 3.0625 | 1381.9519 | 0.4652 |
| HARK-ELTG-SUTH | -1521.7008 | 1765.5847 | -244.3439 | -0.4600 |
| HARK-HRAO-RBTG | -141.0950 | -1384.5492 | 1525.5745 | -0.0697 |
| HARK-HRAO-DNTG | -141.0950 | -1381.9519 | 1522.8886 | -0.1583 |
| HARK-HRAO-ELTG | -141.0950 | -1380.5477 | 1521.7008 | 0.0581 |
| HARK-HRAO-SUTH | -141.0950 | 385.4949 | -244.3439 | 0.0560 |
| HARK-HRAO-SSLR | -141.0950 | 315.5735 | -174.3642 | 0.1143 |
| HARK-ELTG-DNTG | -1521.7008 | -1.8608 | 1522.8886 | -0.6730 |
| SSLR-SUTH-HARK | 69.8401 | -244.3439 | 174.3642 | -0.1396 |
| HRAO-ELTG-SUTH | -1380.5477 | 1765.5847 | -385.4949 | -0.4579 |

**RMS Ht** = 0.2764

**C.4:** RMS height misclosure for $L1c_{(-Ant)}$

| Triangle | Obs ht. (m) | Obs ht. (m) | Obs ht. (m) | Delta ht. (m) |
|---|---|---|---|---|
| SSLR-PNTG-SATG | -1694.8672 | -1.7602 | 1696.6590 | 0.0316 |
| TBTG-SATG-SSLR | 0.0963 | 1696.6590 | -1696.7568 | -0.0015 |
| TBTG-SBTG-SSLR | 0.3633 | 1696.4207 | -1696.7568 | 0.0272 |
| SSLR-MBTG-SBTG | -1696.4335 | 0.0225 | 1696.4207 | 0.0097 |
| TBTG-UCTN-SBTG | 132.4162 | -132.0659 | -0.3633 | -0.0130 |
| SSLR-MBTG-SUTH | -1696.3771 | 1766.2842 | -69.8807 | 0.0264 |
| MBTG-PETG-SUTH | -1.7446 | 1767.9968 | -1766.2842 | -0.0320 |
| PETG-ELTG-SUTH | 1.1711 | 1766.9641 | -1767.9968 | 0.1384 |
| SUTH-HRAO-SSLR | -385.6516 | 315.6896 | 69.8807 | -0.0813 |
| RBTG-DNTG-HARK | 2.9855 | 1524.2781 | -1527.2502 | 0.0134 |
| HRAO-ELTG-DNTG | -1381.4382 | -1.7251 | 1383.0461 | -0.1172 |
| HARK-PNTG-SSLR | -1520.4549 | 1694.8672 | -174.4677 | -0.0554 |
| HRAO-RBTG-DNTG | -1386.0357 | 2.9855 | 1383.0461 | -0.0041 |
| HARK-ELTG-SUTH | -1522.5207 | 1766.9641 | -244.3965 | 0.0469 |
| HARK-HRAO-RBTG | -141.2125 | -1386.0357 | 1527.2502 | 0.0020 |
| HARK-HRAO-DNTG | -141.2125 | -1383.0461 | 1524.2781 | 0.0195 |
| HARK-HRAO-ELTG | -141.2125 | -1381.4382 | 1522.5207 | -0.1300 |
| HARK-HRAO-SUTH | -141.2125 | 385.6516 | -244.3965 | 0.0426 |
| HARK-HRAO-SSLR | -141.2125 | 315.6896 | -174.4677 | 0.0094 |
| HARK-ELTG-DNTG | -1522.5207 | -1.7251 | 1524.2781 | 0.0323 |
| SSLR-SUTH-HARK | 69.8807 | -244.3965 | 174.4677 | -0.0481 |
| HRAO-ELTG-SUTH | -1381.4382 | 1766.9641 | -385.6516 | -0.1257 |

**RMS Ht** = 0.0629

**C.5:** RMS height misclosure for precise L1c

| Triangle | Obs ht. (m) | Obs ht. (m) | Obs ht. (m) | Delta ht. (m) |
|---|---|---|---|---|
| SSLR-PNTG-SATG | -1694.8723 | -1.8274 | 1696.6153 | -0.0844 |
| TBTG-SATG-SSLR | 0.1418 | 1696.6153 | -1696.7969 | -0.0398 |
| TBTG-SBTG-SSLR | 0.3573 | 1696.4395 | -1696.7969 | -0.0001 |
| SSLR-MBTG-SBTG | -1696.4696 | 0.0798 | 1696.4395 | 0.0497 |
| TBTG-UCTN-SBTG | 132.4161 | -132.0710 | -0.3573 | -0.0122 |
| SSLR-MBTG-SUTH | -1696.4374 | 1766.3448 | -69.8972 | 0.0102 |
| MBTG-PETG-SUTH | -1.7292 | 1768.1157 | -1766.3448 | 0.0417 |
| PETG-ELTG-SUTH | 1.1804 | 1766.9402 | -1768.1157 | 0.0049 |
| SUTH-HRAO-SSLR | -385.5639 | 315.6425 | 69.8972 | -0.0242 |
| RBTG-DNTG-HARK | 2.9807 | 1524.2204 | -1527.2236 | -0.0225 |
| HRAO-ELTG-DNTG | -1381.3258 | -1.6586 | 1383.0277 | 0.0433 |
| HARK-PNTG-SSLR | -1520.4340 | 1694.8723 | -174.4411 | -0.0028 |
| HRAO-RBTG-DNTG | -1386.0223 | 2.9807 | 1383.0277 | -0.0139 |
| HARK-ELTG-SUTH | -1522.5529 | 1766.9402 | -244.3605 | 0.0268 |
| HARK-HRAO-RBTG | -141.2125 | -1386.0223 | 1527.2236 | -0.0112 |
| HARK-HRAO-DNTG | -141.2125 | -1383.0277 | 1524.2204 | -0.0198 |
| HARK-HRAO-ELTG | -141.2125 | -1381.3258 | 1522.5529 | 0.0146 |
| HARK-HRAO-SUTH | -141.2125 | 385.5639 | -244.3605 | -0.0091 |
| HARK-HRAO-SSLR | -141.2125 | 315.6425 | -174.4411 | -0.0111 |
| HARK-ELTG-DNTG | -1522.5529 | -1.6586 | 1524.2204 | 0.0089 |
| SSLR-SUTH-HARK | 69.8972 | -244.3605 | 174.4411 | -0.0222 |
| HRAO-ELTG-SUTH | -1381.3258 | 1766.9402 | -385.5639 | 0.0505 |

**RMS Ht** = 0.0310

**C.6:** RMS height misclosure for precise $L1c_{(NOAA)}$

| Triangle | Obs ht. (m) | Obs ht. (m) | Obs ht. (m) | Delta ht. (m) |
|---|---|---|---|---|
| SSLR-PNTG-SATG | -1694.8700 | -1.8283 | 1696.6142 | -0.0841 |
| TBTG-SATG-SSLR | 0.1416 | 1696.6142 | -1696.7991 | -0.0433 |
| TBTG-SBTG-SSLR | 0.3573 | 1696.4398 | -1696.7991 | -0.0020 |
| SSLR-MBTG-SBTG | -1696.4704 | 0.0122 | 1696.4398 | -0.0184 |
| TBTG-UCTN-SBTG | 132.4161 | -132.0708 | -0.3573 | -0.0120 |
| SSLR-MBTG-SUTH | -1696.4295 | 1766.3642 | -69.8932 | 0.0415 |
| MBTG-PETG-SUTH | -1.7280 | 1768.1287 | -1766.3642 | 0.0365 |
| PETG-ELTG-SUTH | 1.1818 | 1766.9867 | -1768.1287 | 0.0398 |
| SUTH-HRAO-SSLR | -385.5597 | 315.6179 | 69.8932 | -0.0486 |
| RBTG-DNTG-HARK | 2.9790 | 1524.2378 | -1527.2523 | -0.0355 |
| HRAO-ELTG-DNTG | -1381.3727 | -1.6544 | 1383.0410 | 0.0139 |
| HARK-PNTG-SSLR | -1520.4517 | 1694.8700 | -174.4077 | 0.0106 |
| HRAO-RBTG-DNTG | -1386.0335 | 2.9790 | 1383.0410 | -0.0135 |
| HARK-ELTG-SUTH | -1522.5750 | 1766.9867 | -244.3560 | 0.0557 |
| HARK-HRAO-RBTG | -141.2126 | -1386.0335 | 1527.2523 | 0.0062 |
| HARK-HRAO-DNTG | -141.2126 | -1383.0410 | 1524.2378 | -0.0158 |
| HARK-HRAO-ELTG | -141.2126 | -1381.3727 | 1522.5750 | -0.0103 |
| HARK-HRAO-SUTH | -141.2126 | 385.5597 | -244.3560 | -0.0089 |
| HARK-HRAO-SSLR | -141.2126 | 315.6179 | -174.4077 | -0.0024 |
| HARK-ELTG-DNTG | -1522.5750 | -1.6544 | 1524.2378 | 0.0084 |
| SSLR-SUTH-HARK | 69.8932 | -244.3560 | 174.4077 | -0.0551 |
| HRAO-ELTG-SUTH | -1381.3727 | 1766.9867 | -385.5597 | 0.0543 |

**RMS Ht** = 0.0356

## Appendix D: XForm-Datum Transformation parameters

**D.1:** Translations and Scale factor for L1c/L1

DETERMINATION OF DATUM TRANSFORMATION PARAMETERS

SOURCE DATUM CO-ORDINATES (L1)
(Ellipsoidal Heights)

| Name | Latitude | Longitude | Height |
|---|---|---|---|
| DNTG | -29 52 27.36501 | 31 03 03.52957 | 31.601 |
| ELTG | -33 01 37.79680 | 27 54 52.90499 | 33.076 |
| HARK | -25 53 13.59274 | 27 42 27.92812 | 1555.408 |
| HRAO | -25 53 24.38254 | 27 41 13.12495 | 1414.196 |
| MBTG | -34 10 46.58916 | 22 08 49.71317 | 33.466 |
| PETG | -33 57 35.26607 | 25 37 45.48579 | 31.817 |
| PNTG | -29 15 24.63753 | 16 52 02.53461 | 34.918 |
| RBTG | -28 47 45.33271 | 32 04 42.47235 | 28.502 |
| SATG | -33 01 24.75796 | 17 57 37.57296 | 33.417 |
| SBTG | -34 11 17.43872 | 18 26 22.65889 | 33.578 |
| SSLR | -32 22 45.04734 | 20 48 08.96170 | 1729.922 |
| SUTH | -32 22 48.75044 | 20 48 37.66864 | 1799.819 |
| TBTG | -33 54 19.86420 | 18 26 00.56615 | 33.206 |
| UCTN | -33 57 30.62739 | 18 27 36.70020 | 165.619 |

TARGET DATUM CO-ORDINATES (L1c)
(Ellipsoidal Heights)

| Name | Latitude | Longitude | Height |
|---|---|---|---|
| DNTG | -29 52 27.37206 | 31 03 03.53230 | 31.141 |
| ELTG | -33 01 37.80777 | 27 54 52.90786 | 32.866 |
| HARK | -25 53 13.59274 | 27 42 27.92812 | 1555.409 |
| HRAO | -25 53 24.38254 | 27 41 13.12495 | 1414.196 |
| MBTG | -34 10 46.60559 | 22 08 49.70657 | 33.437 |
| PETG | -33 57 35.28007 | 25 37 45.48371 | 31.697 |
| PNTG | -29 15 24.64251 | 16 52 02.51771 | 34.956 |
| RBTG | -28 47 45.33666 | 32 04 42.47704 | 28.161 |
| SATG | -33 01 24.77123 | 17 57 37.55484 | 33.187 |
| SBTG | -34 11 17.45476 | 18 26 22.64237 | 33.445 |
| SSLR | -32 22 45.05976 | 20 48 08.95083 | 1729.851 |
| SUTH | -32 22 48.76285 | 20 48 37.65776 | 1799.748 |
| TBTG | -33 54 19.87959 | 18 26 00.54960 | 33.087 |
| UCTN | -33 57 30.64287 | 18 27 36.68370 | 165.507 |

DATUM TRANSFORMATION PARAMETERS

X-shift : -2.348 ± 0.206 metres
Y-shift : -1.224 ± 0.091 metres
Z-shift : 1.236 ± 0.138 metres

Scale Factor : 1.0000004 ± 0.0000000
0.4318 ppm ± 0.0411 ppm

RMS ERROR : 0.0888 metres

RESIDUALS (Cartesian)

| Name | X | Y | Z |
|---|---|---|---|
| DNTG | 0.172 | 0.207 | -0.169 |
| ELTG | 0.048 | -0.039 | -0.088 |
| HARK | -0.153 | -0.072 | 0.040 |
| HRAO | -0.151 | -0.072 | 0.040 |
| MBTG | -0.013 | -0.092 | 0.099 |
| PETG | -0.002 | -0.040 | -0.004 |
| PNTG | -0.138 | -0.078 | 0.050 |
| RBTG | 0.070 | 0.141 | -0.141 |
| SATG | 0.102 | 0.064 | -0.040 |
| SBTG | 0.050 | 0.021 | 0.031 |
| SSLR | -0.024 | -0.037 | 0.054 |
| SUTH | -0.024 | -0.037 | 0.053 |
| TBTG | 0.034 | 0.018 | 0.035 |
| UCTN | 0.029 | 0.015 | 0.039 |

RESIDUALS (Geographical - Metres)

| Name | Latitude | Longitude | Height |
|---|---|---|---|
| DNTG | -0.020 | 0.088 | 0.305 |
| ELTG | -0.061 | -0.057 | 0.068 |
| HARK | -0.037 | 0.008 | -0.169 |
| HRAO | -0.037 | 0.007 | -0.168 |
| MBTG | 0.056 | -0.080 | -0.094 |
| PETG | -0.013 | -0.035 | -0.014 |
| PNTG | -0.032 | -0.034 | -0.160 |
| RBTG | -0.059 | 0.082 | 0.185 |
| SATG | 0.030 | 0.029 | 0.119 |
| SBTG | 0.056 | 0.004 | 0.028 |
| SSLR | 0.026 | -0.026 | -0.059 |
| SUTH | 0.026 | -0.026 | -0.059 |
| TBTG | 0.050 | 0.006 | 0.012 |
| UCTN | 0.050 | 0.006 | 0.005 |

## D.2: Translations, Scale factor and Rotations for L1c/L1

DETERMINATION OF DATUM TRANSFORMATION PARAMETERS

SOURCE DATUM CO-ORDINATES (L1)
(Ellipsoidal Heights)

| Name | Latitude | Longitude | Height |
|---|---|---|---|
| DNTG | -29 52 27.36501 | 31 03 03.52957 | 31.601 |
| ELTG | -33 01 37.79680 | 27 54 52.90499 | 33.076 |
| HARK | -25 53 13.59274 | 27 42 27.92812 | 1555.408 |
| HRAO | -25 53 24.38254 | 27 41 13.12495 | 1414.196 |
| MBTG | -34 10 46.58916 | 22 08 49.71317 | 33.466 |
| PETG | -33 57 35.26607 | 25 37 45.48579 | 31.817 |
| PNTG | -29 15 24.63753 | 16 52 02.53461 | 34.918 |
| RBTG | -28 47 45.33271 | 32 04 42.47235 | 28.502 |
| SATG | -33 01 24.75796 | 17 57 37.57296 | 33.417 |
| SBTG | -34 11 17.43872 | 18 26 22.65889 | 33.578 |
| SSLR | -32 22 45.04734 | 20 48 08.96170 | 1729.922 |
| SUTH | -32 22 48.75044 | 20 48 37.66864 | 1799.819 |
| TBTG | -33 54 19.86420 | 18 26 00.56615 | 33.206 |
| UCTN | -33 57 30.62739 | 18 27 36.70020 | 165.619 |

TARGET DATUM CO-ORDINATES (L1c)
(Ellipsoidal Heights)

| Name | Latitude | Longitude | Height |
|---|---|---|---|
| DNTG | -29 52 27.37206 | 31 03 03.53230 | 31.141 |
| ELTG | -33 01 37.80777 | 27 54 52.90786 | 32.866 |
| HARK | -25 53 13.59274 | 27 42 27.92812 | 1555.409 |
| HRAO | -25 53 24.38254 | 27 41 13.12495 | 1414.196 |
| MBTG | -34 10 46.60559 | 22 08 49.70657 | 33.437 |
| PETG | -33 57 35.28007 | 25 37 45.48371 | 31.697 |
| PNTG | -29 15 24.64251 | 16 52 02.51771 | 34.956 |
| RBTG | -28 47 45.33666 | 32 04 42.47704 | 28.161 |
| SATG | -33 01 24.77123 | 17 57 37.55484 | 33.187 |
| SBTG | -34 11 17.45476 | 18 26 22.64237 | 33.445 |
| SSLR | -32 22 45.05976 | 20 48 08.95083 | 1729.851 |
| SUTH | -32 22 48.76285 | 20 48 37.65776 | 1799.748 |
| TBTG | -33 54 19.87959 | 18 26 00.54960 | 33.087 |
| UCTN | -33 57 30.64287 | 18 27 36.68370 | 165.507 |

DATUM TRANSFORMATION PARAMETERS

X-shift : -1.047 ± 0.343 metres
Y-shift : -1.984 ± 0.248 metres
Z-shift : 2.697 ± 0.406 metres

Scale Factor : 1.0000004 ± 0.0000000
0.4318 ppm ± 0.0332 ppm

X-rotation : -0.00608 ± 0.00750 seconds
Y-rotation : -0.06323 ± 0.01492 seconds
Z-rotation : -0.02748 ± 0.00914 seconds

RMS ERROR : 0.0716 metres

RESIDUALS (Cartesian)

| Name | X | Y | Z |
|---|---|---|---|
| DNTG | 0.124 | 0.172 | -0.078 |
| ELTG | -0.045 | -0.067 | -0.003 |
| HARK | -0.057 | -0.072 | 0.021 |
| HRAO | -0.056 | -0.073 | 0.021 |
| MBTG | -0.070 | -0.095 | 0.119 |
| PETG | -0.093 | -0.059 | 0.061 |
| PNTG | -0.004 | -0.036 | -0.075 |
| RBTG | 0.038 | 0.102 | -0.045 |
| SATG | 0.123 | 0.084 | -0.091 |
| SBTG | 0.035 | 0.034 | 0.005 |
| SSLR | -0.020 | -0.026 | 0.026 |
| SUTH | -0.021 | -0.025 | 0.026 |
| TBTG | 0.026 | 0.032 | 0.004 |
| UCTN | 0.019 | 0.029 | 0.009 |

RESIDUALS (Geographical - Metres)

| Name | Latitude | Longitude | Height |
|---|---|---|---|
| DNTG | 0.030 | 0.083 | 0.208 |
| ELTG | -0.042 | -0.038 | -0.058 |
| HARK | -0.017 | -0.038 | -0.085 |
| HRAO | -0.018 | -0.038 | -0.084 |
| MBTG | 0.042 | -0.061 | -0.150 |
| PETG | -0.010 | -0.013 | -0.125 |
| PNTG | -0.073 | -0.034 | 0.025 |
| RBTG | 0.002 | 0.066 | 0.097 |
| SATG | 0.002 | 0.042 | 0.169 |
| SBTG | 0.029 | 0.021 | 0.034 |
| SSLR | 0.007 | -0.017 | -0.037 |
| SUTH | 0.006 | -0.016 | -0.037 |
| TBTG | 0.023 | 0.022 | 0.026 |
| UCTN | 0.023 | 0.022 | 0.018 |

## D.3: Translations and Scale factor for L1c/L1c$_{(-trop)}$

DETERMINATION OF DATUM TRANSFORMATION PARAMETERS

SOURCE DATUM CO-ORDINATES (L1c$_{(-trop)}$)
(Ellipsoidal Heights)

| Name | Latitude | Longitude | Height |
|---|---|---|---|
| DNTG | -29 52 27.38740 | 31 03 03.54312 | 32.529 |
| ELTG | -33 01 37.83710 | 27 54 52.90578 | 33.740 |
| HARK | -25 53 13.59266 | 27 42 27.92826 | 1555.291 |
| HRAO | -25 53 24.38254 | 27 41 13.12495 | 1414.196 |
| MBTG | -34 10 46.63894 | 22 08 49.68490 | 34.535 |
| PETG | -33 57 35.31356 | 25 37 45.47350 | 32.653 |
| PNTG | -29 15 24.65025 | 16 52 02.47160 | 36.038 |
| RBTG | -28 47 45.34859 | 32 04 42.48934 | 29.500 |
| SATG | -33 01 24.79665 | 17 57 37.51532 | 34.267 |
| SBTG | -34 11 17.48654 | 18 26 22.60487 | 34.542 |
| SSLR | -32 22 45.08312 | 20 48 08.92446 | 1729.707 |
| SUTH | -32 22 48.78623 | 20 48 37.63144 | 1799.547 |
| TBTG | -33 54 19.90991 | 18 26 00.51225 | 34.176 |
| UCTN | -33 57 30.67349 | 18 27 36.64655 | 166.476 |

TARGET DATUM CO-ORDINATES (L1c)
(Ellipsoidal Heights)

| Name | Latitude | Longitude | Height |
|---|---|---|---|
| DNTG | -29 52 27.37206 | 31 03 03.53230 | 31.141 |
| ELTG | -33 01 37.80777 | 27 54 52.90786 | 32.866 |
| HARK | -25 53 13.59274 | 27 42 27.92812 | 1555.409 |
| HRAO | -25 53 24.38254 | 27 41 13.12495 | 1414.196 |
| MBTG | -34 10 46.60559 | 22 08 49.70657 | 33.437 |
| PETG | -33 57 35.28007 | 25 37 45.48371 | 31.697 |
| PNTG | -29 15 24.64251 | 16 52 02.51771 | 34.956 |
| RBTG | -28 47 45.33666 | 32 04 42.47704 | 28.161 |
| SATG | -33 01 24.77123 | 17 57 37.55484 | 33.187 |
| SBTG | -34 11 17.45476 | 18 26 22.64237 | 33.445 |
| SSLR | -32 22 45.05976 | 20 48 08.95083 | 1729.851 |
| SUTH | -32 22 48.76285 | 20 48 37.65776 | 1799.748 |
| TBTG | -33 54 19.87959 | 18 26 00.54960 | 33.087 |
| UCTN | -33 57 30.64287 | 18 27 36.68370 | 165.507 |

DATUM TRANSFORMATION PARAMETERS

X-shift : 5.335 ± 0.780 metres
Y-shift : 2.821 ± 0.346 metres
Z-shift : -2.869 ± 0.523 metres

Scale Factor : 0.9999988 ± 0.0000002
-1.1535 ppm ± 0.1558 ppm

RMS ERROR : 0.3365 metres

RESIDUALS (Cartesian)

| Name | X | Y | Z |
|---|---|---|---|
| DNTG | 0.545 | 0.276 | -0.327 |
| ELTG | 0.117 | -0.005 | -0.116 |
| HARK | -0.625 | -0.305 | 0.379 |
| HRAO | -0.531 | -0.257 | 0.325 |
| MBTG | 0.208 | 0.135 | -0.226 |
| PETG | 0.136 | 0.036 | -0.172 |
| PNTG | 0.341 | 0.006 | -0.031 |
| RBTG | 0.535 | 0.206 | -0.313 |
| SATG | 0.233 | 0.089 | -0.127 |
| SBTG | 0.198 | 0.096 | -0.184 |
| SSLR | -0.709 | -0.213 | 0.519 |
| SUTH | -0.755 | -0.230 | 0.549 |
| TBTG | 0.203 | 0.099 | -0.171 |
| UCTN | 0.105 | 0.069 | -0.106 |

RESIDUALS (Geographical - Metres)

| Name | Latitude | Longitude | Height |
|---|---|---|---|
| DNTG | 0.020 | -0.045 | 0.691 |
| ELTG | -0.042 | -0.059 | 0.147 |
| HARK | 0.037 | 0.021 | -0.790 |
| HRAO | 0.035 | 0.019 | -0.672 |
| MBTG | -0.050 | 0.046 | 0.328 |
| PETG | -0.065 | -0.026 | 0.211 |
| PNTG | 0.133 | -0.093 | 0.301 |
| RBTG | -0.003 | -0.109 | 0.644 |
| SATG | 0.029 | 0.012 | 0.278 |
| SBTG | -0.030 | 0.028 | 0.284 |
| SSLR | 0.043 | 0.052 | -0.902 |
| SUTH | 0.042 | 0.053 | -0.959 |
| TBTG | -0.017 | 0.029 | 0.281 |
| UCTN | -0.020 | 0.032 | 0.160 |

**D.4:** Translations, Scale factor and Rotations for L1c/ $L1c_{(-trop)}$

DETERMINATION OF DATUM TRANSFORMATION PARAMETERS

SOURCE DATUM CO-ORDINATES ($L1c_{(-trop)}$)

(Ellipsoidal Heights)

| Name | Latitude | Longitude | Height |
|---|---|---|---|
| DNTG | -29 52 27.38740 | 31 03 03.54312 | 32.529 |
| ELTG | -33 01 37.83710 | 27 54 52.90578 | 33.740 |
| HARK | -25 53 13.59266 | 27 42 27.92826 | 1555.291 |
| HRAO | -25 53 24.38254 | 27 41 13.12495 | 1414.196 |
| MBTG | -34 10 46.63894 | 22 08 49.68490 | 34.535 |
| PETG | -33 57 35.31356 | 25 37 45.47350 | 32.653 |
| PNTG | -29 15 24.65025 | 16 52 02.47160 | 36.038 |
| RBTG | -28 47 45.34859 | 32 04 42.48934 | 29.500 |
| SATG | -33 01 24.79665 | 17 57 37.51532 | 34.267 |
| SBTG | -34 11 17.48654 | 18 26 22.60487 | 34.542 |
| SSLR | -32 22 45.08312 | 20 48 08.92446 | 1729.707 |
| SUTH | -32 22 48.78623 | 20 48 37.63144 | 1799.547 |
| TBTG | -33 54 19.90991 | 18 26 00.51225 | 34.176 |
| UCTN | -33 57 30.67349 | 18 27 36.64655 | 166.476 |

TARGET DATUM CO-ORDINATES (L1c)

(Ellipsoidal Heights)

| Name | Latitude | Longitude | Height |
|---|---|---|---|
| DNTG | -29 52 27.37206 | 31 03 03.53230 | 31.141 |
| ELTG | -33 01 37.80777 | 27 54 52.90786 | 32.866 |
| HARK | -25 53 13.59274 | 27 42 27.92812 | 1555.409 |
| HRAO | -25 53 24.38254 | 27 41 13.12495 | 1414.196 |
| MBTG | -34 10 46.60559 | 22 08 49.70657 | 33.437 |
| PETG | -33 57 35.28007 | 25 37 45.48371 | 31.697 |
| PNTG | -29 15 24.64251 | 16 52 02.51771 | 34.956 |
| RBTG | -28 47 45.33666 | 32 04 42.47704 | 28.161 |
| SATG | -33 01 24.77123 | 17 57 37.55484 | 33.187 |
| SBTG | -34 11 17.45476 | 18 26 22.64237 | 33.445 |
| SSLR | -32 22 45.05976 | 20 48 08.95083 | 1729.851 |
| SUTH | -32 22 48.76285 | 20 48 37.65776 | 1799.748 |
| TBTG | -33 54 19.87959 | 18 26 00.54960 | 33.087 |
| UCTN | -33 57 30.64287 | 18 27 36.68370 | 165.507 |

DATUM TRANSFORMATION PARAMETERS

```
X-shift :    9.168 ±   1.502 metres
Y-shift :    1.608 ±   1.088 metres
Z-shift :    2.106 ±   1.777 metres

Scale Factor :  0.9999988  ±  0.0000001
                -1.1535 ppm ±  0.1452 ppm
```

X-rotation : 0.03721 ± 0.03283 seconds
Y-rotation : -0.19030 ± 0.06534 seconds
Z-rotation : -0.07507 ± 0.04003 seconds

RMS ERROR : 0.3136 metres

RESIDUALS (Cartesian)

| Name | X | Y | Z |
|---|---|---|---|
| DNTG | 0.425 | 0.219 | -0.241 |
| ELTG | -0.151 | -0.120 | 0.044 |
| HARK | -0.318 | -0.167 | 0.181 |
| HRAO | -0.223 | -0.119 | 0.127 |
| MBTG | 0.029 | 0.059 | -0.124 |
| PETG | -0.133 | -0.079 | -0.015 |
| PNTG | 0.727 | 0.173 | -0.264 |
| RBTG | 0.469 | 0.167 | -0.246 |
| SATG | 0.277 | 0.105 | -0.148 |
| SBTG | 0.136 | 0.063 | -0.133 |
| SSLR | -0.707 | -0.204 | 0.497 |
| SUTH | -0.753 | -0.221 | 0.527 |
| TBTG | 0.162 | 0.077 | -0.136 |
| UCTN | 0.060 | 0.045 | -0.068 |

RESIDUALS (Geographical - Metres)

| Name | Latitude | Longitude | Height |
|---|---|---|---|
| DNTG | 0.028 | -0.032 | 0.534 |
| ELTG | -0.067 | -0.035 | -0.183 |
| HARK | 0.006 | 0.000 | -0.402 |
| HRAO | 0.004 | -0.002 | -0.283 |
| MBTG | -0.075 | 0.044 | 0.110 |
| PETG | -0.099 | -0.013 | -0.119 |
| PNTG | 0.134 | -0.045 | 0.780 |
| RBTG | 0.018 | -0.107 | 0.545 |
| SATG | 0.037 | 0.015 | 0.329 |
| SBTG | -0.027 | 0.017 | 0.198 |
| SSLR | 0.027 | 0.060 | -0.886 |
| SUTH | 0.026 | 0.060 | -0.943 |
| TBTG | -0.013 | 0.022 | 0.224 |
| UCTN | -0.017 | 0.024 | 0.097 |

## Appendix E: Tables of Coordinates and Standard errors

**E.1:** Final positions - ITRF97(1998.0) reference frame, WGS84 ellipsoid.
Network constrained at HRAO (Broadcast L1c).

| Site code | Latitude ° ′ ″ | Longitude ° ′ ″ | Height (metres) | $\sigma_\phi$ | $\sigma_\lambda$ | $\sigma_h$ |
|---|---|---|---|---|---|---|
| | | | | (metres) | | |
| DNTG | -29 52 27.37206 | 031 03 03.53230 | 31.141 | 0.009 | 0.018 | 0.045 |
| ELTG | -33 01 37.80777 | 027 54 52.90786 | 32.866 | 0.010 | 0.020 | 0.053 |
| HARK | -25 53 13.59274 | 027 42 27.92812 | 1555.409 | 0.001 | 0.001 | 0.008 |
| HRAO | -25 53 24.38254 | 027 41 13.12495 | 1414.196 | 0.000 | 0.000 | 0.000 |
| MBTG | -34 10 46.60559 | 022 08 49.70657 | 33.437 | 0.010 | 0.019 | 0.048 |
| PETG | -33 57 35.28007 | 025 37 45.48371 | 31.697 | 0.010 | 0.020 | 0.052 |
| PNTG | -29 15 24.64251 | 016 52 02.51771 | 34.956 | 0.012 | 0.026 | 0.059 |
| RBTG | -28 47 45.33666 | 032 04 42.47704 | 28.161 | 0.008 | 0.018 | 0.042 |
| SATG | -33 01 24.77123 | 017 57 37.55484 | 33.187 | 0.010 | 0.020 | 0.054 |
| SBTG | -34 11 17.45476 | 018 26 22.64237 | 33.445 | 0.010 | 0.020 | 0.051 |
| SSLR | -32 22 45.05976 | 020 48 08.95083 | 1729.851 | 0.009 | 0.019 | 0.046 |
| SUTH | -32 22 48.76285 | 020 48 37.65776 | 1799.748 | 0.010 | 0.019 | 0.046 |
| TBTG | -33 54 19.87959 | 018 26 00.54960 | 33.087 | 0.010 | 0.020 | 0.052 |
| UCTN | -33 57 30.64287 | 018 27 36.68370 | 165.507 | 0.010 | 0.020 | 0.054 |

**E.2:** Final positions - ITRF97(1998.0) reference frame, WGS84 ellipsoid.
Network constrained at HRAO and SUTH (Broadcast L1c).

| Site code | Latitude ° ′ ″ | Longitude ° ′ ″ | Height (metres) | $\sigma_\phi$ | $\sigma_\lambda$ | $\sigma_h$ |
|---|---|---|---|---|---|---|
| | | | | (metres) | | |
| DNTG | -29 52 27.37045 | 031 03 03.53269 | 31.142 | 0.014 | 0.018 | 0.044 |
| ELTG | -33 01 37.80627 | 027 54 52.90979 | 32.883 | 0.012 | 0.017 | 0.042 |
| HARK | -25 53 13.59273 | 027 42 27.92812 | 1555.410 | 0.001 | 0.001 | 0.008 |
| HRAO | -25 53 24.38254 | 027 41 13.12495 | 1414.196 | 0.000 | 0.000 | 0.000 |
| MBTG | -34 10 46.60505 | 022 08 49.71009 | 33.459 | 0.006 | 0.008 | 0.020 |
| PETG | -33 57 35.27885 | 025 37 45.48643 | 31.716 | 0.010 | 0.015 | 0.036 |
| PNTG | -29 15 24.64421 | 016 52 02.52089 | 34.972 | 0.014 | 0.021 | 0.046 |
| RBTG | -28 47 45.33505 | 032 04 42.47688 | 28.162 | 0.013 | 0.018 | 0.041 |
| SATG | -33 01 24.77184 | 017 57 37.55889 | 33.209 | 0.006 | 0.011 | 0.031 |
| SBTG | -34 11 17.45501 | 018 26 22.64667 | 33.468 | 0.005 | 0.011 | 0.025 |
| SSLR | -32 22 45.05989 | 020 48 08.95408 | 1729.875 | 0.001 | 0.001 | 0.008 |
| SUTH | -32 22 48.76298 | 020 48 37.66102 | 1799.773 | 0.000 | 0.000 | 0.000 |
| TBTG | -33 54 19.87990 | 018 26 00.55381 | 33.110 | 0.005 | 0.010 | 0.026 |
| UCTN | -33 57 30.64317 | 018 27 36.68793 | 165.529 | 0.005 | 0.011 | 0.030 |

**E.3:** Final positions - ITRF97(1998.0) reference frame, WGS84 ellipsoid.
Network constrained at HRAO (Broadcast L1).

| Site code | Latitude ° ′ ″ | Longitude ° ′ ″ | Height (metres) | $\sigma_\phi$ | $\sigma_\lambda$ | $\sigma_h$ |
|---|---|---|---|---|---|---|
| | | | | (metres) | | |
| DNTG | -29 52 27.36501 | 031 03 03.52957 | 31.601 | 0.027 | 0.059 | 0.132 |
| ELTG | -33 01 37.79680 | 027 54 52.90499 | 33.076 | 0.029 | 0.050 | 0.132 |
| HARK | -25 53 13.59274 | 027 42 27.92812 | 1555.408 | 0.001 | 0.001 | 0.006 |
| HRAO | -25 53 24.38254 | 027 41 13.12495 | 1414.196 | 0.000 | 0.000 | 0.000 |
| MBTG | -34 10 46.58916 | 022 08 49.71317 | 33.466 | 0.030 | 0.059 | 0.154 |
| PETG | -33 57 35.26607 | 025 37 45.48579 | 31.817 | 0.030 | 0.056 | 0.150 |
| PNTG | -29 15 24.63753 | 016 52 02.53461 | 34.918 | 0.036 | 0.079 | 0.189 |
| RBTG | -28 47 45.33271 | 032 04 42.47235 | 28.502 | 0.027 | 0.060 | 0.138 |
| SATG | -33 01 24.75796 | 017 57 37.57296 | 33.417 | 0.033 | 0.063 | 0.173 |
| SBTG | -34 11 17.43872 | 018 26 22.65889 | 33.578 | 0.031 | 0.061 | 0.159 |
| SSLR | -32 22 45.04734 | 020 48 08.96170 | 1729.922 | 0.030 | 0.058 | 0.149 |
| SUTH | -32 22 48.75044 | 020 48 37.66864 | 1799.819 | 0.030 | 0.058 | 0.149 |
| TBTG | -33 54 19.86420 | 018 26 00.56615 | 33.206 | 0.031 | 0.061 | 0.159 |
| UCTN | -33 57 30.62739 | 018 27 36.70020 | 165.619 | 0.031 | 0.061 | 0.159 |

**E.4:** Final positions - ITRF97(1998.0) reference frame, WGS84 ellipsoid.
Network constrained at HRAO and SUTH (Broadcast L1).

| Site code | Latitude ° ′ ″ | Longitude ° ′ ″ | Height (metres) | $\sigma_\phi$ | $\sigma_\lambda$ | $\sigma_h$ |
|---|---|---|---|---|---|---|
| | | | | (metres) | | |
| DNTG | -29 52 27.36979 | 031 03 03.53676 | 31.593 | 0.042 | 0.059 | 0.128 |
| ELTG | -33 01 37.80748 | 027 54 52.90930 | 33.061 | 0.035 | 0.043 | 0.106 |
| HARK | -25 53 13.59273 | 027 42 27.92815 | 1555.408 | 0.001 | 0.001 | 0.006 |
| HRAO | -25 53 24.38254 | 027 41 13.12495 | 1414.196 | 0.000 | 0.000 | 0.000 |
| MBTG | -34 10 46.60393 | 022 08 49.70874 | 33.427 | 0.017 | 0.030 | 0.069 |
| PETG | -33 57 35.27907 | 025 37 45.48699 | 31.791 | 0.028 | 0.041 | 0.099 |
| PNTG | -29 15 24.64658 | 016 52 02.51884 | 34.888 | 0.042 | 0.057 | 0.133 |
| RBTG | -28 47 45.33543 | 032 04 42.48061 | 28.498 | 0.042 | 0.060 | 0.134 |
| SATG | -33 01 24.77245 | 017 57 37.56085 | 33.380 | 0.019 | 0.032 | 0.097 |
| SBTG | -34 11 17.45481 | 018 26 22.64819 | 33.538 | 0.014 | 0.031 | 0.066 |
| SSLR | -32 22 45.05988 | 020 48 08.95407 | 1729.876 | 0.001 | 0.001 | 0.006 |
| SUTH | -32 22 48.76298 | 020 48 37.66102 | 1799.773 | 0.000 | 0.000 | 0.000 |
| TBTG | -33 54 19.87987 | 018 26 00.55529 | 33.166 | 0.013 | 0.031 | 0.066 |
| UCTN | -33 57 30.64313 | 018 27 36.68941 | 165.579 | 0.013 | 0.031 | 0.067 |

**E.5:** Final positions - ITRF97(1998.0) reference frame, WGS84 ellipsoid.
Network constrained at HRAO (Broadcast $L1c_{(-trop)}$).

| Site code | Latitude ° ′ ″ | Longitude ° ′ ″ | Height (metres) | $\sigma_\phi$ | $\sigma_\lambda$ | $\sigma_h$ |
|---|---|---|---|---|---|---|
| | | | | (metres) | | |
| DNTG | -29 52 27.38740 | 031 03 03.54312 | 32.529 | 0.033 | 0.096 | 0.082 |
| ELTG | -33 01 37.83710 | 027 54 52.90578 | 33.740 | 0.031 | 0.087 | 0.082 |
| HARK | -25 53 13.59266 | 027 42 27.92826 | 1555.291 | 0.002 | 0.002 | 0.005 |
| HRAO | -25 53 24.38254 | 027 41 13.12495 | 1414.196 | 0.000 | 0.000 | 0.000 |
| MBTG | -34 10 46.63894 | 022 08 49.68490 | 34.535 | 0.032 | 0.084 | 0.082 |
| PETG | -33 57 35.31356 | 025 37 45.47350 | 32.653 | 0.033 | 0.090 | 0.086 |
| PNTG | -29 15 24.65025 | 016 52 02.47160 | 36.038 | 0.041 | 0.113 | 0.105 |
| RBTG | -28 47 45.34859 | 032 04 42.48934 | 29.500 | 0.032 | 0.096 | 0.080 |
| SATG | -33 01 24.79665 | 017 57 37.51532 | 34.267 | 0.036 | 0.091 | 0.090 |
| SBTG | -34 11 17.48654 | 018 26 22.60487 | 34.542 | 0.035 | 0.090 | 0.088 |
| SSLR | -32 22 45.08312 | 020 48 08.92446 | 1729.707 | 0.029 | 0.078 | 0.075 |
| SUTH | -32 22 48.78623 | 020 48 37.63144 | 1799.547 | 0.029 | 0.078 | 0.075 |
| TBTG | -33 54 19.90991 | 018 26 00.51225 | 34.176 | 0.035 | 0.090 | 0.088 |
| UCTN | -33 57 30.67349 | 018 27 36.64655 | 166.476 | 0.035 | 0.090 | 0.089 |

**E.6:** Final positions - ITRF97(1998.0) reference frame, WGS84 ellipsoid.
Network constrained at HRAO and SUTH (Broadcast $L1c_{(-trop)}$).

| Site code | Latitude ° ′ ″ | Longitude ° ′ ″ | Height (metres) | $\sigma_\phi$ | $\sigma_\lambda$ | $\sigma_h$ |
|---|---|---|---|---|---|---|
| | | | | (metres) | | |
| DNTG | -29 52 27.37134 | 031 03 03.53141 | 32.535 | 0.059 | 0.105 | 0.089 |
| ELTG | -33 01 37.80987 | 027 54 52.90674 | 33.829 | 0.057 | 0.084 | 0.079 |
| HARK | -25 53 13.59267 | 027 42 27.92818 | 1555.293 | 0.002 | 0.002 | 0.006 |
| HRAO | -25 53 24.38254 | 027 41 13.12495 | 1414.196 | 0.000 | 0.000 | 0.000 |
| MBTG | -34 10 46.60849 | 022 08 49.70973 | 34.738 | 0.028 | 0.050 | 0.046 |
| PETG | -33 57 35.28341 | 025 37 45.48419 | 32.784 | 0.050 | 0.080 | 0.074 |
| PNTG | -29 15 24.64039 | 016 52 02.51568 | 36.228 | 0.056 | 0.092 | 0.085 |
| RBTG | -28 47 45.33635 | 032 04 42.47317 | 29.503 | 0.059 | 0.106 | 0.087 |
| SATG | -33 01 24.77195 | 017 57 37.55686 | 34.473 | 0.029 | 0.060 | 0.058 |
| SBTG | -34 11 17.45725 | 018 26 22.64492 | 34.750 | 0.025 | 0.061 | 0.055 |
| SSLR | -32 22 45.05988 | 020 48 08.95408 | 1729.931 | 0.001 | 0.001 | 0.004 |
| SUTH | -32 22 48.76298 | 020 48 37.66102 | 1799.773 | 0.000 | 0.000 | 0.000 |
| TBTG | -33 54 19.88169 | 018 26 00.55221 | 34.384 | 0.025 | 0.060 | 0.055 |
| UCTN | -33 57 30.64507 | 018 27 36.68643 | 166.684 | 0.025 | 0.060 | 0.055 |

**E.7:** Final positions - ITRF97(1998.0) reference frame, WGS84 ellipsoid.
Network constrained at HRAO (Broadcast $L1c_{(-Ant)}$).

| Site code | Latitude ° ′ ″ | Longitude ° ′ ″ | Height (metres) | $\sigma_\phi$ | $\sigma_\lambda$ | $\sigma_h$ |
|---|---|---|---|---|---|---|
| | | | | (metres) | | |
| DNTG | -29 52 27.37200 | 031 03 03.53240 | 31.154 | 0.008 | 0.017 | 0.044 |
| ELTG | -33 01 37.80734 | 027 54 52.90975 | 32.865 | 0.009 | 0.019 | 0.043 |
| HARK | -25 53 13.59274 | 027 42 27.92812 | 1555.409 | 0.001 | 0.001 | 0.008 |
| HRAO | -25 53 24.38254 | 027 41 13.12495 | 1414.196 | 0.000 | 0.000 | 0.000 |
| MBTG | -34 10 46.60492 | 022 08 49.70820 | 33.499 | 0.009 | 0.019 | 0.040 |
| PETG | -33 57 35.27952 | 025 37 45.48551 | 31.722 | 0.009 | 0.020 | 0.044 |
| PNTG | -29 15 24.64210 | 016 52 02.51953 | 35.019 | 0.011 | 0.027 | 0.055 |
| RBTG | -28 47 45.33679 | 032 04 42.47712 | 28.163 | 0.008 | 0.017 | 0.040 |
| SATG | -33 01 24.77051 | 017 57 37.55666 | 33.261 | 0.010 | 0.021 | 0.047 |
| SBTG | -34 11 17.45398 | 018 26 22.64412 | 33.518 | 0.009 | 0.020 | 0.043 |
| SSLR | -32 22 45.05914 | 020 48 08.95254 | 1729.925 | 0.008 | 0.019 | 0.037 |
| SUTH | -32 22 48.76219 | 020 48 37.65936 | 1799.808 | 0.009 | 0.019 | 0.038 |
| TBTG | -33 54 19.87883 | 018 26 00.55136 | 33.160 | 0.009 | 0.020 | 0.044 |
| UCTN | -33 57 30.64211 | 018 27 36.68546 | 165.580 | 0.009 | 0.020 | 0.046 |

**E.8:** Final positions - ITRF97(1998.0) reference frame, WGS84 ellipsoid.
Network constrained at HRAO and SUTH (Broadcast $L1c_{(-Ant)}$).

| Site code | Latitude ° ′ ″ | Longitude ° ′ ″ | Height (metres) | $\sigma_\phi$ | $\sigma_\lambda$ | $\sigma_h$ |
|---|---|---|---|---|---|---|
| | | | | (metres) | | |
| DNTG | -29 52 27.37125 | 031 03 03.53306 | 31.153 | 0.014 | 0.018 | 0.044 |
| ELTG | -33 01 37.80700 | 027 54 52.91121 | 32.843 | 0.012 | 0.016 | 0.036 |
| HARK | -25 53 13.59273 | 027 42 27.92812 | 1555.409 | 0.001 | 0.001 | 0.008 |
| HRAO | -25 53 24.38254 | 027 41 13.12495 | 1414.196 | 0.000 | 0.000 | 0.000 |
| MBTG | -34 10 46.60541 | 022 08 49.71020 | 33.469 | 0.006 | 0.009 | 0.023 |
| PETG | -33 57 35.27948 | 025 37 45.48728 | 31.696 | 0.010 | 0.015 | 0.034 |
| PNTG | -29 15 24.64368 | 016 52 02.52067 | 34.993 | 0.014 | 0.021 | 0.047 |
| RBTG | -28 47 45.33592 | 032 04 42.47749 | 28.162 | 0.013 | 0.018 | 0.040 |
| SATG | -33 01 24.77172 | 017 57 37.55857 | 33.231 | 0.007 | 0.011 | 0.034 |
| SBTG | -34 11 17.45505 | 018 26 22.64627 | 33.487 | 0.006 | 0.011 | 0.028 |
| SSLR | -32 22 45.05993 | 020 48 08.95420 | 1729.895 | 0.003 | 0.003 | 0.015 |
| SUTH | -32 22 48.76298 | 020 48 37.66102 | 1799.773 | 0.000 | 0.000 | 0.000 |
| TBTG | -33 54 19.87991 | 018 26 00.55345 | 33.130 | 0.006 | 0.011 | 0.029 |
| UCTN | -33 57 30.64319 | 018 27 36.68756 | 165.549 | 0.006 | 0.011 | 0.033 |

**E.9:** Final positions - ITRF97(1998.0) reference frame, WGS84 ellipsoid.
Network constrained at HRAO. (Precise L1c)

| Site code | Latitude ° ′ ″ | Longitude ° ′ ″ | Height (metres) | $\sigma_\phi$ | $\sigma_\lambda$ | $\sigma_h$ |
|---|---|---|---|---|---|---|
| | | | | (metres) | | |
| DNTG | -29 52 27.37030 | 031 03 03.53319 | 31.171 | 0.004 | 0.004 | 0.024 |
| ELTG | -33 01 37.80646 | 027 54 52.91169 | 32.847 | 0.004 | 0.003 | 0.024 |
| HARK | -25 53 13.59275 | 027 42 27.92812 | 1555.408 | 0.001 | 0.001 | 0.009 |
| HRAO | -25 53 24.38254 | 027 41 13.12495 | 1414.196 | 0.000 | 0.000 | 0.000 |
| MBTG | -34 10 46.60480 | 022 08 49.71127 | 33.403 | 0.004 | 0.004 | 0.025 |
| PETG | -33 57 35.27906 | 025 37 45.48776 | 31.673 | 0.005 | 0.004 | 0.034 |
| PNTG | -29 15 24.64147 | 016 52 02.52240 | 34.991 | 0.005 | 0.007 | 0.036 |
| RBTG | -28 47 45.33538 | 032 04 42.47716 | 28.188 | 0.004 | 0.005 | 0.029 |
| SATG | -33 01 24.77006 | 017 57 37.55938 | 33.203 | 0.006 | 0.006 | 0.039 |
| SBTG | -34 11 17.45364 | 018 26 22.64718 | 33.428 | 0.004 | 0.004 | 0.027 |
| SSLR | -32 22 45.05895 | 020 48 08.95484 | 1729.867 | 0.003 | 0.003 | 0.019 |
| SUTH | -32 22 48.76204 | 020 48 37.66178 | 1799.766 | 0.003 | 0.003 | 0.018 |
| TBTG | -33 54 19.87849 | 018 26 00.55448 | 33.072 | 0.005 | 0.004 | 0.029 |
| UCTN | -33 57 30.64177 | 018 27 36.68856 | 165.493 | 0.005 | 0.005 | 0.034 |

**E.10:** Final positions - ITRF97(1998.0) reference frame, WGS84 ellipsoid.
Network constrained at HRAO and SUTH (Precise L1c).

| Site code | Latitude ° ′ ″ | Longitude ° ′ ″ | Height (metres) | $\sigma_\phi$ | $\sigma_\lambda$ | $\sigma_h$ |
|---|---|---|---|---|---|---|
| | | | | (metres) | | |
| DNTG | -29 52 27.37075 | 031 03 03.53370 | 31.171 | 0.005 | 0.004 | 0.024 |
| ELTG | -33 01 37.80735 | 027 54 52.91189 | 32.851 | 0.004 | 0.003 | 0.023 |
| HARK | -25 53 13.59275 | 027 42 27.92813 | 1555.409 | 0.001 | 0.001 | 0.009 |
| HRAO | -25 53 24.38254 | 027 41 13.12495 | 1414.196 | 0.000 | 0.000 | 0.000 |
| MBTG | -34 10 46.60594 | 022 08 49.71074 | 33.409 | 0.003 | 0.002 | 0.018 |
| PETG | -33 57 35.28011 | 025 37 45.48767 | 31.677 | 0.005 | 0.005 | 0.033 |
| PNTG | -29 15 24.64205 | 016 52 02.52103 | 34.997 | 0.005 | 0.006 | 0.034 |
| RBTG | -28 47 45.33567 | 032 04 42.47779 | 28.189 | 0.005 | 0.006 | 0.028 |
| SATG | -33 01 24.77112 | 017 57 37.55824 | 33.209 | 0.005 | 0.005 | 0.036 |
| SBTG | -34 11 17.45485 | 018 26 22.64613 | 33.434 | 0.003 | 0.003 | 0.021 |
| SSLR | -32 22 45.05989 | 020 48 08.95408 | 1729.873 | 0.001 | 0.001 | 0.009 |
| SUTH | -32 22 48.76298 | 020 48 37.66102 | 1799.773 | 0.000 | 0.000 | 0.000 |
| TBTG | -33 54 19.87965 | 018 26 00.55342 | 33.079 | 0.004 | 0.003 | 0.024 |
| UCTN | -33 57 30.64294 | 018 27 36.68751 | 165.500 | 0.004 | 0.004 | 0.030 |

**E.11:** Final positions - ITRF97(1998.0) reference frame, WGS84 ellipsoid.
Network constrained at HRAO (Precise $L1c_{(NOAA)}$).

| Site code | Latitude ° ′ ″ | Longitude ° ′ ″ | Height (metres) | $\sigma_\phi$ | $\sigma_\lambda$ | $\sigma_h$ |
|---|---|---|---|---|---|---|
| | | | | (metres) | | |
| DNTG | -29 52 27.37082 | 031 03 03.53386 | 31.150 | 0.004 | 0.004 | 0.025 |
| ELTG | -33 01 37.80770 | 027 54 52.91190 | 32.818 | 0.005 | 0.003 | 0.026 |
| HARK | -25 53 13.59275 | 027 42 27.92815 | 1555.406 | 0.001 | 0.001 | 0.009 |
| HRAO | -25 53 24.38254 | 027 41 13.12495 | 1414.196 | 0.000 | 0.000 | 0.000 |
| MBTG | -34 10 46.60641 | 022 08 49.71029 | 33.396 | 0.004 | 0.004 | 0.024 |
| PETG | -33 57 35.28049 | 025 37 45.48751 | 31.640 | 0.005 | 0.004 | 0.033 |
| PNTG | -29 15 24.64192 | 016 52 02.52021 | 34.981 | 0.005 | 0.006 | 0.034 |
| RBTG | -28 47 45.33570 | 032 04 42.47814 | 28.168 | 0.004 | 0.005 | 0.026 |
| SATG | -33 01 24.77145 | 017 57 37.55722 | 33.191 | 0.006 | 0.005 | 0.037 |
| SBTG | -34 11 17.45526 | 018 26 22.64512 | 33.418 | 0.004 | 0.004 | 0.025 |
| SSLR | -32 22 45.06013 | 020 48 08.95351 | 1729.859 | 0.003 | 0.003 | 0.019 |
| SUTH | -32 22 48.76327 | 020 48 37.66045 | 1799.754 | 0.003 | 0.003 | 0.018 |
| TBTG | -33 54 19.88009 | 018 26 00.55237 | 33.058 | 0.004 | 0.004 | 0.028 |
| UCTN | -33 57 30.64337 | 018 27 36.68648 | 165.481 | 0.005 | 0.005 | 0.032 |

**E.12:** Final positions - ITRF97(1998.0) reference frame, WGS84 ellipsoid.
Network constrained at HRAO and SUTH (Precise $L1c_{(NOAA)}$).

| Site code | Latitude ° ′ ″ | Longitude ° ′ ″ | Height (metres) | $\sigma_\phi$ | $\sigma_\lambda$ | $\sigma_h$ |
|---|---|---|---|---|---|---|
| | | | | (metres) | | |
| DNTG | -29 52 27.37052 | 031 03 03.53373 | 31.152 | 0.005 | 0.004 | 0.025 |
| ELTG | -33 01 37.80727 | 027 54 52.91203 | 32.823 | 0.005 | 0.003 | 0.026 |
| HARK | -25 53 13.59275 | 027 42 27.92815 | 1555.409 | 0.001 | 0.001 | 0.009 |
| HRAO | -25 53 24.38254 | 027 41 13.12495 | 1414.196 | 0.000 | 0.000 | 0.000 |
| MBTG | -34 10 46.60599 | 022 08 49.71081 | 33.414 | 0.003 | 0.002 | 0.017 |
| PETG | -33 57 35.28003 | 025 37 45.48782 | 31.649 | 0.005 | 0.005 | 0.032 |
| PNTG | -29 15 24.64190 | 016 52 02.52097 | 34.994 | 0.005 | 0.006 | 0.032 |
| RBTG | -28 47 45.33546 | 032 04 42.47793 | 28.169 | 0.004 | 0.005 | 0.026 |
| SATG | -33 01 24.77116 | 017 57 37.55799 | 33.208 | 0.005 | 0.004 | 0.033 |
| SBTG | -34 11 17.45490 | 018 26 22.64589 | 33.436 | 0.003 | 0.003 | 0.019 |
| SSLR | -32 22 45.05984 | 020 48 08.95408 | 1729.877 | 0.001 | 0.001 | 0.009 |
| SUTH | -32 22 48.76298 | 020 48 37.66102 | 1799.773 | 0.000 | 0.000 | 0.000 |
| TBTG | -33 54 19.87974 | 018 26 00.55313 | 33.076 | 0.003 | 0.003 | 0.022 |
| UCTN | -33 57 30.64301 | 018 27 36.68724 | 165.499 | 0.004 | 0.004 | 0.028 |

**E.13:** Final positions - ITRF97 (1998.0) reference frame, WGS84 ellipsoid.
Columbus Adjustment. Network constrained at HRAO (Precise L1c $_{(NOAA)}$).

| Site Code | Latitude ° ′ ″ | Longitude ° ′ ″ | Height (metres) | $\sigma_\phi$ | $\sigma_\lambda$ | $\sigma_h$ |
|---|---|---|---|---|---|---|
| | | | | (metres) | | |
| DNTG | -29 52 27.37079 | 031 03 03.53387 | 31.154 | 0.004 | 0.004 | 0.023 |
| ELTG | -33 01 37.80781 | 027 54 52.91204 | 32.831 | 0.005 | 0.003 | 0.023 |
| HARK | -25 53 13.59273 | 027 42 27.92815 | 1555.407 | 0.001 | 0.001 | 0.008 |
| HRAO | -25 53 24.38254 | 027 41 13.12495 | 1414.196 | 0.000 | 0.000 | 0.000 |
| MBTG | -34 10 46.60652 | 022 08 49.71042 | 33.396 | 0.004 | 0.003 | 0.022 |
| PETG | -33 57 35.28057 | 025 37 45.48769 | 31.659 | 0.005 | 0.004 | 0.029 |
| PNTG | -29 15 24.64218 | 016 52 02.52020 | 34.981 | 0.005 | 0.006 | 0.031 |
| RBTG | -28 47 45.33564 | 032 04 42.47815 | 28.172 | 0.004 | 0.005 | 0.024 |
| SATG | -33 01 24.77166 | 017 57 37.55732 | 33.200 | 0.005 | 0.005 | 0.035 |
| SBTG | -34 11 17.45545 | 018 26 22.64526 | 33.415 | 0.004 | 0.004 | 0.024 |
| SSLR | -32 22 45.06028 | 020 48 08.95358 | 1729.857 | 0.003 | 0.003 | 0.018 |
| SUTH | -32 22 48.76343 | 020 48 37.66052 | 1799.750 | 0.003 | 0.003 | 0.017 |
| TBTG | -33 54 19.88029 | 018 26 00.55251 | 33.059 | 0.004 | 0.004 | 0.026 |
| UCTN | -33 57 30.64356 | 018 27 36.68661 | 165.480 | 0.005 | 0.005 | 0.030 |

**E.14:** Final positions - ITRF97 (1998.0) reference frame, WGS84 ellipsoid.
Columbus Adjustment. Network constrained at HRAO and SUTH (Precise L1c $_{(NOAA)}$).

| Site Code | Latitude ° ′ ″ | Longitude ° ′ ″ | Height (metres) | $\sigma_\phi$ | $\sigma_\lambda$ | $\sigma_h$ |
|---|---|---|---|---|---|---|
| | | | | (metres) | | |
| DNTG | -29 52 27.37075 | 031 03 03.53384 | 31.159 | 0.005 | 0.005 | 0.027 |
| ELTG | -33 01 37.80752 | 027 54 52.91208 | 32.850 | 0.005 | 0.003 | 0.026 |
| HARK | -25 53 13.59271 | 027 42 27.92817 | 1555.411 | 0.001 | 0.001 | 0.009 |
| HRAO | -25 53 24.38254 | 027 41 13.12495 | 1414.196 | 0.000 | 0.000 | 0.000 |
| MBTG | -34 10 46.60605 | 022 08 49.71090 | 33.419 | 0.002 | 0.002 | 0.018 |
| PETG | -33 57 35.28020 | 025 37 45.48782 | 31.683 | 0.005 | 0.005 | 0.033 |
| PNTG | -29 15 24.64191 | 016 52 02.52079 | 35.007 | 0.005 | 0.006 | 0.033 |
| RBTG | -28 47 45.33561 | 032 04 42.47813 | 28.176 | 0.004 | 0.005 | 0.027 |
| SATG | -33 01 24.77122 | 017 57 37.55788 | 33.224 | 0.005 | 0.005 | 0.036 |
| SBTG | -34 11 17.45499 | 018 26 22.64581 | 33.437 | 0.003 | 0.003 | 0.021 |
| SSLR | -32 22 45.05984 | 020 48 08.95408 | 1729.880 | 0.001 | 0.001 | 0.010 |
| SUTH | -32 22 48.76298 | 020 48 37.66102 | 1799.773 | 0.000 | 0.000 | 0.000 |
| TBTG | -33 54 19.87983 | 018 26 00.55306 | 33.081 | 0.003 | 0.003 | 0.024 |
| UCTN | -33 57 30.64311 | 018 27 36.68716 | 165.502 | 0.004 | 0.004 | 0.030 |